

## ABSTRACT

AGUDA, REMIL MARTINEZ. Preparation and Characterization of Modified Biomass as Functional Carbon-based Materials. (Under the direction of Dr Richard Venditti and Dr Stephen Kelley.)

Biomass can be modified to make value-added products, such as resins, carbon fibers and activated carbon. This work focuses on two systems, modification of softwood Kraft lignin as a precursor for carbon fiber, and conversion of pine wood and switchgrass into activated biochar. The first chapter of this thesis reports on the modification of softwood Kraft lignin (SKL), a by-product of the papermaking process, with naphthanol and phenol to produce materials that may be useful as carbon fiber precursors. The purified phenolated and naphthanolated SKL samples were tested for changes relative to unmodified SKL, in their chemical and thermal properties including, carbon yield, glass transition temperature ( $T_g$ ), chemical structure, molecular weight and molecular ordering. Chemical modification lowered the  $T_g$  of SKL, but did not significantly change the carbon yield, molecular weight and molecular ordering of the SKL. The  $T_g$  increased after repeated heating cycles for modified and unmodified lignins, which could help with stabilization in carbon fiber production. The temperature at 5% weight loss (around 180 -195 °C) and  $T_g$  (110-120 °C from the first heating cycle) suggested a processing range of 110 to 200 °C for melt spinning modified SKL into carbon fiber precursors. The second chapter of this thesis is focused on preparation of activated biochars from pine wood and switchgrass. These biomass feedstocks were pyrolyzed under a nitrogen atmosphere to produce initial biochars, followed by heating under moist nitrogen at 900 °C to make steam activated biochar. Biomass, biochar and activated biochar samples, along with commercially available steam-activated carbon samples, were analyzed for their elemental composition, moisture content, specific surface

area and surface chemistry. The specific surface area of the biochar increased after steam activation (from 4 to 562 m<sup>2</sup>/g for pine wood and 3 to 128 m<sup>2</sup>/g for switchgrass). The increased specific surface area resulted in an increased sorption of the activated biochars, relative to the non-activated biochar, for furfural and gallic acid. Pine wood and switchgrass activated biochars were observed to adsorb around 310 and 255 mg/g for furfural; and 102 and 28 mg/g for gallic acid, respectively, for the conditions evaluated. This research demonstrated the production of functional carbon-based materials from biomass.

© Copyright 2017 by Remil Martinez Aguda

All Rights Reserved

Preparation and Characterization of Modified Biomass as Functional Carbon-based Materials

by  
Remil Martinez Aguda

A thesis submitted to the Graduate Faculty of  
North Carolina State University  
in partial fulfillment of the  
requirements for the Degree of  
Master of Science

Forest Biomaterials

Raleigh, North Carolina

2017

APPROVED BY:

---

Stephen Kelley  
Committee Co-chair

---

Richard Venditti  
Committee Co-chair

---

Sunkyu Park

---

Praveen Kolar

## **BIOGRAPHY**

Remil Martinez Aguda was born and raised in the science and nature city of Los Baños, Laguna, Philippines. His parents are Remedios Jucutan Martinez, an entomology researcher and financial services professional, and Angelito Aguinaldo Aguda, an agricultural engineer and entrepreneur. Together with his siblings, Reman and Rembo, his parents influenced them to have a drive for lifelong learning, sincere service and continuous wholistic self-development in a neighborhood of well-rounded scholars. With an early exposure in national high school science contests and regular visits in his parents' workplaces at international research institutes and processing plants, he was encouraged to pursue a college degree in chemical engineering, an emerging interdisciplinary field of applied science and engineering at the University of the Philippines Los Baños. After teaching in this university for three years, he pursued graduate studies in chemical engineering at North Carolina State University, and after graduation, worked for five years as a manufacturing associate and process development engineer/scientist at two protein biotherapeutics companies with multiple locations in the Research Triangle Park, Raleigh and Clayton in North Carolina. He then returned to University of the Philippines Los Baños, where he taught basic science and engineering, conducted basic research, extension in science education; and facilitated workshops for industry professionals. For professional growth as an academic scholar, teacher and researcher in science and engineering, he joined the department of forest biomaterials at North Carolina State University to complete another graduate degree in forest biomaterials.

## ACKNOWLEDGEMENTS

My academic journey is full of intellectual and personal connections with scholars from around the world. This work is made possible with the following people who have been helpful and supportive in my academic endeavors:

To my advisors, Drs Richard Venditti and Stephen Kelley, and committee members, Drs Sunkyu Park and Praveen Kolar who have been patient about giving clear directions, allowing independence as a graduate student and generous support

To fellow graduate students, post doctoral scholars, visiting scholars and adjunct professors in the department of Forest Biomaterials: Ali Ayoub, Wissam Farhat, Ganesh Narayanan, Parham Tayeb, Peggy Tayeb, Tiago de Assis, Camila Abbati de Assis, Guizhou Wang, Seughyun Yoo, Grant Culbertson, Jesse Daystar, Neethi Rajagopalan, Carter Reeb, Robert Radics, Robert Narron, Jing Du, Xiao Jiang, Egbe Eni, Eliezer Antonio Molina, Junyeong Park, Kim Chaehoon, Lu Liu, Timo Leskinen, Carlos Aizpurua, Carlos Carillo, Nithima Nakthong, Wenhui Geng, Anna Ferrer, Ingrid Hoeger, Yuhan Wang, Zahra Ashrafi, Matthew Kollman, Derek Corbett, Preeti Tyagi, Adam Scouse, Ashish Virmani, Zachary Miller, Carolina Londono Zuluaga, Maria Herrera Diaz, Eliezer Reyes, Fangda Zhang, Xiaohang Sun, Guanqun Luo, Haleh Sanaei, Xin Zhang, , Michael Joyce, Juliana Jardim, Jiadeng Zhu, Mohammad Khalilzadeh, Seona Ro, Ben Jeuck, Xueyu Du, Abdus Salam, Valeria Gomez, Chao Wang, Hasan Sadeghifar , Xiaomin Li, Sachin Agate, Michael Joyce and Marielis Zambrano

To the faculty and staff of the department of Forest Biomaterials: Barbara White, Beverly Miller, Carlos Salas, Cullen Alexander, David Tillota, Dimitris Argyropoulos, Guillermo Veralde, Hasan Jameel, Hou-min Chang, Ilona Peszlen, Jim Bray, Joel Pawlak, Leena Kathuria, Jie Liu, Lokendra Pal, Lucian Lucia, Marian McCord, Martin Hubbe, Med Byrd, Melissa Rabil, Mike

Maltby, Paula Harrod, Perry Peralta, Richard Phillips, Ronalds Gonzalez, Tricia Brown, Ved Naithani, Jim and Linda Murray and Pat Hill

For the first chapter of this thesis, the following colleagues are acknowledged for their training, maintenance and technical assistance of the following equipment with their associated data processing software: Jing Du and Xiao Jiang (phenolation set-up), Lu Liu (GPC), David Tillota, Jie Liu, Lewis Reynolds and Jacob Majikes (FT-IR), Hana Gracz, Robert Narron and Wissam Farhat (NMR) , Barbara White (DSC and TGA). The methods developed by Lu Liu (GPC), Hanna Gracz and Robert Narron (NMR) were used. The estimated cost of phenolated lignin as carbon fiber precursor and lignin as a fuel was from the economic analysis using cost models by Charles Grant Culbertson. Petroleum pitch for X-ray diffraction was provided by Amit Naskar of Oak Ridge National Laboratories, Knoxville, TN, USA through an industry collaborator. The X-ray diffraction work was performed by Ching-Chang Chung in part at the Analytical Instrumentation Facility (AIF) at North Carolina State University, which is supported by the State of North Carolina and the National Science Foundation (award number ECCS-1542015). The AIF is a member of the North Carolina Research Triangle Nanotechnology Network (RTNN), a site in the National Nanotechnology Coordinated Infrastructure (NNCI). The United States Department of Agriculture Southeastern Integrated Biomass Supply Systems Consortium (IBSS) funded this project.

For the second chapter of this thesis, technical support and guidance by the following people are duly acknowledged in the Department of Forest Biomaterials, NCSU: Seugyun Yoo, Eliezer Antonio Reyes Molina (pyrolysis), Barbara White (lab operations), Nathan Niles (preparation of the pinewood chips), Ali Ayoub (switchgrass samples) and Camilla Abbati de Assis (market trends analysis). The Kolar research group in Weaver Labs, Department of Biological and

Agricultural Engineering are acknowledged for their technical assistance on this project: Zachary Lentz, Han Jin and Brianna Massie. The following vendors are also very helpful in the completing the experimental set up and chemicals: Dayton Campos and Jordan Grigston (Swagelok Corporation, Wake Forest, NC), Parker Liu (MTI Corporation Inc., Richmond, CA) and Rob Blackman (VWR International LLC, Suwanee, GA). Lisa Lentz performed the elemental analysis of the samples at the NCSU Environmental and Agricultural Testing Services Lab. Andrew Whitaker of Soil Biogeochemistry lab trained me to do BET surface area analysis at the Department of Crop and Soil Science. Andy McClure of Jacobi Carbons gave free commercially available AC, without any proprietary and confidentiality issues. Dr Henry Nowicki of PACS testing, consulting and training center on activated carbon has been emailing useful information on the production and testing of AC. The Department of Energy LEAF funded this project.

I also wanted to extend my personal note of thanks to the following individuals and groups for their support and patience during my stay at NCSU:

To Sam Reyes, Julian and Mera Cacho, Iaconis family, Villazor-Baluyot family, Carino family, Kevin and Kristi Smith, Brendan Hardy, Joseph Gartrell, Karen and Reginald Valencia, Tim Tucker, Juliet Lindo, Florentino dela Cruz, Dennis Pacardo, Ganesh Narayanan and Ted Gonzalez for their generosity of their time and resources; and giving me a positive outlook in life To the ES King Village community, for sharing their time and resources, and recognizing our efforts for serving the well-being of the community towards diversity and inclusion: Tim Blair, Mandy Geiger, Joel Oliver, Rena Gobble, Bruno Ferreira, LaTonya Johnson, Farhan Rahman, Preslyn Phillips, Salil Kulkarni, Ryu family, Abhilash Kunatoor Margabandu, Kevin Walser,

Kristin Hummel, Kylie Hoffman, Lakeisha George, Bagus and Rasi Wibowo, Ana Patricia Malotro, Jasmine Alsaied, Mera Cacho, Chanel Spencer and the rest of the ESKV staff

To my relatives for their support: Uncle Fred and Auntie Mercy Martinez, Uncle Jun and Auntie Wilma Aguda, Lolo Manning and Lola Julieta Aguda, Uncle Nante, Auntie Ester Martinez, and my cousins, Edmer and Sou Martinez, Edmundo and Jude Martinez, Jonathan Rene and Joseph Aguda; and other relatives in the USA that I was not able to mention but also very generous of their time and resources

To my family who have been in constant communication for the encouragement, empathy and prayers: Papa, Mama, Kuya Reman, Ate Lani, Rembo, Aira & Ate Josie

To the NCSU Health Center for a great resource for my overall health and well-being

To my St. Francis of Assisi church group in Raleigh for the spiritual nourishment

To the Almighty God, the creator of forest biomaterials, my sincerest praise and thanks

## TABLE OF CONTENTS

LIST OF TABLES .....	ix
LIST OF FIGURES .....	xi
CHAPTER 1 .....	1
Softwood Kraft Lignin Modified with Phenols and Naphthanols as Carbon Fiber Precursors.....	1
ABSTRACT.....	1
ABBREVIATIONS .....	3
1.1 INTRODUCTION .....	4
1.2 MATERIALS AND METHODS.....	6
1.2.1 Naphthanolation and phenolation of lignin in a solvent system and purification using solvent extraction .....	6
1.2.2 Gel Permeation Chromatography (GPC) .....	8
1.2.3 <sup>1</sup> H Nuclear Magnetic Resonance ( <sup>1</sup> H NMR).....	9
1.2.4 Fourier Transform Infrared (FT IR) Spectroscopy .....	11
1.2.5 Thermogravimetic Analysis (TGA) .....	12
1.2.6 Differential Scanning Calorimetry (DSC).....	13
1.2.7 In-situ X-ray Diffraction (XRD) .....	14
1.3 RESULTS AND DISCUSSION.....	14
1.3.1 Chemical modification of softwood Kraft lignin .....	14
1.3.1.1 Organic reaction mechanisms.....	14
1.3.1.2 Molecular Weights of Purified Chemically Modified Lignins.....	18
1.3.1.3 Degree of Substitution from <sup>1</sup> H NMR.....	23
1.3.1.4 Principal Component Analysis of FT IR spectra.....	31
1.3.2 Thermal Properties of Chemically Modified Lignins .....	40
1.3.2.1 Weight losses during heating from Thermogravimetric analysis (TGA).....	40
1.3.2.2 Glass Transition Temperatures from DSC .....	49
1.3.2.3 Recommended Thermal Processing Conditions for Fiber Formation.....	65
1.3.3 Relationships between Chemical Properties and Thermal Properties.....	68
1.3.4 Molecular Ordering of Chemically Modified Lignin for Fiber Formation.....	73
1.4 SUMMARY AND CONCLUSIONS .....	75
1.5 REFERENCES .....	76

CHAPTER 2 .....	81
Production and Properties of Activated Biochar and its Utilization as Adsorbent Material .....	81
ABSTRACT .....	81
ABBREVIATIONS .....	82
2.1 INTRODUCTION .....	83
2.2 RELATED STUDIES ON STEAM ACTIVATION OF BIOCHAR.....	85
2.3 RELATED STUDIES ON ADSORPTION OF SELECTED MODEL COMPOUNDS ON ACTIVATED CARBON .....	100
2.4 MATERIALS AND METHODS.....	103
2.4.1 Biochar production.....	104
2.4.2 Activation of biochar using moist nitrogen mixture .....	106
2.4.3 Physical properties of biochar, activated biochar and commercially available activated carbon.....	108
2.4.3.1 Elemental compositional analysis .....	108
2.4.3.2 Moisture content.....	109
2.4.3.3 Thermogravimetric analysis of biochar.....	109
2.4.3.4 BET surface area .....	110
2.4.3.5 Boehm titration for Surface chemistry .....	110
2.4.4 Adsorption of model compounds .....	111
2.5 RESULTS AND DISCUSSION.....	113
2.5.1 Yield, moisture content, elemental analysis and thermogravimetric analysis of biochar .....	113
2.5.2 Moisture content, elemental analysis and yield of the activated biochar.....	117
2.5.3 Boehm titration for surface chemistry.....	118
2.5.4 BET surface area .....	119
2.5.5 Adsorption Behavior of Activated Biochar.....	121
2.6 SUMMARY AND CONCLUSION .....	128
2.7 REFERENCES .....	129

## LIST OF TABLES

### CHAPTER 1

Table 1.1. Chemical properties of softwood Kraft lignin modified with phenols and naphthanols at 2 hours reaction time and 90 °C .....	19
Table 1.2. Chemical properties of softwood Kraft lignin modified with phenols and naphthanols at increasing reaction time at 100 °C .....	20
Table 1.3. Molecular weights of SKL reported in the literature .....	22
Table 1.4 Degree of substitution of the chemically modified lignin and percent mass addition at increasing reaction times (calculated using equations in Figure 1).....	28
Table 1.5. FT IR band assignments on softwood Kraft lignin and phenolated lignin.....	32
Table 1.6. TGA Results (set at 100% at 105° C) for softwood Kraft lignin and chemically modified lignin samples at increasing reaction time: maximum weight loss temperature, $T_{max}$ (temperature at the highest weight %/°C), weight % at the $T_{max}$ , temperature at 5% weight loss, and weight % at 700 °C of lignin samples.....	65
Table 1.7. Glass transition temperatures of lignin chemically modified with naphthanol and phenol over 4 cycles of heating and cooling at different temperature ranges with an isothermal hold after heating.....	55
Table 1.8 Molecular weight (MRwR and MRnR) of softwood Kraft lignin and phenolated lignin heated in TGA heated from 40 °C to 200°C at 20 °C/minute and then held at 200 °C for 8 minutes.....	64

CHAPTER 2

Table 2.1. Studies on activation of biochar using steam or steam-inert gas mixtures, the product properties and its intended application.....98

Table 2.2 Percent Carbon and Weight % from TGA from elemental analysis of biochar batches from pinewood and switchgrass combined for activation.....115

Table 2.3 Moisture content and elemental composition of the steam activated commercial activated carbon, biomass source, combined biochar batches and activated biochar.....117

Table 2.4 Acidic and basic groups on the biochar and activated carbon.....119

Table 2.5 Comparisons of the BET surface area of the biochar and activated biochar samples with commercially available AC and reported values in the literature.....120

## LIST OF FIGURES

### CHAPTER 1

Figure 1.1. Equations for calculating the degree of substitution from the peak intensities of $^1\text{H}$ NMR, and the % mass of reactant added (phenol or naphthanol) per gram of $\text{C}_9$ units.....	10
Figure 1.2. Reaction of 1-naphthanol (upper) and 2-naphthanol (lower) with unsaturated carbon bonds in lignin, hydroxyl and carbonyl portions of the lignin macromolecule.....	15
Figure 1.3. Gel permeation chromatograms showed the absence of unreacted naphthanol after three washing and precipitation steps of the product made in dioxane-water mixture.....	18
Figure 1.4. $^1\text{H}$ NMR of Softwood Kraft lignins modified with naphthanol made in dioxane-water mixtures at increasing reaction time.....	24
Figure 1.5. $^1\text{H}$ NMR of Softwood Kraft lignins modified with naphthanol and phenol made in dioxane-water for 2 hours of reaction time.....	25
Figure 1.6. $^1\text{H}$ NMR of Softwood Kraft lignins modified with phenol at 1 and 2 hours.....	27
Figure 1.7. Degree of substitution versus reaction time for different chemical modifications at $100\text{ }^\circ\text{C}$ .....	30
Figure 1.8. FT IR of lignin samples that were identified from IR band assignments reported in the literature.....	33
Figure 1.9. FT IR spectra of Bio Choice Lignin (BCL) and phenolated lignin samples (P1, P2, P4 and P8 are prepared at 1,2,4 and 8 hours reaction time, respectively).....	34
Figure 1.10. FT IR spectra of Bio Choice Lignin (BCL) and naphthanolated lignin samples (2N4 and 2N8) are 2-naphthanolated lignin samples prepared at 4 and 8 hours reaction time, respectively; 1N4 and 1N8 are 1-naphthanolated lignin samples prepared at 4 and 8 hours reaction time, respectively.....	35

Figure 1.11. Principal Component Analysis (PCA) score plots for PC-1 (81%) versus PC-2 (9%); and PC-2 (9%) and PC-3 (4%) for FT IR of lignin samples from 4000 to 850  $\text{cm}^{-1}$  .....37

Figure 1.12. Principal Component Analysis (PCA) loading plots for X-variables for PC-1, PC-2 and PC-3 for the FT IR lignin samples from 4000 to 850  $\text{cm}^{-1}$  .....38

Figure 1.13. TGA curve of the softwood Kraft lignin as a starting material.....41

Figure 1.14. TGA curves of phenolated lignins made in 1 and 2 hours reaction time (sampled from the same reaction mixture).....42

Figure 1.15. TGA curves of 1-naphthanolated and phenolated lignins made in 2 hours reaction time.....43

Figure 1.16. TGA curves of phenolated and naphthanolated lignins made in 4 hours reaction time.....44

Figure 1.18. TGA curves of phenolated and naphthanolated lignins made in 8 hours reaction time.....45

Figure 1.19. DSC scan of softwood Kraft lignin showing the  $T_g$  at the each cycle.....50

Figure 1.20. DSC scan of phenolated lignin made at 8 hours reaction showing the  $T_g$  at each cycle.....51

Figure 1.21. DSC of 1-naphthanolated lignin made at 8 hours reaction showing the  $T_g$  at each cycle.....52

Figure 1.22. DSC of 2-naphthanolated lignin made at 8 hours reaction showing the  $T_g$  at each cycle.....53

Figure 1.23. TGA curve of softwood Kraft lignin heated at 20  $^{\circ}\text{C}$  per minute from 40 to 200  $^{\circ}\text{C}$  with an isothermal hold at 8 minutes at 200  $^{\circ}\text{C}$ .....59

Figure 1.24. TGA curve of phenolated lignin made in 1 and 2 hours reaction time, heated at 20 °C per minute from 40 to 200 °C with an isothermal hold at 8 minutes at 200 °C.....	60
Figure 1.25. TGA curve of 1-naphthanolated lignin made in 4 and 8 hours reaction time, heated at 20 °C per minute from 40 to 200 °C with an isothermal hold at 8 minutes at 200 °C.....	61
Figure 1.26. TGA curve of 2-naphthanolated lignin made in 4 and 8 hours reaction time, heated at 20 °C per minute from 40 to 200 °C with an isothermal hold at 8 minutes at 200 °C.....	62
Figure 1.27. Suggested processing range of the modified lignins for thermal processing based on the $T_g$ and temperature at 5% weight loss (without residual solvent content) for the lignin samples, prepared at 8 hours reaction time.....	66
Figure 1.28. Correlation of the $M_w$ and $T_g$ using the Fox Flory equation for the chemically modified lignins prepared in this study.....	68
Figure 1.29. Glass transition temperatures of naphthanolated and phenolated lignin predicted using Fox equation.....	70
Figure 1.30. Correlation of the $M_n$ and $T_g$ using the Fox Flory equation for the chemically modified lignins prepared in this study.....	72
Figure 1.31. X-ray diffraction patterns of 1-naphthanolated lignin and phenolated lignin samples, compared with petroleum pitch at room temperature.....	73

## CHAPTER 2

Figure 2.1 Schematic model of activated carbon affected by type of activation and biomass source (Henning & von Kienle, 2012).....	86
Figure 2.2. Steam activation of biochar using a porous case fixed in a reactor tube (Abbas, 2014).....	89
Figure 2.3. Biochar pellet press (a), pellets (b) and physical activation equipment (Abbas, 2014).....	89
Figure 2.4. Steam activation set-up with nitrogen and water combined and fed to a reactor (Azargohar & Dalai, 2008).....	90
Figure 2.5 A packed bed reactor for carbonization, oxygenation and activation of biomass for production of activation carbon by a controlled, low temperature oxidation of biomass charcoal in liquid water (Antal & Grønli, 2003).....	92
Figure 2.6. Experimental set up for steam activation of biochar using the same set-up for making biochar (Daud, Ali, & Sulaiman, 2000).....	96
Figure 2.7 Process diagram for the pyrolysis of biomass.....	104
Figure 2.8 Muffle furnace containing the metal box for heating the biomass.....	104
Figure 2.9 Steam activation set-up.....	107
Figure 2.10 Metal tube attachment at the inlet to the metal container for distribution of the moist nitrogen mixture.....	107
Figure 2.11 Yield and average percent moisture content (% MC) of the biochar batches from pinewood and switchgrass.....	113
Figure 2.12 Thermogravimetric analysis of biochar batches from pinewood and switchgrass.....	116

Figure 2.13. Absorbance of furfural solution (3.6 mg/L) from 200 to 330 nm, showing maximum absorbance at 277 nm.....122

Figure 2.14. Absorbance of furfural solutions with known concentrations (0.9 to 5.5 mg/L) showing a linear relationship for interpolation on absorbance range of 0.2 to 0.8 for determining the concentration of unknown solutions from sorption experiments.....122

Figure 2.15. Absorbance of gallic acid solution (mg/L) from 235 to 380 nm, showing a maximum absorbance at 260 nm.....123

Figure 2.16. Absorbances of gallic acid solutions with concentrations from 1.0 to 20.0 mg/L, showing a linear relationship of absorbance and concentration for interpolation on absorbance range of 0 to 0.99 for determining the concentration of unknown solutions from sorption experiments.....123

Figure 2.17. Batch adsorption isotherm indicating equilibrium concentrations at adsorption of furfural for 2 hours contact time at 25 °C.....124

Figure 2.18. Batch adsorption isotherm indicating equilibrium concentrations of gallic acid at 1 hour contact time at 25 °C.....125

## CHAPTER 1

### Softwood Kraft Lignin Modified with Phenols and Naphthanols as Carbon Fiber Precursors

#### ABSTRACT

Lignin is an abundant natural biomaterial that can be converted to high-value products such as carbon fibers. This study aims to evaluate the changes in lignin upon reaction with hydroxylated aromatic compounds and show that the hydroxylated aromatic compounds would increase the overall carbon content and act as ordering sites in the structure of lignin. To achieve this, Softwood Kraft Lignin (SKL) was chemically combined with phenol, 1-naphthanol or 2-naphthanol in a dioxane-water solvent system and purified through solvent extraction. The purified products were tested with gel permeation chromatography (GPC) to determine the molecular weight and confirm the absence of unreacted phenol or naphthanol, prior to measuring the degree of substitution (DS) by  $^1\text{H}$  NMR. FT IR confirmed an increase in the phenolic functional groups after incorporation of these hydroxylated aromatic compounds into the lignin structure. After heating the lignin samples to 700 °C in TGA, the yield of the naphthanolated lignin, phenolated lignin, and SKL were comparable in the range of 43 to 46 weight %, due to a low degree of substitution (0.02 to 0.29 mole of reactant per mol of  $\text{C}_9$  lignin unit). However, as shown in Differential Scanning Calorimetry (DSC), naphthanolation and phenolation lowered the glass transition temperature of SKL by 20-40 °C. Relationships of the molecular weight and glass transition temperature,  $T_g$ , were correlated by Fox equations for polymer mixtures. During four DSC heating and cooling cycles, the  $T_g$  increased, which suggested that the thermal stability of these lignin materials are expected to improve after the heat treatment and cooling steps in the fiber formation by melt-spinning, thermostabilization and carbonization steps in carbon fiber manufacturing. In situ X-ray diffraction did not show any ordering of the unmodified and

modified lignin indicating that the addition of these hydroxylated aromatic compounds at the measured DS values did not induce ordering. Increasing the reaction time increased the degree of substitution and lowered the glass transition temperature but did not significantly change the molecular weight and yield after carbonization. These chemical and thermal properties suggested a temperature range of 110 to 200 °C for processing the modified lignin samples for melt-spinning into carbon fiber precursors.

## ABBREVIATIONS

BCL™	Bio Choice Lignin
SKL	Softwood Kraft Lignin
GPC	Gel Permeation Chromatography
SEC	Size Exclusion Chromatography
M <sub>w</sub>	Weight average molecular weight
M <sub>n</sub>	Number average molecular weight
MALDI TOF	Matrix-Assisted Laser Desorption Ionization Time of Flight
<sup>1</sup> H NMR	Proton Nuclear Magnetic Resonance
DS	Degree of Substitution
FT IR	Fourier Transform Infrared Spectroscopy
PCA	Principal Component Analysis
PC	Principal Component
TGA	Thermogravimetric Analysis
T <sub>max</sub>	Temperature at maximum change in weight % or Maximum weight loss temperature (Weight %/°C)
DSC	Differential Scanning Calorimetry
T <sub>g</sub>	Glass transition temperature
T <sub>m</sub>	Melting temperature
XRD	X-ray Diffraction

## 1.1 INTRODUCTION

The valorization of lignin as a polymeric biomaterial has motivated biomaterials researchers to creatively utilize it as a carbon fiber precursor because of its graphite-like structure after carbonization. Currently, there is a great interest in using lignin, a by-product of the papermaking process, for carbon fibers to replace other more expensive raw carbon fiber polymer precursors. Lignin-based carbon fibers can be sold at \$1800/ton (Ellringmann, Wilms, Warnecke, Seide, & Gries, 2015) as compared to lignin being sold as fuel for approximately \$180 per ton, based on its heating value (Svensson, 2014). Hence, there have been ongoing efforts on conversion of lignin to carbon fiber; and also setting standards for lignin properties that would be necessary for its conversion (Saito et al., 2013). Supply chain analysis of carbon fibers in their applications in wind energy, aerospace, automotive and pressure vessels (Das et al., 2016) anticipated demand for carbon fibers in these industries to be 92,802 metric tons by 2018. For the aerospace and automotive industries, lignin can be an alternative low-cost biomass-based precursor for carbon fiber-based fabrics. Lignin-based carbon fibers have been made into thermal insulation mats in a scalable process (Paul et al., 2015). Significant advancements in the study of producing lignin-based carbon fibers showed that this material can be used as alternative cheaper components in catalyst supports, thermal insulators and electrodes for power storage devices (Dallmayer & Kadla, 2014).

The industrial conversion of softwood Kraft lignin (SKL) into value-added products such as carbon fibers involves modification of the lignin, melt-spinning by extrusion, thermostabilization, carbonization and surface modification (Bajpai, 2013) in order to meet the desired properties as a mechanical support, insulator or conductor of electricity. For instance, the conversion of phenolated lignin to carbon fiber involved heating it at 180 °C for 3 to 4 hours

in a non-oxidizing atmosphere (nitrogen stream) and reduced pressure ( $< 10$  mm Hg) for increased viscosity and density; melt-spinning into a fiber at  $200$  °C at a constant heating rate; and finally carbonizing the fiber under an inert atmosphere (nitrogen stream) up to  $800$ °C at a rate of  $200$ °C per hour (Sudo, Kenichi; Shimizu, 1994).

Lignin is a complex, heterogeneous biomolecule that needs to be modified to have uniform properties for fiber formation. Chemical modification of lignin as a carbon fiber precursor has been performed in previous studies such as acetylation (Zhang, Jin, & Ogale, 2015; Zhang & Ogale, 2014), UV cross linkable thermoplastic graft copolymers (Wang & Venditti, 2015) or condensation (Kadla, Kubo, Venditti, Gilbert, & Compere, 2002). The strategies for the conversion of lignin to high-value polymeric materials through polymerization of the monolignols and the aforementioned lignin derivatives have also been explored and documented (Upton & Kasko, 2016). Naphthanolation is explored in this study as another way for chemically modifying lignin. This study demonstrated the use of a solvent system to ensure the complete mixing of the reactants as a solution, compared to previous studies on phenolation where phenol was used as a solvent, in addition to its role as a reactant (Matsushita, Sano, Imai, Imai, & Fukushima, 2007; Podschun, Stücker, Saake, & Lehnen, 2015; S. Yang, Wen, Yuan, & Sun, 2014). This study also demonstrated the removal of unreacted phenol or naphthanol in the product mixture by multiple dispersion and precipitation steps.

In this study, lignin is chemically modified to add aromatic carbons to its structure to increase its carbon content during thermal treatment and to lower its glass transition temperature,  $T_g$ , for thermal processing (melt spinning or extrusion) and in addition, such modification is expected to induce ordering in the lignin structure by increasing sites for pi-pi stacking. Thus, ordering the lignin macromolecule during heating and fiber formation is expected to create more order in

subsequent carbonized structures. Phenolated and naphthanolated lignin was produced and analyzed with respect to properties important to producing carbon-based material.

## 1.2 MATERIALS AND METHODS

### 1.2.1 Naphthanolation and phenolation of lignin in a solvent system and purification using solvent extraction

Bio Choice™ (BCL) softwood Kraft lignin from Domtar (Plymouth, NC, USA) was used in this study. BCL is a lignin by-product from the Lignoboost process, which is a process using carbon dioxide as an acid for precipitation of the softwood Kraft lignin and a two-pass slurry washing process with sulfuric acid to remove contaminants. To further remove ash, approximately two kilograms of Bio Choice lignin (BCL) was mixed with 20 L deionized water and then the pH adjusted to 2-3 by addition of 1 M sulfuric acid and stirred for 12 hours. The lignin was then filtered through a ceramic membrane with a coarse porosity (40-60 microns) and washed using deionized water until the pH reached 6 to 7. The ash content of the washed lignin was 0.11 %. The material was oven dried for 3 hours at 60°C and then kept in sealable plastic bags until further use.

BCL™ is chemically modified with the following hydroxylated aromatic compounds: phenol (from Fisher Scientific, Atlanta, GA, USA; used as received), 1-naphthanol and 2-naphthanol (from Sigma Aldrich, St. Louis, MO, USA; used as received). The solvents for the reaction (1,4 dioxane) and purification (ethyl acetate, and diethyl ether) were purchased from Fisher Scientific (Atlanta, GA, USA) and used as received.

Softwood Kraft Lignin was mixed with naphthanol or phenol at a 3: 5 w/w ratio, added to a mixture of 1,4 dioxane-water (9:1 v/v) at a concentration of 20 % w/v. Sulfuric acid was added as a catalyst, which is 5% of the BCL mass (for instance, adding 5 g H<sub>2</sub>SO<sub>4</sub> per 100 g lignin). The reaction was

allowed to complete at 90°C for 2 hours with continuous stirring. All reaction product mixtures were cooled to room temperature, dispersed in 40 mL ethyl acetate and precipitated in 900 mL diethyl ether in order to separate the lignin from unreacted naphthanol or phenol. Diethyl ether dissolved phenol and ethyl acetate; but did not dissolve the phenolated lignin. This washing and precipitation step was performed three times, resulting in a yield of at least 1 gram of sample. After vacuum filtration, 200 mL deionized water was added to remove the sulfuric acid in the recovered phenolated lignin and to adjust its pH to 7. The final product was dried in an oven at 60°C for at least 12 hours (overnight). As a basis for comparison, lignin without a reactant was also made in the same mass ratios and reaction conditions.

To obtain samples at increasing reaction times, another batch of lignin reacting with phenol or naphthanol was made in a dioxane-water system, where 50-mL samples of the reaction mixture were obtained (at a set time) : phenol (1, 2, 4 and 8 hours), and 1-naphthanol or 2-naphthanol (4 and 8 hours). In these reaction mixtures, 20 grams of the starting BCL material was mixed with 0.5 mole of phenol or naphthanol. Like the previous experiments performed at 2 hours reaction time, this solid mixture was added to a mixture of 1,4 dioxane-water (90:10 v/v) at a concentration of 20 % w/v. However, the reaction temperature during the reflux of the 90% dioxane-water mixture was at 100-105 °C (near the boiling points of 1,4 dioxane and water, which are 101 °C and 100 °C, respectively). When the phenol and lignin were thoroughly mixed in the dioxane-water, sulfuric acid was added at 5% of the mass of the BCL. As a basis for comparison, another batch of lignin (with a known mass) without a reactant (phenol or naphthanol) was also added to the same 1,4 dioxane-water mixture in the presence of sulfuric acid at 5% of the mass of the lignin at the same reaction temperature, reactant to solvent ratios and reaction times of 1, 4 and 8 hours.

### 1.2.2 Gel Permeation Chromatography (GPC)

Gel Permeation Chromatography (GPC), also known as Size Exclusion Chromatography (SEC), measured the molecular weight distribution of the lignin. GPC also identifies the components in the reaction mixture, the lignin-carbohydrate complex molecules, the Softwood Kraft lignin molecules and unreacted phenol or naphthanol. The acetylation reagents, (pyridine and acetic anhydride) and chromatography solvent (tetrahydrofuran) were purchased from Fisher Scientific (Atlanta, GA, USA) and were used as received. Lignin samples were acetylated with equal volumes of pyridine and acetic anhydride for at least 72 hours in the dark. The samples were recovered by precipitation in deionized icewater and then filtered on ceramic crucibles with fine porosity (4-5.5 microns). After air drying, the acetylated naphthanolated or phenolated samples were dissolved in tetrahydrofuran at a concentration of 0.1 mg/mL, filtered through a 0.5 micron filter and loaded into two columns in series, HR-1 and HR-E (Waters Corporation, Milford, MA) with a UV detector (to measure absorbance at 280 nm) at 35°C. These chromatography columns were packed with highly cross-linked styrene-divinylbenzene copolymer with controlled pore size. Tetrahydrofuran was used as the eluent at a flowrate of 0.7 mL/minute. The acetylated forms of the phenol or naphthanol, phenyl acetate, 1-naphthanyl acetate and 2-naphthanyl acetate, were also tested in order to identify the unreacted acetylated reactants in the chromatograms of the acetylated lignin samples. These acetylated phenol, 1-naphthanol and 2-naphthanol standards were obtained from Sigma Aldrich (> 98% purity) and were used as received. The molecular weights of the lignin samples were determined from a calibration curve of known retention times and molecular weights of polystyrene standards, with molecular weights ranging from 38,640 to 380 g/mol. Data collection and processing was performed using Shimadzu LC Software.

### 1.2.3 $^1\text{H}$ Nuclear Magnetic Resonance ( $^1\text{H}$ NMR)

After GPC confirmed that absence of unreacted naphthanol or phenol in the chromatograms and shown that multiple washing and precipitations had removed the naphthanol or phenol in the purified naphthanolated or phenolated samples, the purified lignin samples were analyzed in  $^1\text{H}$  NMR. The purified lignin samples were dissolved in DMSO- $d_6$  (Sigma Aldrich, St Louis, MO) and loaded into a Bruker NMR 500 MHz spectrometer in the following conditions: sweep width of 18 ppm, O1P of 5 ppm, pulse width of 10.25 and delay of 1 second with an acquisition time of 1.8 seconds for 256 scans at 298 K. The  $^1\text{H}$  NMR spectra was processed using TopSpin, and plotted using Mestrenova. Phase and baseline corrections were applied before signal integration against the resonance within the  $\delta$ -region of the methoxy hydrogens (2.6 to 4.2 ppm), which was assigned a value of 1 and other peak signals relative to this spectral region.

The degree of substitution (DS) was expressed as the ratio of the moles of the added reactant (phenol or naphthanol) to the mole of the C<sub>9</sub> unit of the lignin. This DS value is calculated from the ratio of the peak intensities of the aromatic hydrogens (> 6 ppm) to the methoxy hydrogens (2.6 to 4.2 ppm), which is assumed to be the ratio of the aromatic hydrogen atoms in the chemically modified lignin to the methoxy hydrogen atoms in the lignin. In this calculation, the peak intensities of the aromatic hydrogens in the lignin starting material and methoxy hydrogen atoms in the unmodified lignin are assumed to remain intact, even after the chemical modification (equations are shown in Figure 1.1). These equations set the degree of substitution of zero to the lignin as a starting material.

$$\text{Degree of Substitution} = \frac{\text{moles of added reactant}}{\text{moles of C}_9 \text{ unit}}$$

*Degree of Substitution, DS*

$$= \frac{\frac{(\text{peak intensity of aromatic H in chemically modified lignin} - \text{peak intensity of aromatic H in lignin})}{\left(\frac{\text{moles of H}}{\text{moles of added reactant}}\right)}}{\left(\frac{\text{peak intensity of methoxy H}}{\frac{3 \text{ moles of H}}{\text{moles of methoxy}}}\right) \left(\frac{\text{moles of C}_9 \text{ unit}}{0.814 \text{ moles of methoxy}}\right)}$$

$$\begin{aligned} \% \text{ mass of reactant added} &= \frac{\text{mass of added reactant to C}_9 \text{ unit}}{\text{mass of added reactant} + \text{mass of C}_9 \text{ unit}} \\ &= \frac{(\text{Degree of substitution, moles of reactant per mole C}_9 \text{ unit}) \left(\frac{\text{molecular weight of C}_9 \text{ unit}}{\text{molecular weight of reactant}}\right)}{\left(\text{Degree of substitution, moles of reactant per mole of C}_9 \text{ unit}\right) \left(\frac{\text{molecular weight of C}_9 \text{ unit}}{\text{molecular weight of reactant}}\right) + (1 \text{ mole C}_9 \text{ unit})(\text{Molar mass of C}_9 \text{ unit})} \end{aligned}$$

Figure 1.1. Equations for calculating the degree of substitution from the peak intensities of <sup>1</sup>H NMR, and the % mass of reactant added (phenol or naphthanol) to grams of C<sub>9</sub> units.

These  $^1\text{H}$  NMR ppm ranges were based on a method of measuring the degree of substitution of phenolated liginosulfonates (M. V. Alonso et al., 2001; Ma V. Alonso et al., 2005). The areas of the residual solvent peaks were subtracted. The peak assignment of the  $^1\text{H}$  NMR of the residual solvents, diethyl ether and ethyl acetate, were from a tabulated list of commonly detected residual solvents in the literature for  $^1\text{H}$  NMR of purified organic molecules (Gottlieb, Kotlyar, & Nudelman, 1997). The moles and amount of  $\text{C}_9$  units are calculated from the molecular formula of the Biochoice™ (BCL) softwood kraft lignin, which is  $\text{C}_9\text{H}_{8.93}\text{O}_{2.37}(\text{OCH}_3)_{0.814}\text{S}_{0.079}$  and its reported average molecular weight of 182.6 g/mol (Pawar, Venditti, Jameel, Chang, & Ayoub, 2016).

The degree of substitution was the basis for calculating percent of the reactant in the chemically modified BCL. The calculation of the percent of reactant (phenol, 1-naphthol or 2-naphthol) did not include the hydrogen in hydroxyl groups, but the hydrogen in the aromatic groups for assigning the number of moles of the aromatic H in the reactant. Moreover, the percent mass addition of the reactant to the lignin can also be calculated from the degree of substitution. The percent carbon in the chemically modified BCL is calculated from the experimental DS, molar mass of lignin (5500 g/mol) reported in the literature for BCL (Pawar et al., 2016), molecular weight of the added hydroxylated aromatic compounds (phenol: 93 g/mol, 1-naphthanol: 143 g/mol, and 2-naphthanol: 143 g/mol).

#### 1.2.4 Fourier Transform Infrared (FT IR) Spectroscopy

FT IR analyses of the oven-dried lignin samples was conducted using Varian 640 Mid FT IR spectrometer equipped with Pike Miracle Attenuated Total Reflection (ATR) accessory containing a ZnSe crystal. The background was collected prior to analysis of each batch of sample. All spectra were collected using 32 scans. Using Spectrum software, the spectra was

baseline corrected to remove the slopes often caused by the scattering of the infrared spectrum beam by the sample; and normalized by setting the absorbance values relative to the maximum absorbance (set at 1). Principal component analysis (PCA) of the FT IR spectra was performed using Unscrambler X 10.4 software. PCA is a multivariate data analysis method for producing linear combinations of the variables such as FTIR band positions with their assignments for bond stretches of the functional groups in the lignin structure.

#### 1.2.5 Thermogravimetric Analysis (TGA)

In this study, thermogravimetric analysis (TGA) measured the weight changes of the samples under nitrogen atmosphere using TGA model Q500 (TA Instruments, DE). TGA estimated the carbon yield at the end of thermal treatment under nitrogen atmosphere, assuming the remaining material at 700°C is carbon with an ash content less than 1%. The lignin samples, prepared at 2 hours of reaction time, were heated from 40 to 105°C, held isothermally at 105 °C for 10 minutes to remove any residual volatile solvents (1,4-dioxane, water, ethyl acetate or diethyl ether), then heated to 700°C at a rate of 10°C per minute. The boiling points of 1,4-dioxane, water, ethyl acetate and diethyl ether are 101, 100, 77 and 35°C, respectively. The lignin samples, which were recovered at increasing reaction times (1, 2, 4 or 8 hours), were heated from 40 to 700°C with a rate of 10°C per minute. The heating rate for this TGA method was chosen to show the weight loss at reasonably low heating rates (< 20 °C per minute), and similar to thermostabilization (0.2 to 3°C/min) up to 250 °C and carbonization at 1000 °C (3°C/min) performed in the production of lignin-based carbon fibers (Kadla et al., 2002). Data analyses were performed using TA Universal Analysis 2000, version 4.5.0.5. The weight % was set at 100 % at 105°C to report the weight % on a dry basis (without moisture or organic solvents from the previous solvent extraction and purification process).

### 1.2.6 Differential Scanning Calorimetry (DSC)

Differential Scanning Calorimetry (DSC) was used to determine the glass transition temperature and the heat capacities of the samples. The DSC model Q2000 (TA Instruments, New Castle, DE, USA) was calibrated with indium and sapphire using standard methods for temperature calibration (ASTM E967) and heat flow calibration (ASTM E968). Approximately 10-15 mg of a lignin sample was heated under nitrogen atmosphere in sealed hermetic pans (Tzero) with a hole in the cover to allow the escape volatiles.

To detect changes in the glass transition temperature,  $T_g$ , over 4 heating and cooling cycles, the sample is heated from 40 °C to different temperatures at a rate of 20 °C per minute: 160°C (first cycle), 180°C (second cycle), 200°C (third cycle) and 220°C (fourth cycle). The sample was at an isothermal hold at 40°C for 5 minutes at the start of each cycle in order to obtain a stable baseline for detecting  $T_g$  then heated to the set temperatures at a heating rate of 20° C/minute to allow condensation and cross-linking, and jump to 40°C to cool the sample. The glass transition temperature and change in heat capacity was analyzed using TA Universal Analysis 2000, version 4.5.0.5.

A TGA method for this DSC method of heating and cooling cycle was performed at the same heating rate up to 200 °C and an isothermal hold at 200 °C for 8 minutes to detect any weight loss over this range of temperature.

### 1.2.7 In-situ X-ray Diffraction (XRD)

For the purified naphthanolated and phenolated lignins at 2 hours of reaction time, temperature-dependent diffraction data were collected with PANalytical Empyrean X-ray diffractometer with Bragg-Brentano optics using fixed receiving slits, a Ni filter and Pixel 1-D detector. The samples were placed in a resistively heated HTK-1200 N hot stage in a nitrogen atmosphere. The samples were heated at a constant rate of  $3^{\circ}\text{C min}^{-1}$  with a theta-two theta pattern capture every 5 minutes. Scanned angles was set between 10 to  $55^{\circ}$ . Data processing was performed using Matlab, High Score Plus and Microsoft Excel.

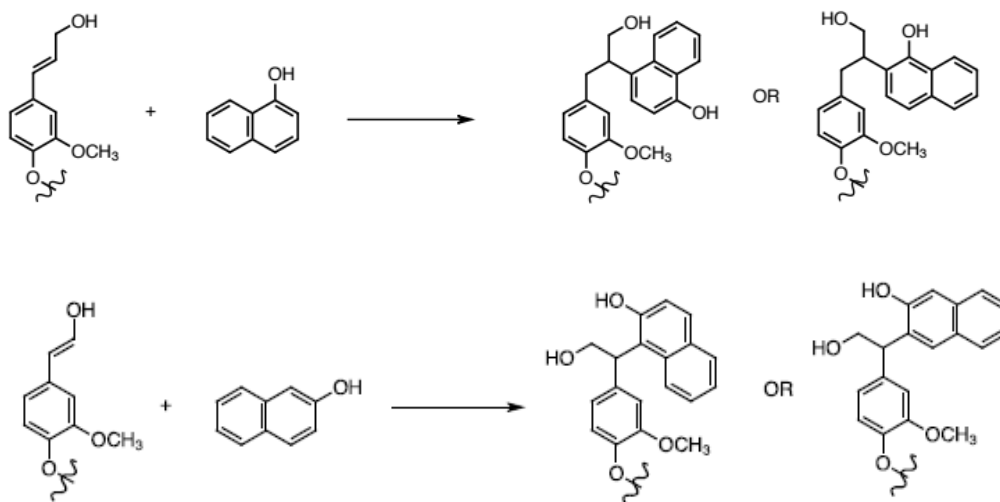
## 1.3 RESULTS AND DISCUSSION

### 1.3.1 Chemical modification of softwood Kraft lignin

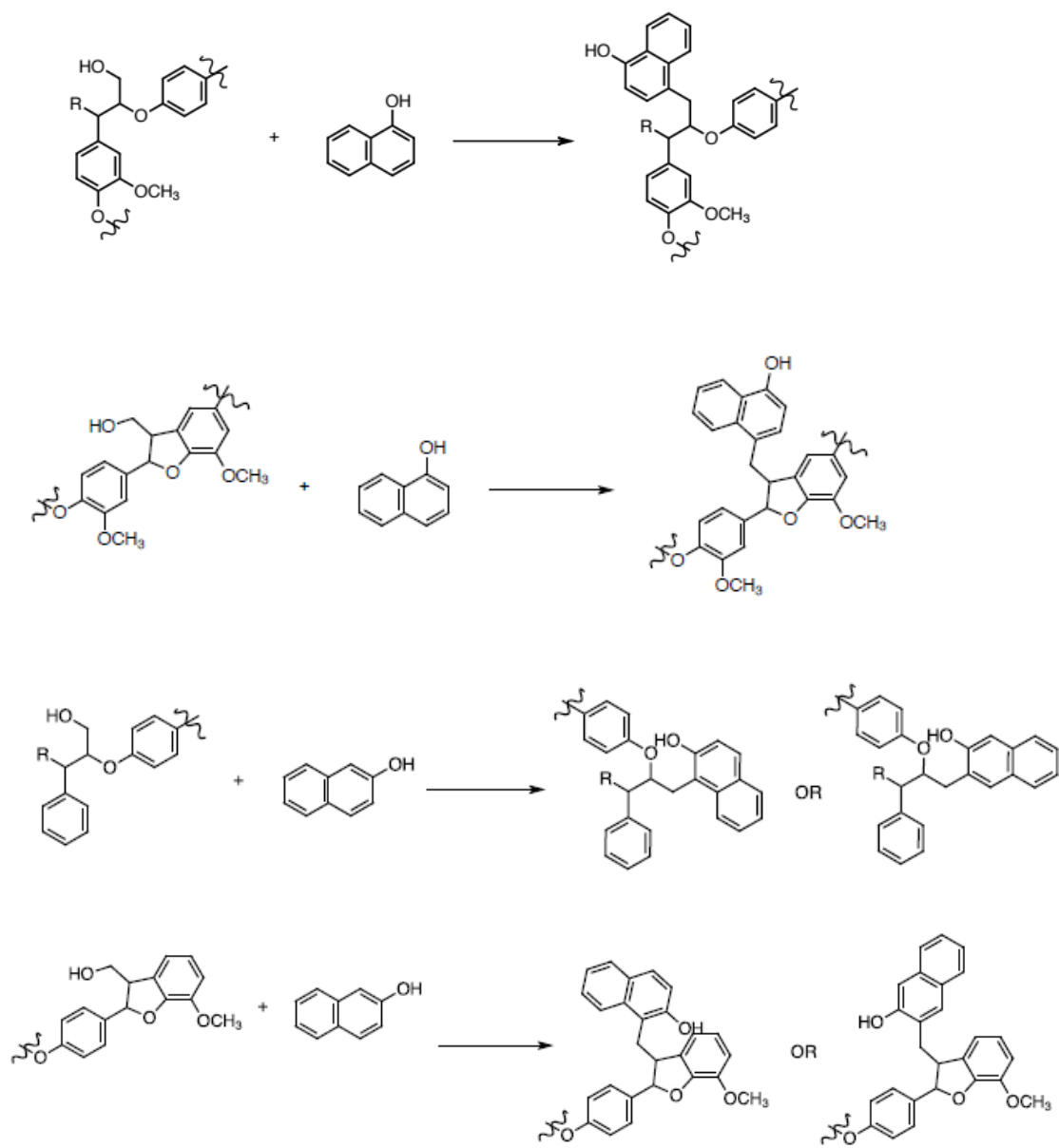
#### 1.3.1.1 Organic reaction mechanisms

The chemical modification of softwood Kraft lignin with phenol or naphthanol involves several sites in the lignin's chemical structure. The chemical reaction mechanism of phenolation and naphthanolation involves nucleophilic aromatic substitution at the stilbene, hydroxyl and carbonyl groups of lignin, with the addition of the phenol or naphthanol at the ortho- or para-position. Figure 1.2 presented the proposed reaction mechanisms for the covalent attachment of 1-naphthanol and 2-naphthanol to the different portions of the softwood Kraft lignin macromolecule. These proposed mechanisms of naphthanolation were based on the reaction mechanisms demonstrated by nuclear magnetic resonance on phenolated lignin from Kraft lignin and Organosolv lignin from hardwood and softwood (Podschun et al., 2015) and other biomass feedstocks such as corn cob, wheat straw and poplar wood (S. Yang et al., 2014). The presence of the methoxy hydrogens in the softwood Kraft lignin near the possible sites for phenolation or naphthanolation were assumed to be not cleaved and not reactive to the phenol or naphthanol.

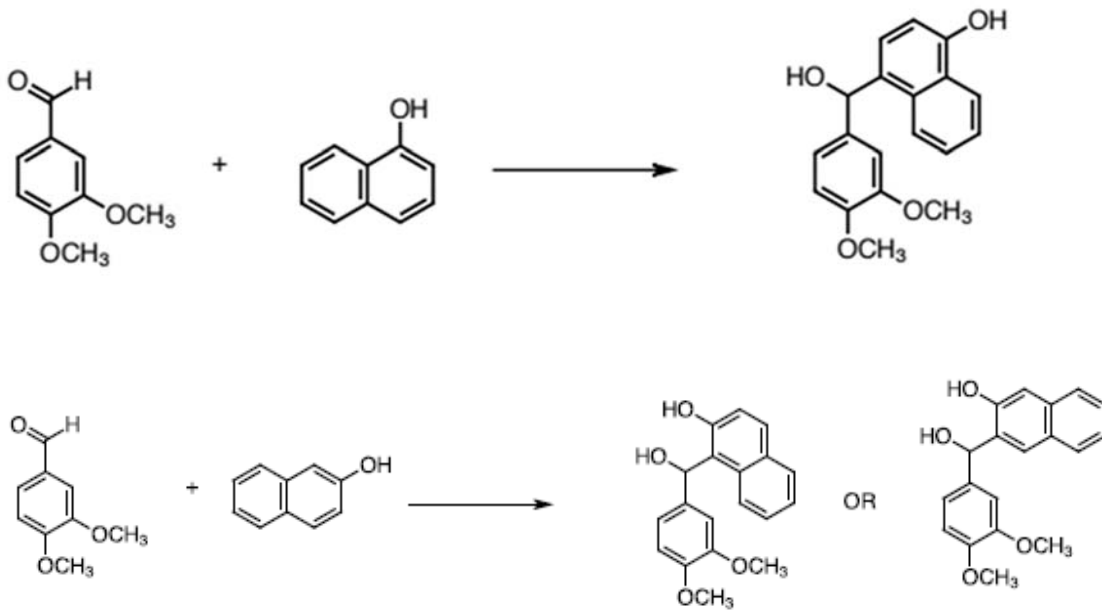
Similar to the reactivity of phenol, the 2-naphthanol reaction mechanisms show the covalent attachment at two ortho- positions, compared to 1-naphthanol with only one reactive site at the ortho- position.



Reaction of naphthanols at the unsaturated carbon bonds



Reaction of naphthanols with hydroxyl groups



Reaction of naphthanol with carbonyl groups

Figure 1.2. Reaction of 1-naphthanol (upper) and 2-naphthanol (lower) with unsaturated carbon bonds in lignin, hydroxyl and carbonyl portions of the lignin macromolecule

### 1.3.1.2 Molecular Weights of Purified Chemically Modified Lignins

Prior to  $^1\text{H}$  NMR measurements, gel permeation chromatography (GPC) was used to ensure purity of the lignin products by showing that the absence of unreacted phenol or naphthanol in the GPC traces, which indicated that they were removed from the product (an example of the removal of 1-naphthanyl acetate in GPC traces shown in Figure 1.3). The same GPC results were observed for the lignin samples chemically modified with phenol and 2-naphthanol, using phenyl acetate and 2-naphthanyl acetate as standards, respectively.

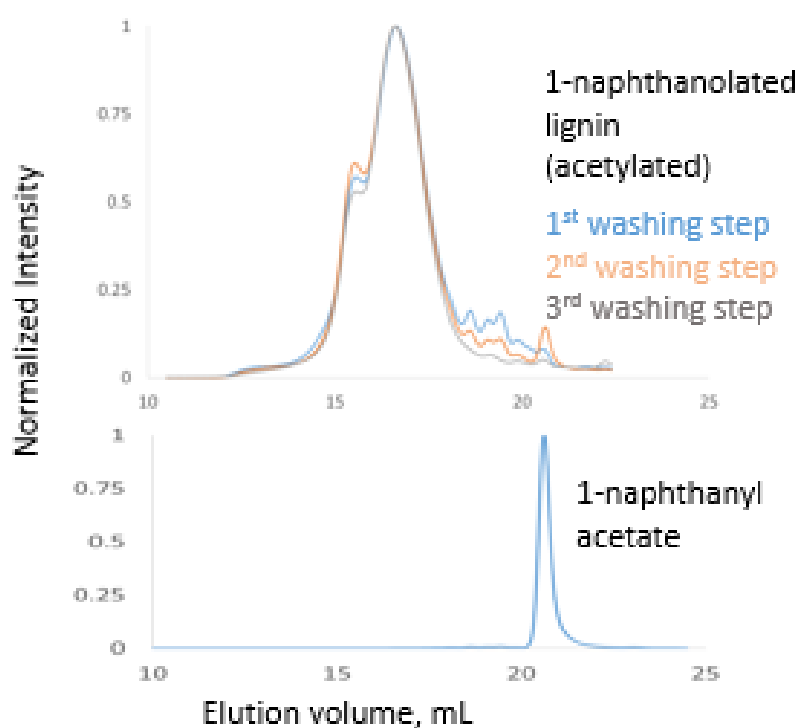


Figure 1.3. Gel permeation chromatograms showed the absence of unreacted naphthanol after three washing and precipitation steps of the product made in dioxane-water mixture.

GPC also measured the molecular weight of lignin and its polydispersity, PD, which is calculated as a ratio of the  $M_w$  (weight average molecular weight) to  $M_n$  (number average molecular weight), shown in Tables 1.1 and 1.2. Table 1.1 presented the lignin samples prepared at 2 hours reaction time at 90 °C while Table 1.2 shows the lignin samples prepared at increasing reaction time at 100 °C. For Table 1.1 the molecular weight of the SKL was not measured with the modified lignin samples because the GPC was used to detect the absence of unreacted phenols but not to compare with the molecular weight of the SKL as a starting material. In summary, both tables show that there are no significant changes in the molecular weights of the SKL after chemical modification.

Table 1.1 Chemical properties of softwood kraft lignin modified with phenols and naphthanols at 2 hours reaction time and 90 °C

Sample	Reaction time, hours	Degree of Substitution	Molecular weight		Polydispersity
			$M_w$	$M_n$	$M_w/M_n$
		moles of reactant per mole of C9 unit	g/mol	g/mol	
Softwood Kraft Lignin	0	0.00	not measured with these samples		
phenolated lignin	2	0.60	2800	3200	0.88
1-naphthanolated lignin	2	0.17	2600	3000	0.87

Table 1.2 Chemical properties of softwood kraft lignin modified with phenols and naphthanols at increasing reaction time at 100 °C

Sample	Reaction time, hours	Degree of Substitution	Molecular weight		Polydispersity
			M <sub>w</sub>	M <sub>n</sub>	M <sub>w</sub> /M <sub>n</sub>
		moles of reactant per mole of C <sub>9</sub> unit	g/mol	g/mol	
Softwood Kraft lignin	starting material	0.00	1900	1100	1.7
phenolated lignin	1	0.12	2400	700	3.4
	2	0.09	2800	1700	1.6
	4	0.10	2800	2100	1.3
	8	0.15	2800	2300	1.2
1-naphthanolated lignin	4	0.02	3250	3100	1.0
	8	0.07	3500	3250	1.1
2-naphthanolated lignin	4	0.24	3500	3250	1.1
	8	0.29	3200	2900	1.1
control (no reactant)	1	not applicable	2800	2400	1.2
	4	not applicable	1600	500	3.2
	8	not applicable	2800	2400	1.2

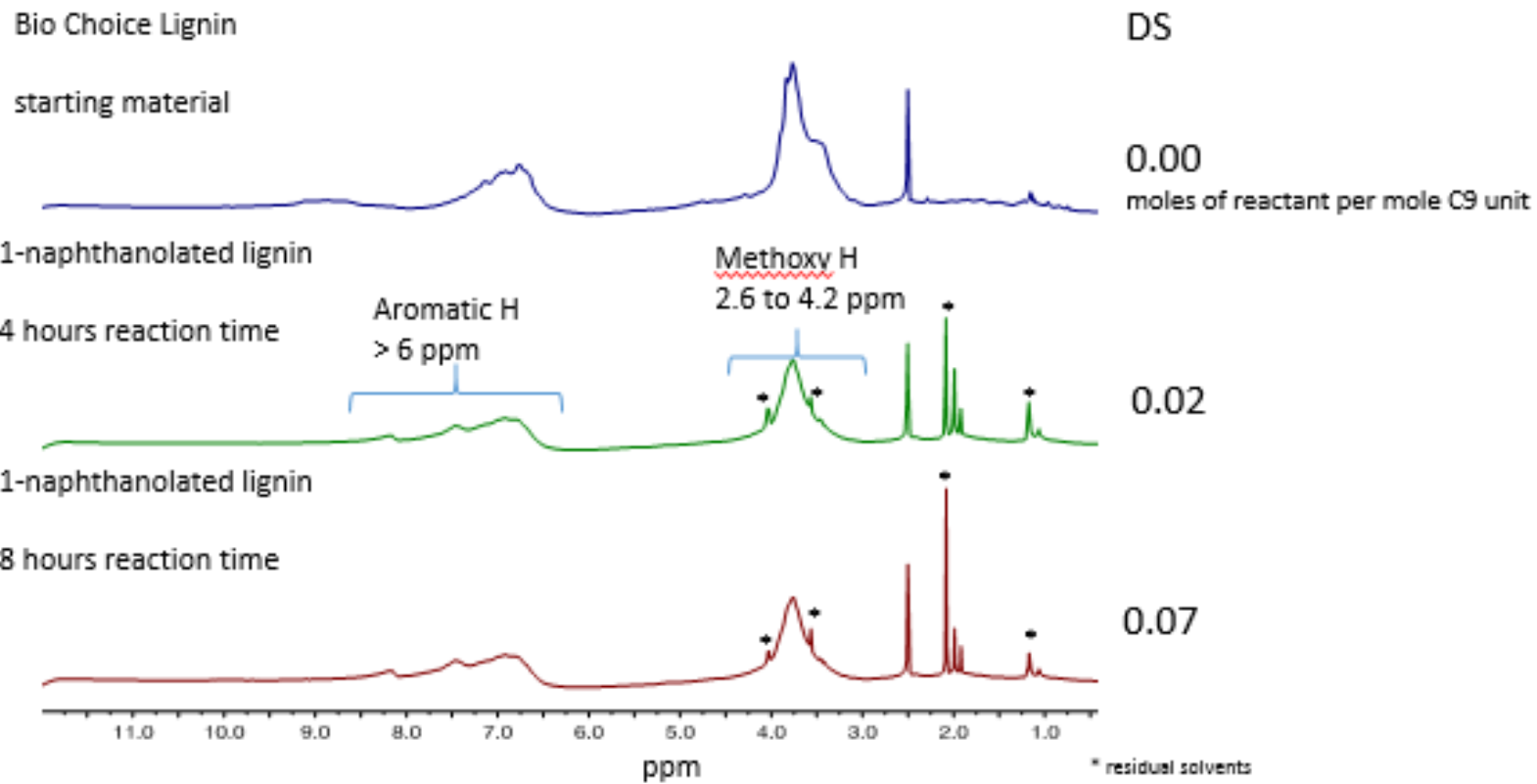
As shown in Tables 1.1 and 1.2, the range of molecular weights in this study for chemically modified lignins were  $M_w$ : 2400 to 3500 g/mol and  $M_n$ : 700 to 3250 g/mol. These ranges of  $M_w$  and  $M_n$  values were similar to acetylated softwood kraft lignin from size exclusion chromatography:  $M_n = 2350$ ,  $M_w = 3600$  and  $PD = 1.5$  and from MALDI-TOF :  $M_n = 2320$ ,  $M_w = 3770$  and  $PD = 1.6$  (Gellerstedt, 2015). The molecular weight ranges of these phenolated or naphthanolated lignin samples from GPC was expected to show slightly higher range of values than the SKL ( $M_w = 1900$ , and  $M_n = 1100$ ) and lignins with the addition of the phenol or naphthanol. Chemically modified SKL were also expected to have a lower range of  $M_w$  and  $M_n$  than unmodified lignin from biorefinery residues:  $M_w = 6500$  to 37800 g/mol,  $M_n = 1300$  to 2800 g/mol (Leskinen, Kelley, & Argyropoulos, 2015) because of the cleavage of the chemical bonds in SKL after processing. The molecular weight of the softwood Kraft lignin reported in the literature ranges from 1600 to 7050 g/mol (shown on Table 1.3). The molecular weight of SKL from this study are not comparable with the  $M_w$  and  $M_n$  values of SKL and its derivatives due to differences in the methods used to measure molecular weight, and the purification and isolation method for the softwood lignin samples.

Table 1.3 Molecular weights of SKL reported in the literature

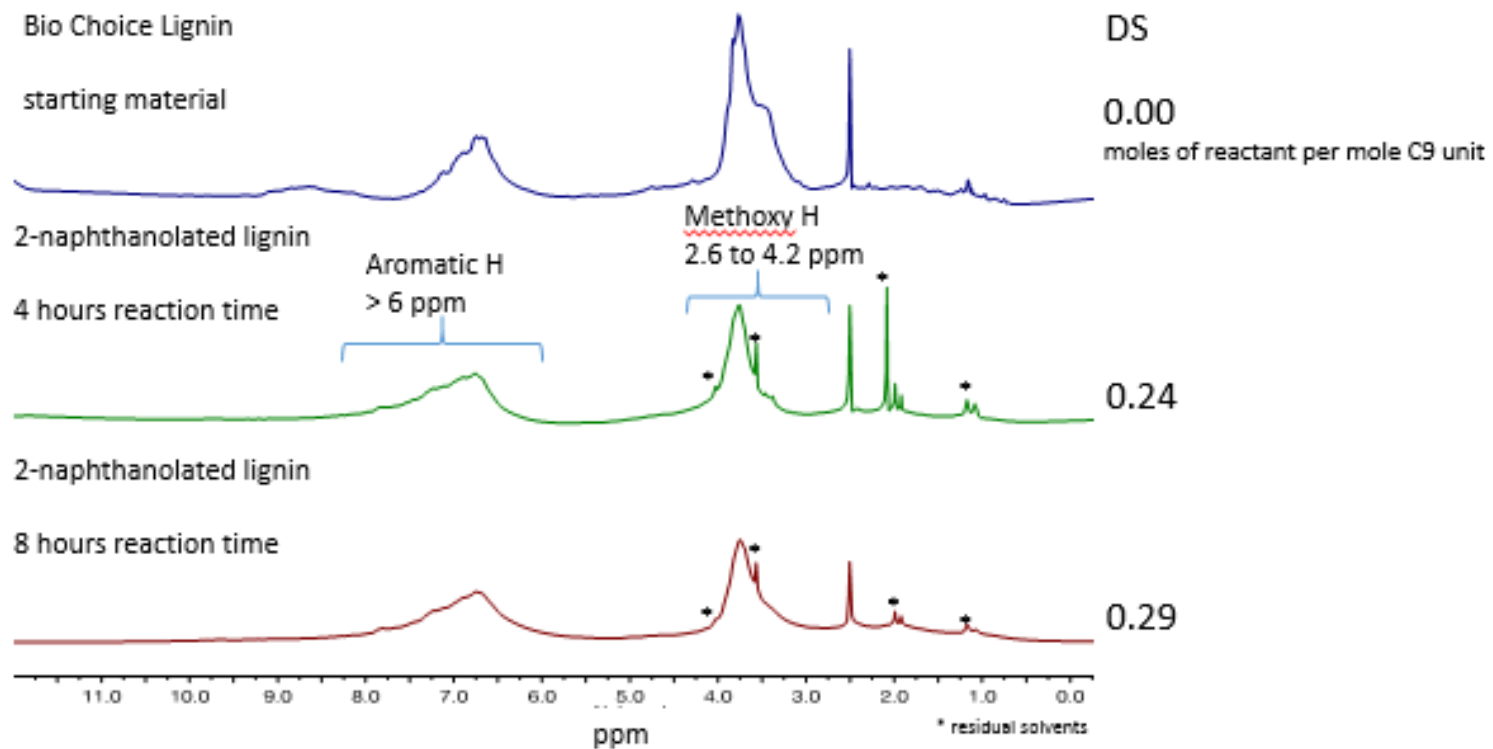
Material	Source	Molecular Weight		Reference
		M <sub>w</sub> , g/mol	M <sub>n</sub> , g/mol	
<hr/>				
Starting material				
<hr/>				
Kraft lignin	softwood	7050	1860	(Banu, El-Aghoury, & Feldman, 2006)
	softwood	1600	not reported	(Ayoub, Venditti, Jameel, & Chang, 2014)
	softwood	3100	1820	(Jacobs & Dahlman, 2000)
	softwood (Indulin AT)	3400	1340	(Jacobs & Dahlman, 2000)
<hr/>				

### 1.3.1.3 Degree of Substitution from $^1\text{H}$ NMR

After the reaction and purification steps, the degree of substitution (DS) was determined on the products based on the NMR results, calculated as the moles of reactant per mole of  $\text{C}_9$  unit using equations in Figure 1.1. Degree of substitution (DS) from  $^1\text{H}$  NMR spectra showed increases in aromatic H peak intensities attributed to the reaction of the phenol or naphthanol.  $^1\text{H}$  NMR spectra of the naphthanolated lignin samples with the corresponding DS values, are shown in Figure 1.4. The  $^1\text{H}$  NMR of the other lignin samples are shown in Figures 1.5 and 1.6. During peak integration, the DS was calculated relative to the methoxy peak with an intensity set to 1. Methoxy peaks from 2.6 to 4.2 ppm also showed different peak sizes in these  $^1\text{H}$  NMR spectra, because the  $^1\text{H}$  NMR spectra were not the baseline corrected and phase corrected in the same manner, resulting in a stack plot that is not drawn to scale. Thus, the DS were calculated from the peak intensities of the aromatic H and methoxy H. Residual solvent peaks were identified with asterisks and their peak intensities were not included in the calculation of the DS. Figure 1.5 shows the DS values for SKL modified for 2 hours reaction time. Figure 1.6 shows similar spectra were observed for SKLs modified with phenol at 1 and 2 hours reaction time. The DS values and percent mass addition of the hydroxylated aromatic compounds were summarized on Table 1.4.



(a) 1-naphthanolated lignin



(b) 2-naphthanolated lignin

Figure 1.4 <sup>1</sup>H NMR of Softwood Kraft lignins modified with naphthanol made in dioxane-water mixtures at increasing reaction time

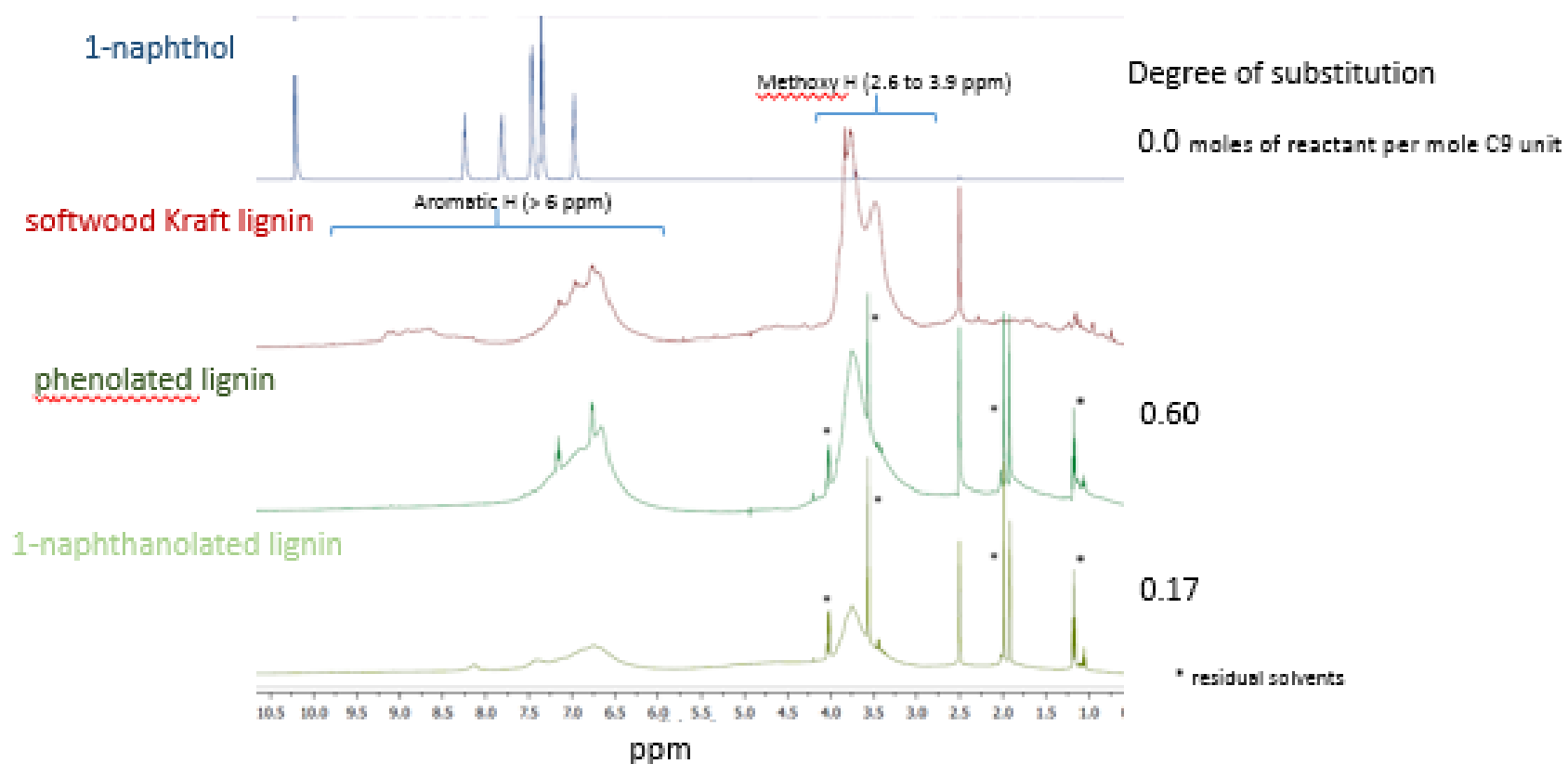


Figure 1.5  $^1\text{H}$  NMR of Softwood Kraft Lignins modified with naphthanol and phenol made in dioxane-water for 2 hours of reaction time.

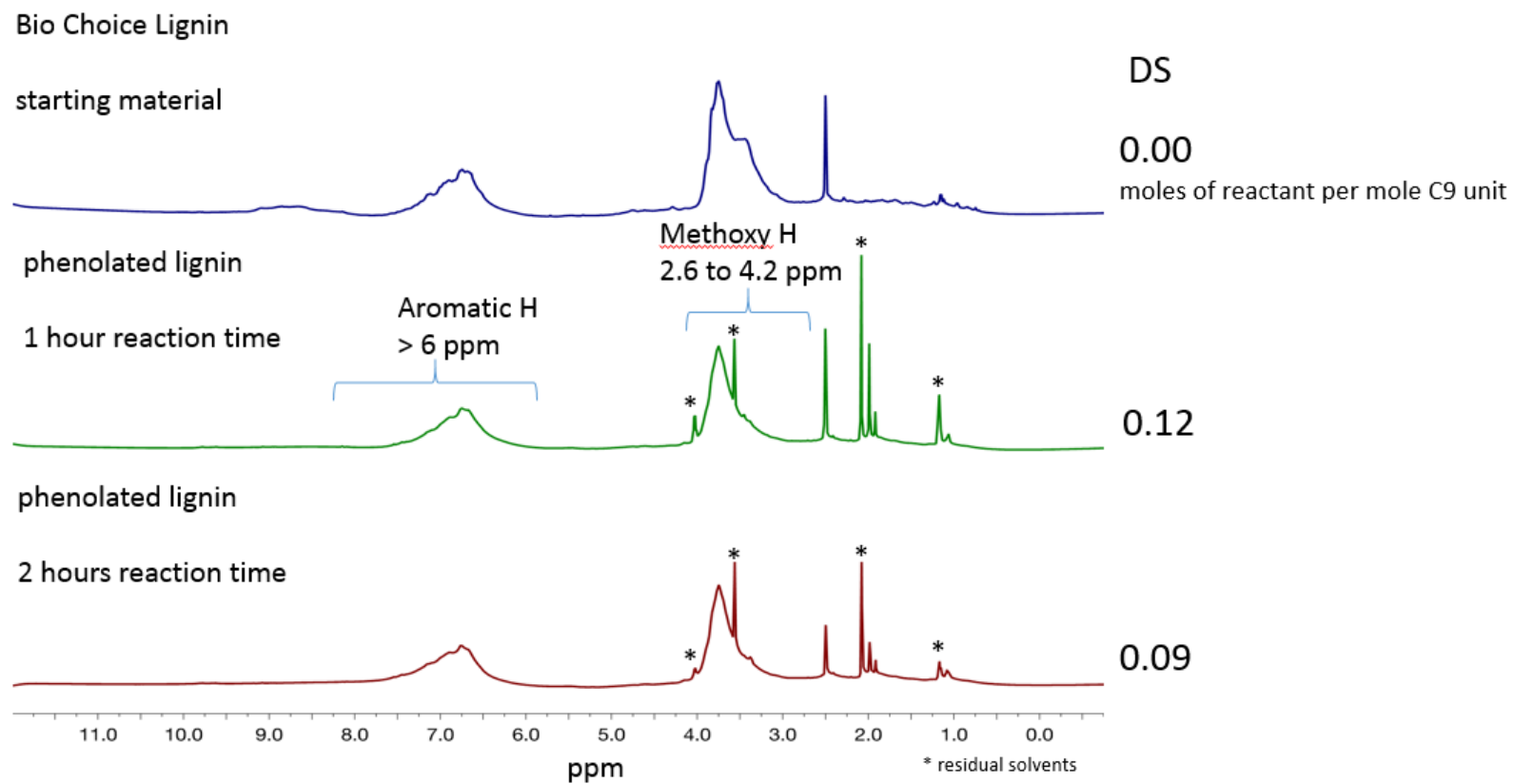


Figure 1.6  $^1\text{H}$  NMR of Softwood Kraft Lignins modified with phenol at 1 and 2 hours.

Table 1.4 Degree of substitution of the chemically modified lignin and percent mass addition at increasing reaction times (calculated using equations in Figure 1)

Sample	Reaction time, hours	Degree of	% mass addition
		Substitution	% mass of reactant added
moles of reactant per mole of C <sub>9</sub> unit			
Softwood Kraft			
lignin	0	0.00	0.0
phenolated			
lignin	1	0.12	5.7
	2	0.09	4.4
	4	0.10	5.0
	8	0.15	6.9
1-			
naphthanolated			
lignin	4	0.02	1.8
	8	0.07	5.1
2-			
naphthanolated			
lignin	4	0.24	16.0
	8	0.29	18.4

As shown in Figure 1.5, the degree of substitution of phenolated lignin (0.60) is higher than the 1-naphthanolated lignin (0.17) made for 2 hours reaction time because phenol has less steric hindrance and two ortho- reactive sites, compared to 1-naphthanol. The 1-naphthanol molecule is a larger molecule with steric hindrance and one ortho- reactive site for nucleophilic aromatic substitution. In the second set of reactions, the 1-naphthanol show lower DS values (0.02 and 0.07), compared to DS values of phenol (0.10 to 0.15) for both 4 and 8 hours ( $^1\text{H}$  NMR of phenolated lignin in Figure 1.4. The DS values for the phenolated lignin (0.60 versus 0.09) at 2 hours reaction time from each set of data were different, probably because of their reaction temperatures (90 versus 100 °C) and limitations of using quantitative  $^1\text{H}$  NMR for expressing the DS, based on peak intensities which are arbitrarily assigned during NMR peak integration. These sets of samples gave contradictory results because lignin is a heterogeneous three-dimensional complex structure, which can have variations in the available sites for incorporation of these hydroxylated aromatic compounds.

Figure 1.7 shows the trends in degree of substitution with increasing reaction time. Increasing the reaction time resulted in different trends in the degree of substitution for the lignin samples

chemically modified with phenol and naphthanols.

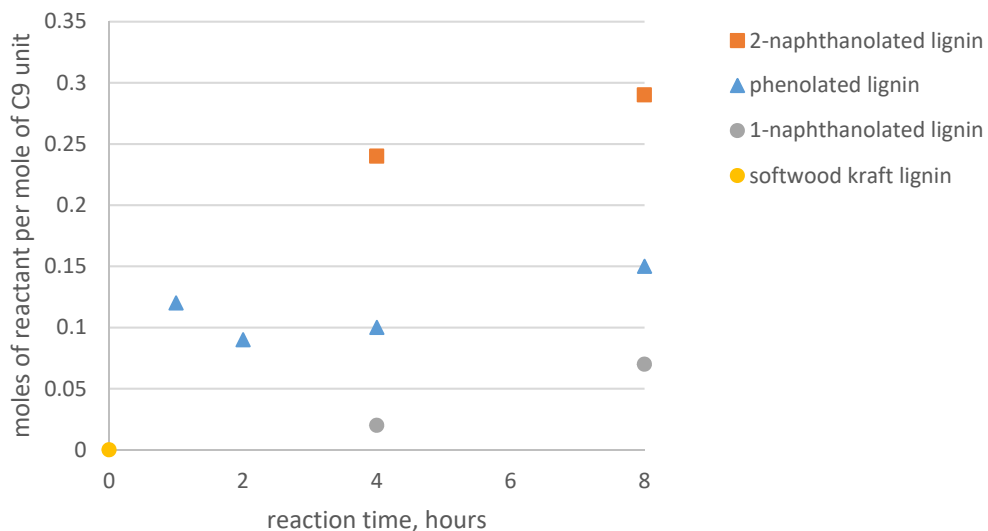


Figure 1.7 Degree of substitution versus reaction time for different chemical modifications at 100 °C.

Both sets of DS data showed phenolated lignin had a higher degree of substitution than 1-naphthanolated lignin. The 2-naphthanolated lignin had the highest DS, followed by phenolated then 1-naphthanolated lignin. For 1-naphthanolated lignins, increasing the reaction time from 4 to 8 hours slightly increased the degree of substitution from 0.02 to 0.07. However, for phenolated lignin, increasing the reaction time from 1 to 8 hours did not significantly change the degree of substitution with comparable DS values from 0.09 to 0.15. For the 2-naphthanolated lignin increasing the reaction time from 4 to 8 hours slightly increased the degree of substitution from 0.24 to 0.29. The 2-naphthanolated lignin had a higher DS than the 1-naphthanolated lignin because the 2-naphthanol had two ortho- reactive positions whereas the 1-naphthanol has only one ortho- reactive position (shown in the reaction mechanisms in Figure 1.2). With an activating group (such as an alpha carbon in the lignin chemical structure), the attack at the ortho-position is faster than the attack at the para- position because of the relatively large

Coulombic population, based on the electron population in the hydroxylated aromatic compound such as phenol or naphthanol (Fleming, 2010). This result is in agreement with a study phenolated lignosulfonates study (Alonso et al., 2005), in which  $^1\text{H}$  NMR showed that the addition of phenol at the ortho- position predominates over the para- position.

#### 1.3.1.4 Principal Component Analysis of FT IR spectra

Fourier Transform Infrared Spectroscopy (FT IR) spectra was used to detect changes in functional groups. The FT IR of the lignin samples are shown on Figure 1.8, to identify bands from 4000 to 850  $\text{cm}^{-1}$  that are compared with the FT IR band assignments for SKL and phenolated lignins, reported in the literature. These FT IR spectra of SKL, phenolated and naphthanolated lignin were baseline corrected and normalized. Table 1.5 listed FT IR band assignments on the observed bands in the lignin samples in this study, which are compared with the FT IR band assignments reported in the literature for softwood Kraft lignin and phenolated lignin. This list shows band assignments that are commonly found in each lignin sample: O-H stretching (phenolic  $-\text{OH}$  and aliphatic  $-\text{OH}$ ), non-conjugated carbonyl and aromatic skeleton (stretching vibration). However, the FT IR methods used in these studies should be noted since a comparison of band assignments from the reported values in the literature and observed bands in this study are different because of the differences in the FT IR methods used. Although different FT IR methods were used, the band assignments have been reported to be similar for the wave numbers of known functional groups in the molecular structure of lignin, such as phenolic  $-\text{OH}$  and aromatic groups. These literature values of the band assignments for SKL were the basis for interpreting the Principal Component Analysis (PCA) plots.

Table 1.5 FT IR band assignments on softwood Kraft lignin and phenolated lignin reported in the literature

Observed bands	Band assignment	Soft-wood Kraft Lignin	Soft-wood Kraft Lignin	Soft-wood Kraft lignin	Phenolated lignin	Phenolated lignin
3366	O-H stretching (phenolic -OH and aliphatic -OH)	3436	3420-3405	3349		
1705	Non-conjugated carbonyl	1701	1705-1715	1704	1703	
1590	Aromatic skeleton (stretching vibration)+ C=O stretching	1598	1600	1594	1600	
1511	Aromatic skeleton (stretching vibration)	1511	1515	1513	1510	
1453	CH <sub>3</sub> + CH <sub>2</sub> (d-asymmetric C-H vibration)		1460	1463	1460	
-	aromatic skeleton (st C-C vibration)		1425			1415
1368	non-etherified phenolic -OH groups		1365			
1210	C-O of guaiacyl (G) ring (st C-O vibration)	1266	1270	1269		
1210	C-C + C-O stretch / phenolic OH + ether (st C-O(H) + C-O (Ar)	1212	1220	1214	1218	
1145	guaiacyl C-H and syringyl C-H / aromatic C-H on-plane deformation in the guaiacyl ring	1146	1125	1150		
1031	aromatic C-H in plane deformation (G > S) / 1st order aliphatic ether (st C-O(H) + C-O) vibration)	1034	1030	1031		1033
853	G (d op Ar C-H)		855			
	Reference:	Awal and Sain (2011)	Mondragon et.al. (2007)	Kadla and Kubo (2005)	Wu Ji-Fu et.al. (2014)	Li Hong-biao et.al. (2009)

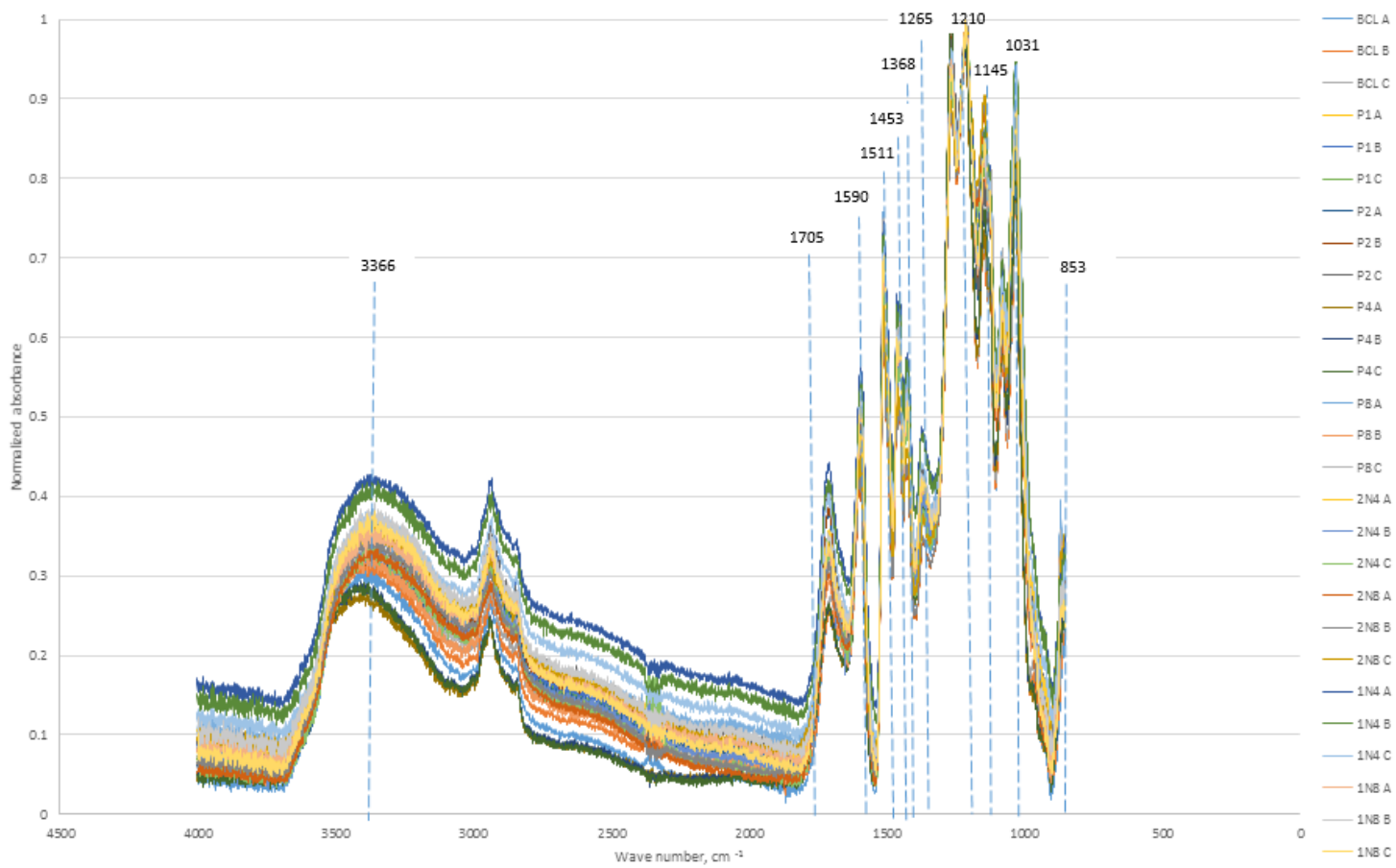


Figure 1.8 FT IR bands of lignin samples that were identified from IR band assignments reported in the literature

For each batch of lignin samples (BCL, P, 1N and 2N) prepared at increasing reaction times (1,2,4 and 8 hours), A, B, and C are the designated FT IR spectra from 3 aliquots tested separately. Figures 1.9 and 1.10 show the FT IR of BCL compared with that of phenolated and naphthanolated lignin samples. The differences were observed in intensities of the normalized absorbances at wave numbers corresponding to –OH stretching for aromatic and aliphatic -OH ( $3366\text{ cm}^{-1}$ ) but no differences in the aromatic skeleton stretching vibrations ( $1511\text{ cm}^{-1}$ ). In Figure 1.9 the FT IR spectra of phenolated lignin samples, P8 A, P1A and P2A (blue, orange and gray lines, respectively) show increased absorbances at the  $3366\text{ cm}^{-1}$  compared to that of BCL (black line) indicated more phenolic groups from phenol added to the lignin structure.

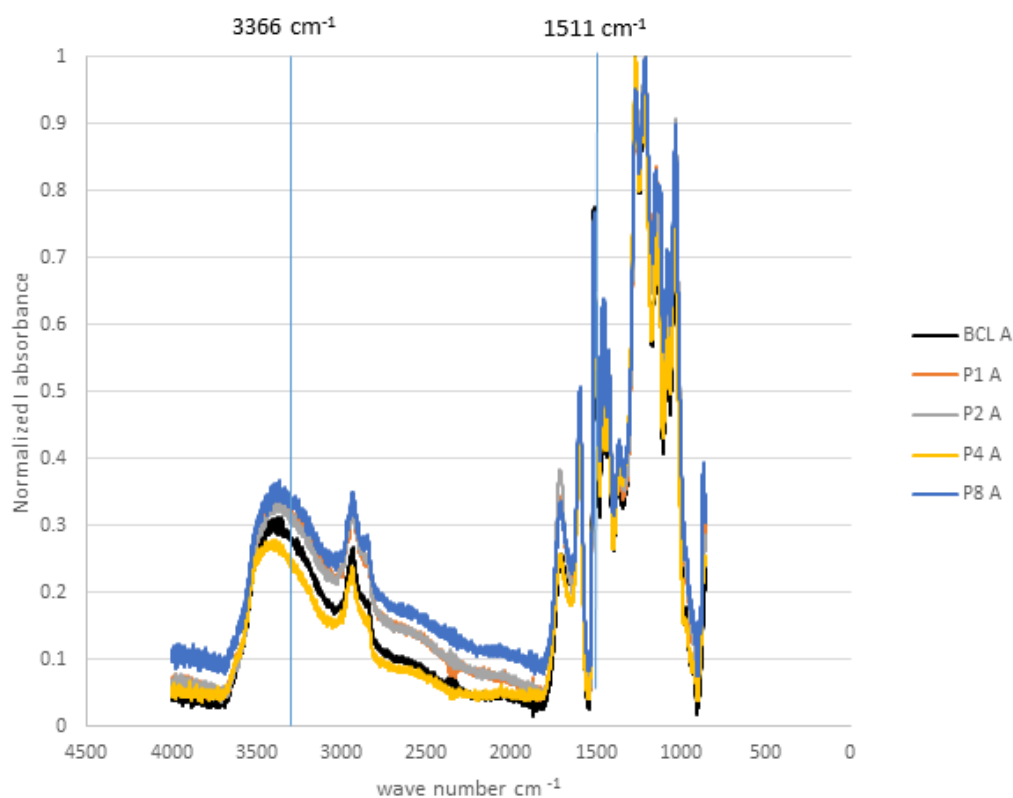


Figure 1.9 FT IR spectra of Bio Choice Lignin (BCL) and phenolated lignin samples (P1, P2, P4 and P8 are prepared at 1,2,4 and 8 hours reaction time, respectively)

Similarly, in Figure 1.10, the FT IR spectra of naphthanolated lignins samples, 1N4 A, 1N8 A, 2N4 A and 2N8 A (yellow, blue, orange and gray lines, respectively) show higher absorbances at  $3366\text{ cm}^{-1}$  compared to that of BCL (black line). These results also indicated an increase in the phenolic groups in the naphthanolated lignin samples.

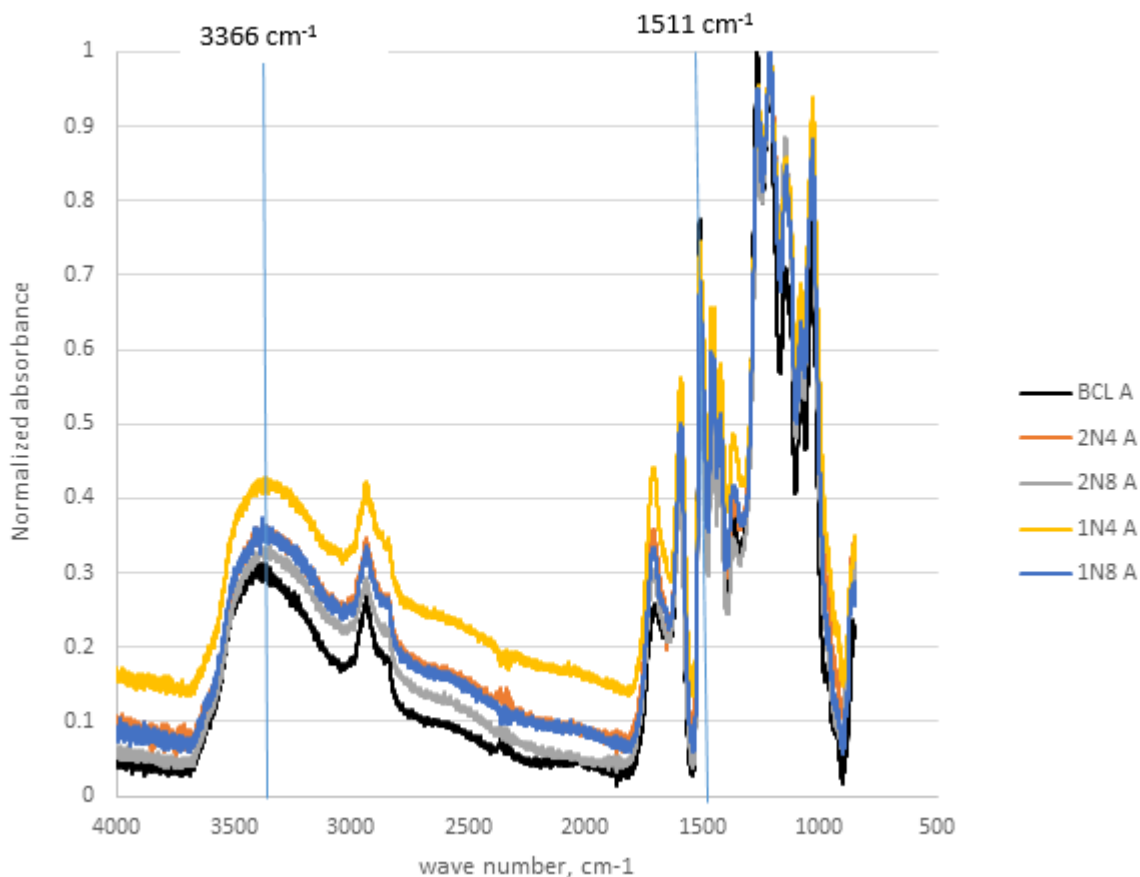


Figure 1.10 FT IR spectra of Bio Choice Lignin (BCL) and naphthanolated lignin samples (2N4 and 2N8 were 2-naphthanolated lignin samples prepared at 4 and 8 hours reaction time, respectively; 1N4 and 1N8 were 1-naphthanolated lignin samples prepared at 4 and 8 hours reaction time, respectively)

Figures 1.9 and 1.10 also showed no significant visual differences in the aromatic skeleton stretching vibrations ( $1511\text{ cm}^{-1}$ ), which indicated that there are no significant amounts of phenols or naphthanols added to the lignin chemical structure.

To quantitatively confirm the spectral differences over a range of wave numbers, principal component analysis (PCA) was used to statistically generate score plots and loading plots. Score plots show data points similar to each other and thus, can be grouped into clusters according to a principal component (PC), which is an FT IR observed band that corresponds to a band assignment in Table 1.5. For each batch of lignin samples (BCL, P, 1N and 2N) at increasing reaction times (1,2,4 and 8 hours), A, B, and C are the designated FT IR spectra from 3 aliquots tested separately. Figure 1.11 shows the PCA score plots for the spectral range of 4000 to 850  $\text{cm}^{-1}$  that have clusters of the phenolated lignins on PC-1 and PC-2 while the naphthanolated lignins and BCL are far from these principal components. Figure 1.12 shows the PCA loading plots for the FT IR lignin samples. However, outliers (shown as encircled dots on the scores plot) indicate errors in data collection or samples that have to be removed from the data set.

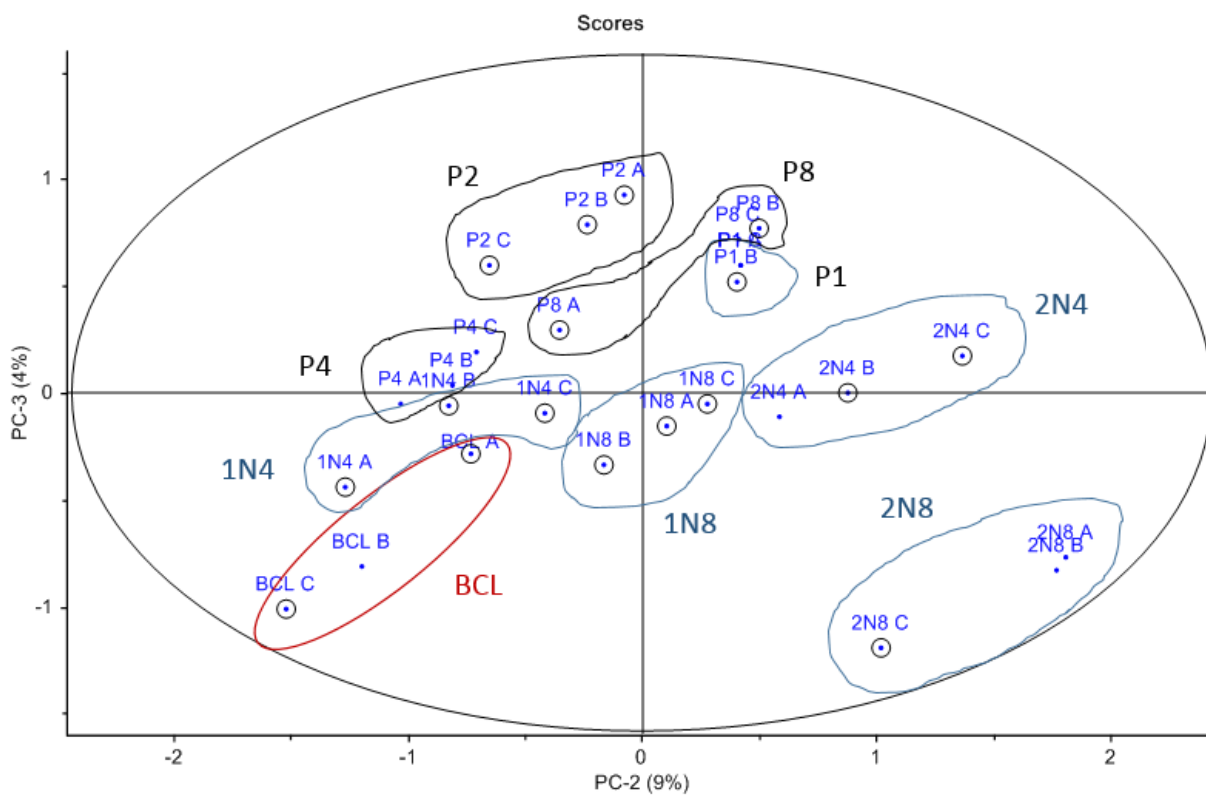
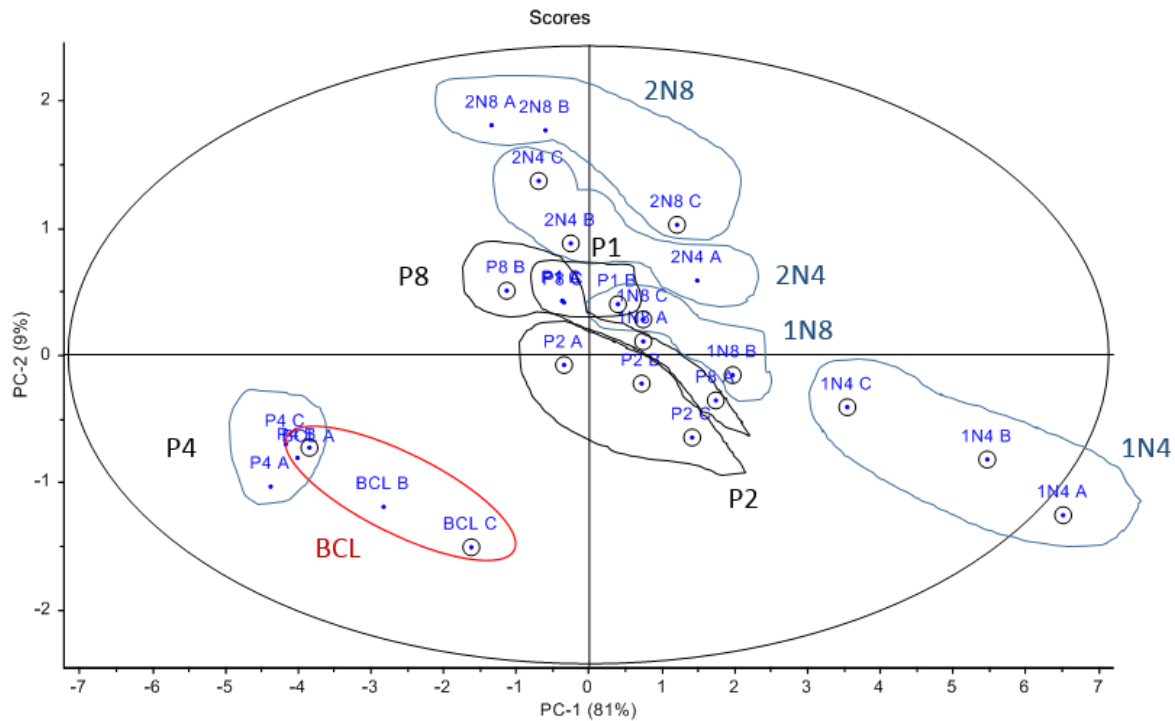
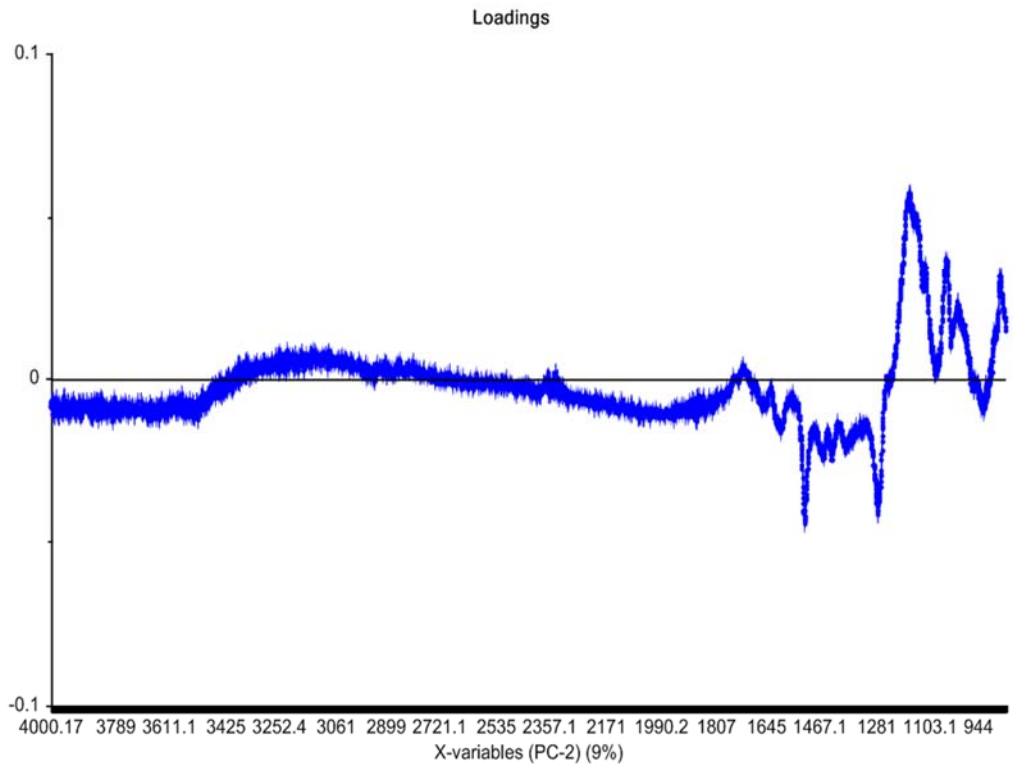
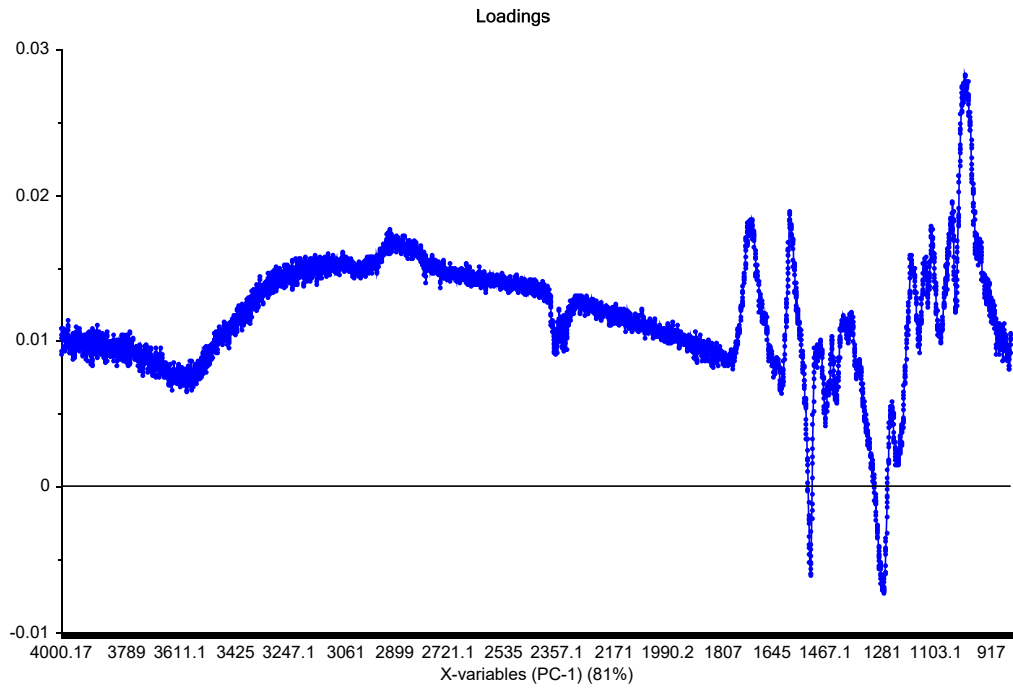


Figure 1.11 Principal Component Analysis (PCA) score plots for PC-1 (81%) versus PC-2 (9%); and PC-2 (9%) and PC-3 (4%) for FT IR of lignin samples from 4000 to 850  $\text{cm}^{-1}$ .



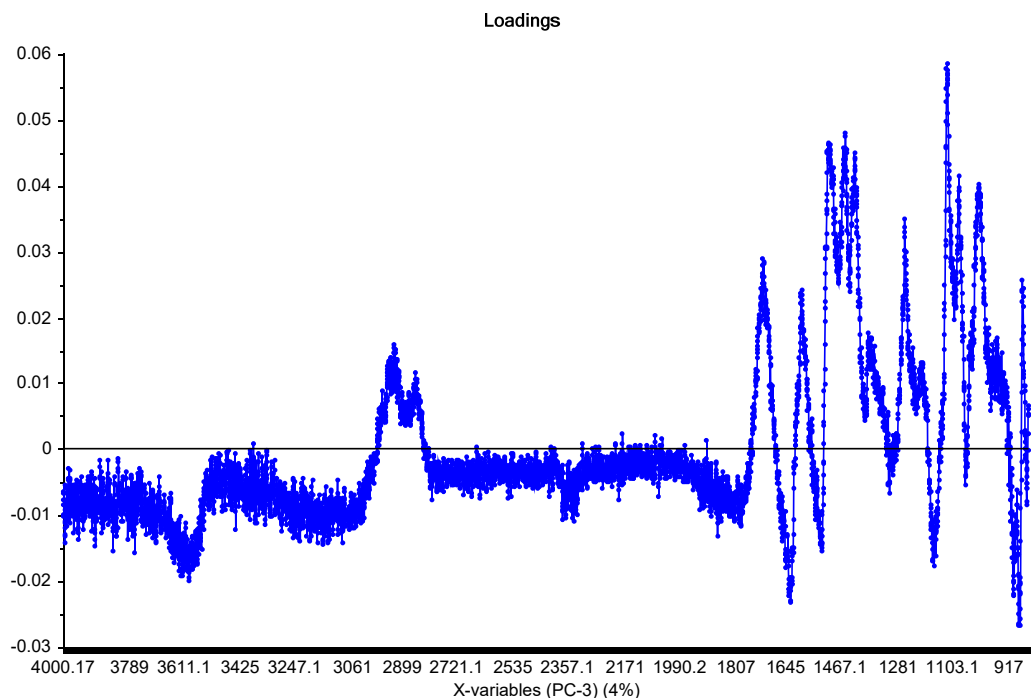


Figure 1.12 Principal Component Analysis (PCA) loading plots for X-variables for PC-1, PC-2 and PC-3 for the FT IR lignin samples from 4000 to 850  $\text{cm}^{-1}$

In a loadings plot, the X-variables (wave numbers) with large loadings (shown as large or broad peaks) are responsible for the greatest differences between the lignin samples. When the sum of the explained variances for the early two principal components (PC-1 and PC-2) are large (for instance 70 to 80 %), the score and loading plots show a large portion of the information in the data. Hence, the relationships between the groupings in the lignin samples and the large loadings in the wave numbers on the loadings plots are interpreted with a high degree of certainty.

However, if the sum of the explained variances for the other remaining principal components (PC-3, PC-4, PC-5 and so on) are lower (for instance, 10 to 20 %), little information from these score and loading plots may not be sufficient to explain the FT IR spectral differences in the lignin samples. The loadings plot for PC-1 (81%) show a broad peak at the range of 3611 to 2357  $\text{cm}^{-1}$  where there are O-H stretching vibrations corresponding to hydrogen bonding

interactions and sharp peaks from 1807 to 1281  $\text{cm}^{-1}$  corresponding to the aromatic skeleton stretching vibrations. PC-2 (9%) loading plot show high loadings from 1467 to 1103  $\text{cm}^{-1}$ , corresponding to the vibrations in the phenolic –OH groups with other groups such as guaiacyl and aromatic C-H groups. However, the score plot for PC-2 (9%) vs PC-3 (4%) showed PCs account for only 13 % of the variability. Overall, the PCA generated score plots show clusters of data points for phenolated lignin (P1, P2, P4 and P8), 1-naphthanolated lignin (1N8) and 2-naphthanolated lignin (2N4, 2N8) but not for BCL, P4 and 1N4. These clusters clearly differentiated from the starting material SKL from the chemically modified lignins. For the score plot of PC-1 vs PC-2, the 1N4 and 1N8 are different but 2N4 and 2N8 are similar based on the PC-1. Likewise, for PC-2 vs PC-3, 1N4, 1N8, 2N4 and 2N8 are different from each other based on PC-2. In the score plot for PC-1 versus PC-2, there are similarities between P4 and BCL. In comparison with the PCA results in studies on FT IR of biorefinery lignins (Leskinen et al., 2015), the PC-1 loading plots do not cross the x-axis, which is different from the loading plots shown on their study. The score plots revealed a large number of outlier data points (which were encircled) which would indicate the type of PCA model used would not be appropriate for these data sets.

### 1.3.2 Thermal Properties of Chemically Modified Lignins

#### 1.3.2.1 Weight losses during heating from Thermogravimetric analysis (TGA)

TGA of the lignin samples show the weight loss of samples over a range of temperatures, when these materials are thermally processed. The TGA curves were derived from the lignin samples heated from 40 to 700 °C. The TGA graphs in Figures 1.13 and 1.19 showed derived data where 100 weight % on the y-axis on the left was normalized at 105 °C when all volatile residual solvents are removed. The derivative weight (measured in weight%/ °C) on the y-axis on the

right, would remain the same regardless of the normalized values at 105°C. The derivative of the weight %/°C versus temperature showed peaks during drastic weight losses, and the highest peak shows a maximum change of weight % or weight loss at a temperature, labeled as  $T_{max}$ . The TGA curves are presented according to the samples taken from the same batch or samples taken at the same reaction time.

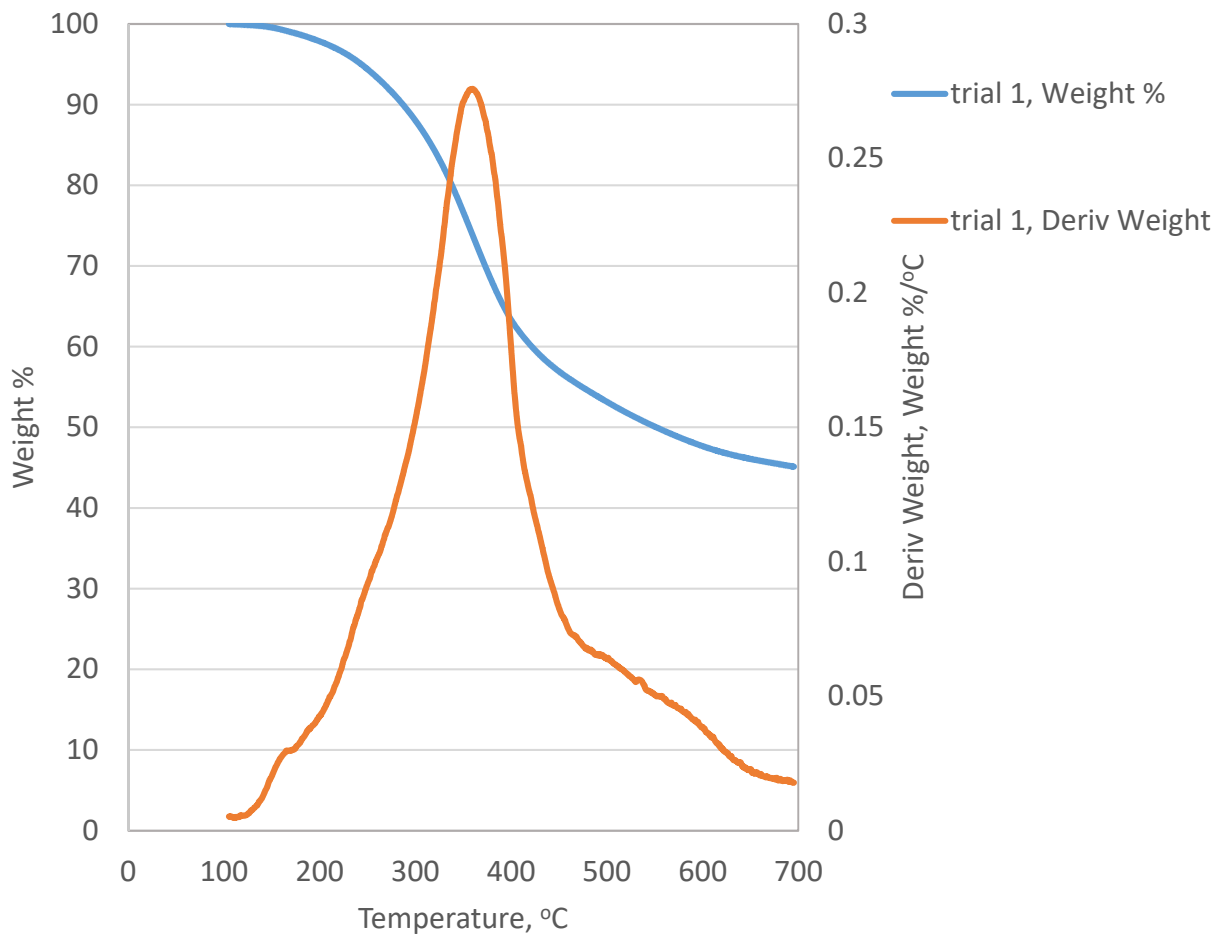


Figure 1.13 TGA curve of the softwood kraft lignin as a starting material

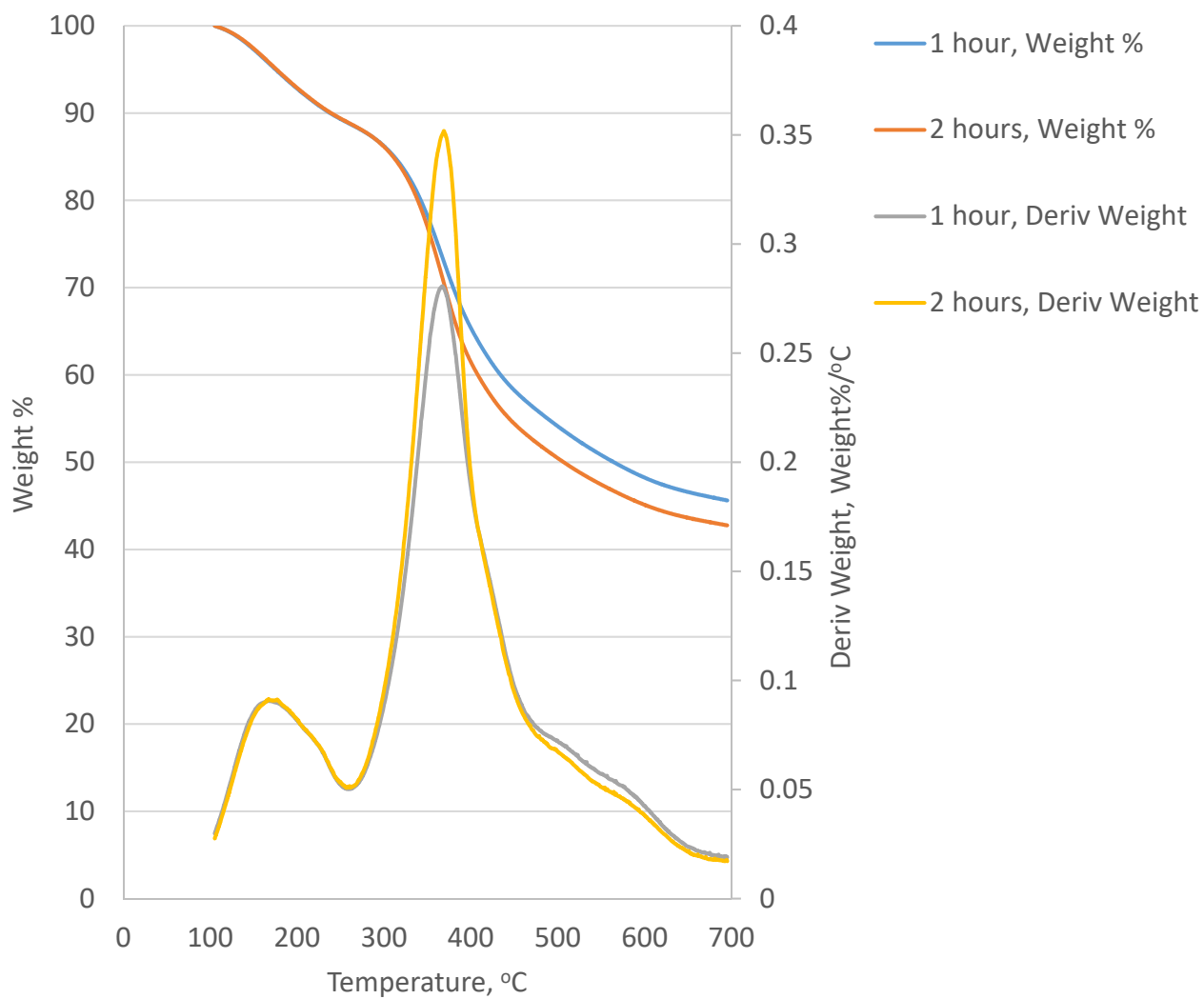


Figure 1.14 TGA curves of phenolated lignins made in 1 and 2 hours reaction time (sampled from the same reaction mixture)

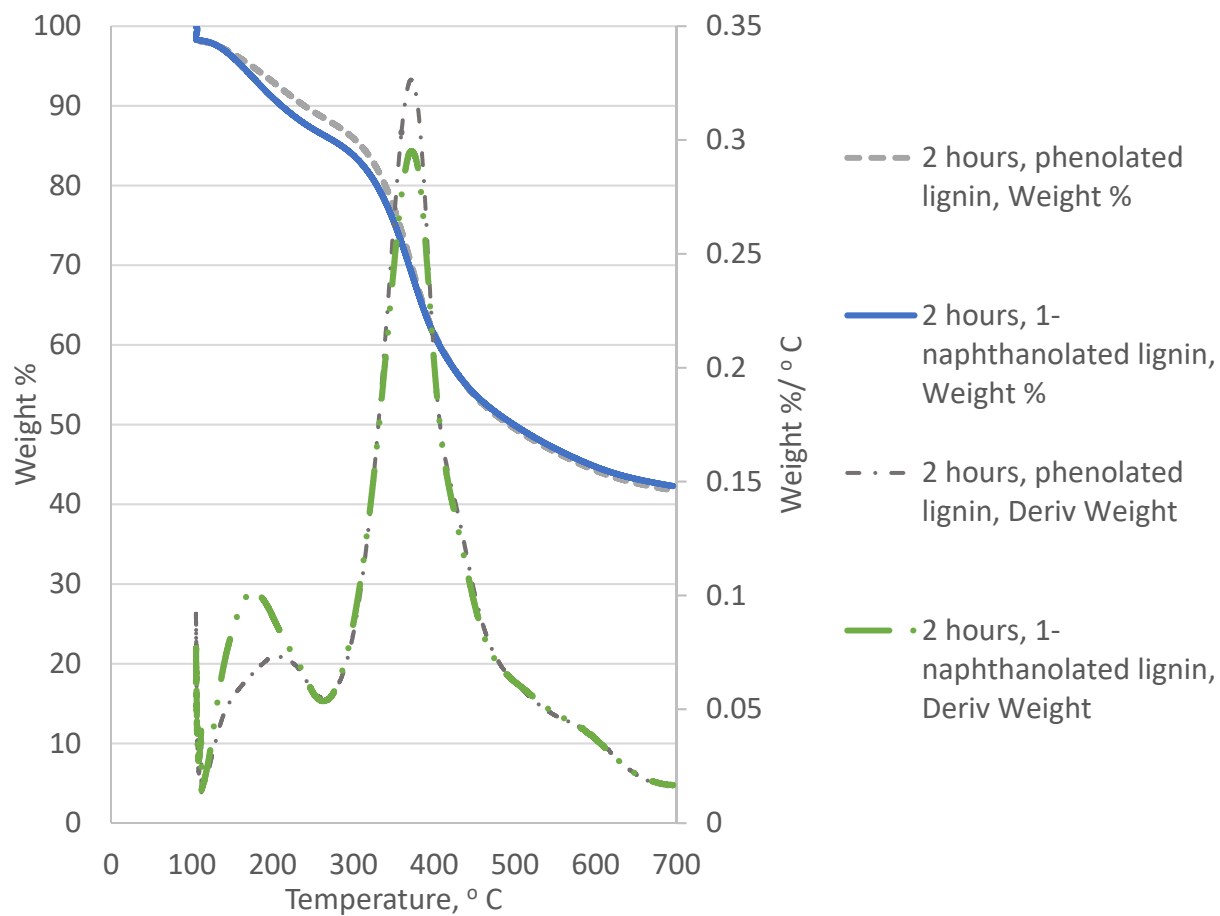


Figure 1.15 TGA curves of 1-naphthanolated and phenolated lignins made in 2 hours reaction time

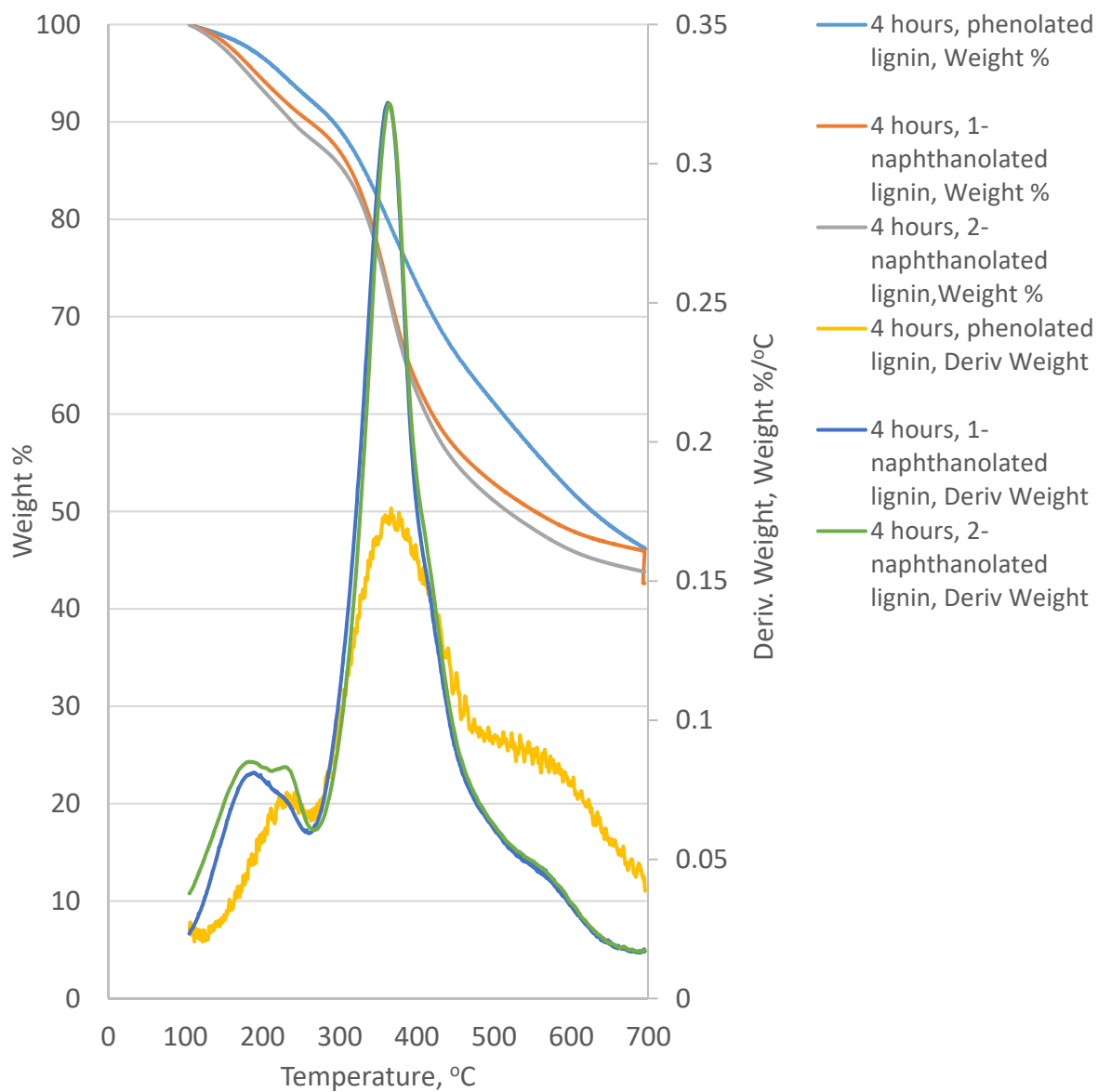


Figure 1.16 TGA curves of phenolated and naphthanolated lignins made in 4 hours reaction time

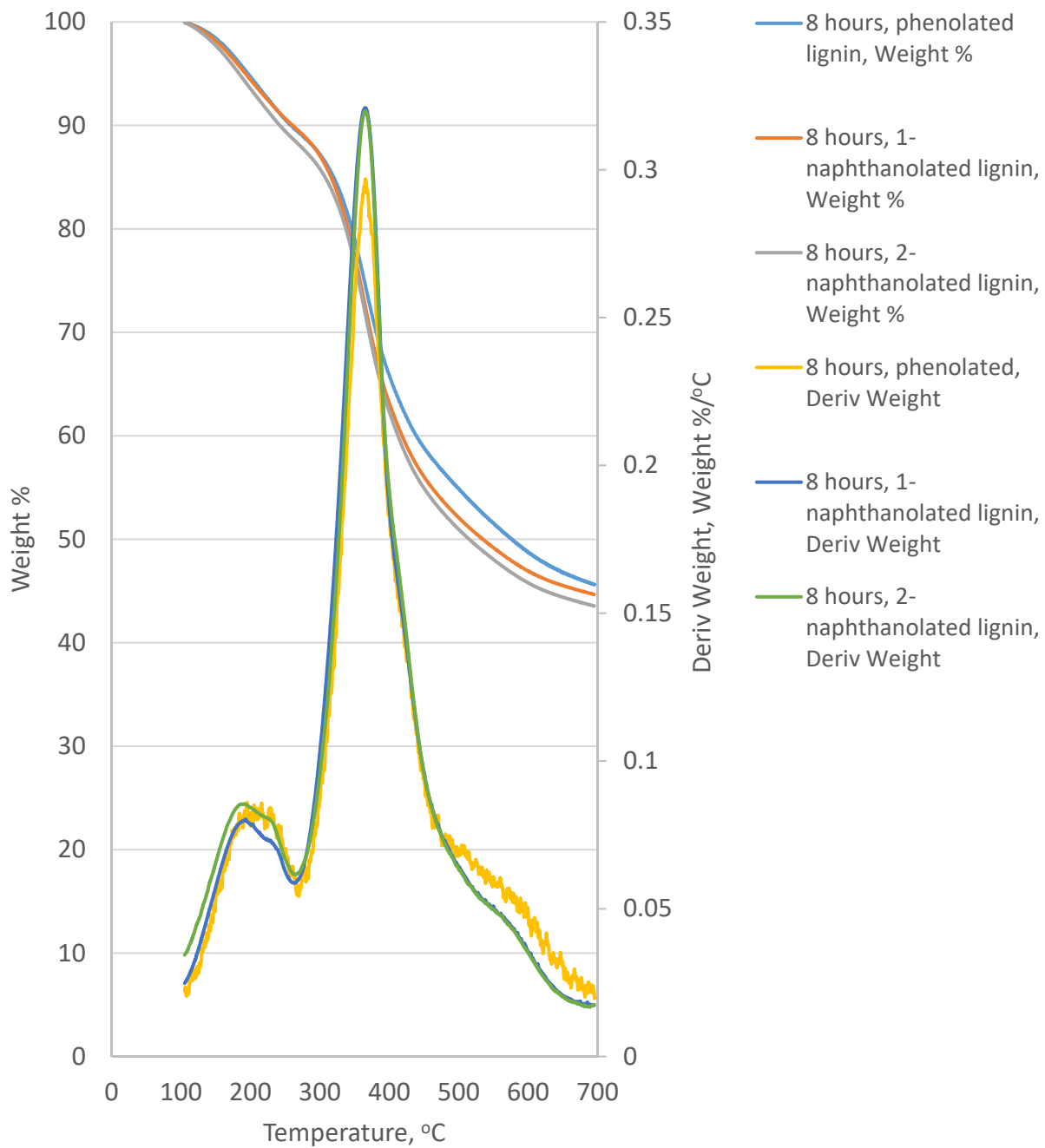


Figure 1.18 TGA curves of phenolated and naphthanolated lignins made in 8 hours reaction time

Table 1.6 shows the derived data from TGA of the chemically modified lignin samples prepared at increasing reaction times. The TGA data is derived from 105 to 700 °C (where the 100 weight % is set at 105 °C) on a tabulated form of the weight % versus temperature. Table 1.6 shows the lignin sample, reaction time,  $T_{max}$ , the weight % at the  $T_{max}$ , temperature at 5% weight loss, and the weight % at 700 °C.  $T_{max}$  is where the temperature has the highest value of weight %/°C and the weight % at  $T_{max}$  are derived from the tabulated TGA data from 105 to 700 °C (data not shown). The temperature at 5% weight loss is at 95 weight % from the tabulated TGA data (not shown) where there is significant thermal degradation and simultaneous evaporation of degradation products. The weight % at 700 °C is the residual mass when the samples reach the highest temperature and can be assumed to be the yield after carbonization under an inert atmosphere with an ash content less than 1%. The lignin samples were tested three times while the chemically modified lignins were only tested once because the TGA method to measure the weight % at 700°C was found to show reproducibility for lignin ( $45.2 \pm 0.4 \%$ ).

Table 1.6 TGA results (set at 100% at 105° C) for softwood kraft lignin and chemically modified lignin samples at increasing reaction time: maximum weight loss temperature,  $T_{max}$  (temperature at the highest weight %/°C), weight % at the  $T_{max}$ , temperature at 5% weight loss, and weight % at 700 °C of lignin samples

Sample	Reaction time, hours	Maximum Weight	Weight %	Temperature	Weight %
		loss temperature, $T_{max}$ ° C	at $T_{max}$	at 5% weight loss	at 700 °C
softwood kraft Lignin	none	365 ± 4	72 ± 3	220 ± 39	45.2 ± 0.4
phenolated lignin	1	367	74	175	46
	2	369	71	176	43
	4	366	79	224	46
	8	366	75	196	46
1-naphtholated lignin	4	362	73	192	43
	8	365	73	193	45
2-naphtholated lignin	4	364	72	181	44
	8	365	72	184	44
control (no reaction)	1	366	71	175	43
	4	364	76	179	49
	8	364	76	179	49

The  $T_{max}$  for the chemically modified lignin samples are comparable (362 to 369 °C) with the starting material, lignin (365 °C). The weight % values at  $T_{max}$  for the chemically modified lignin samples (71-79%) are comparable with the starting material, lignin (74%). The weight % at 700 °C for the chemically modified lignin samples are comparable (43 to 46 weight %) than

the lignin (45 weight %), which indicates no significant change in the yield when these materials are carbonized under an inert atmosphere up to 700 °C. The chemically modified lignin samples have comparable properties with the control lignin samples, which has a similar range of  $T_{\max}$  (364-366 °C), weight % at  $T_{\max}$  (71 to 76%) and show no significant differences in the weight % at 700 °C (43-49 %).

During the TGA of these samples, at 105 °C, the volatile solvents are evaporated (curves in Figures 1.13 to 1.18, values in Table 1.6), then from 105 to 700 °C, thermal degradation with the release of gaseous materials occur. The remaining amount at 700 °C is assumed to be fixed carbon with ash. A review of studies on thermal properties of lignin (Argyropoulos, Sen, & Patil, 2015) reported that the weight loss during the heating of Softwood Kraft lignin (SKL) from 150 to 300°C is due to the evaporation of the products from degradation of the phenylpropane side chains in the chemical structure of lignin. These degradation products are reported to be formic acid, formaldehyde, carbon dioxide, sulfur dioxide and water, which vaporize below 200°C and evolve as gases under an inert atmosphere (H. Yang, Yan, Chen, Lee, & Zheng, 2007) . In this study, the TGA derivative curves of phenolated and naphthanolated samples showed significant weight losses from 105 to 250 °C, compared to lignin with lower losses in the weight over this temperature range, shown in Figures 1.13 to 1.18. These hydroxylated aromatic compounds, which have similar phenolic structures with phenylpropane side chains in the lignin, might also be degraded in this temperature range.

The thermal properties in Table 1.6 suggest the operating temperatures, where these lignin materials would be thermally stable and not prone to thermal degradation into volatile fragments. The operating temperatures for fiber spinning should be below the temperature where there is 5% weight loss and the  $T_{\max}$ . The temperature at 5% weight loss sets an upper limit for thermal

processing conditions if the solvents in the materials were completely removed at 105 °C. The lower limit for thermal processing would be the glass transition temperatures, which were measured by differential scanning calorimetry (DSC).

#### 1.3.2.2 Glass Transition Temperatures from DSC

Differential scanning calorimetry (DSC) was performed to detect phase changes in the lignin during heating from 40 °C to as high as 220 °C, which is below the temperature of 5% weight loss and also below the  $T_{\max}$ . DSC detected the glass transition temperature,  $T_g$ , of the lignin-range molecular movement to a rubbery material with increased molecular mobility. DSC scans of the lignin sample showing how the  $T_g$  values and heat capacities were obtained in the first heating and cooling cycle are shown in Figures 1.19 to 1.22. These are DSC scans of lignin samples at 4 heating and cooling cycles with heating rate at 20 °C per minute from 40 °C to a set temperature with an isothermal hold at the end and rapid cooling to 40 °C. Heat capacities measured at W/g are converted to J/g °C using the heating rate at 20°C per minute. The DSC scans are presented in Figure 1.20 to 1.22 for the lignin samples made for 8 hours, which showed the highest degrees of substitution.

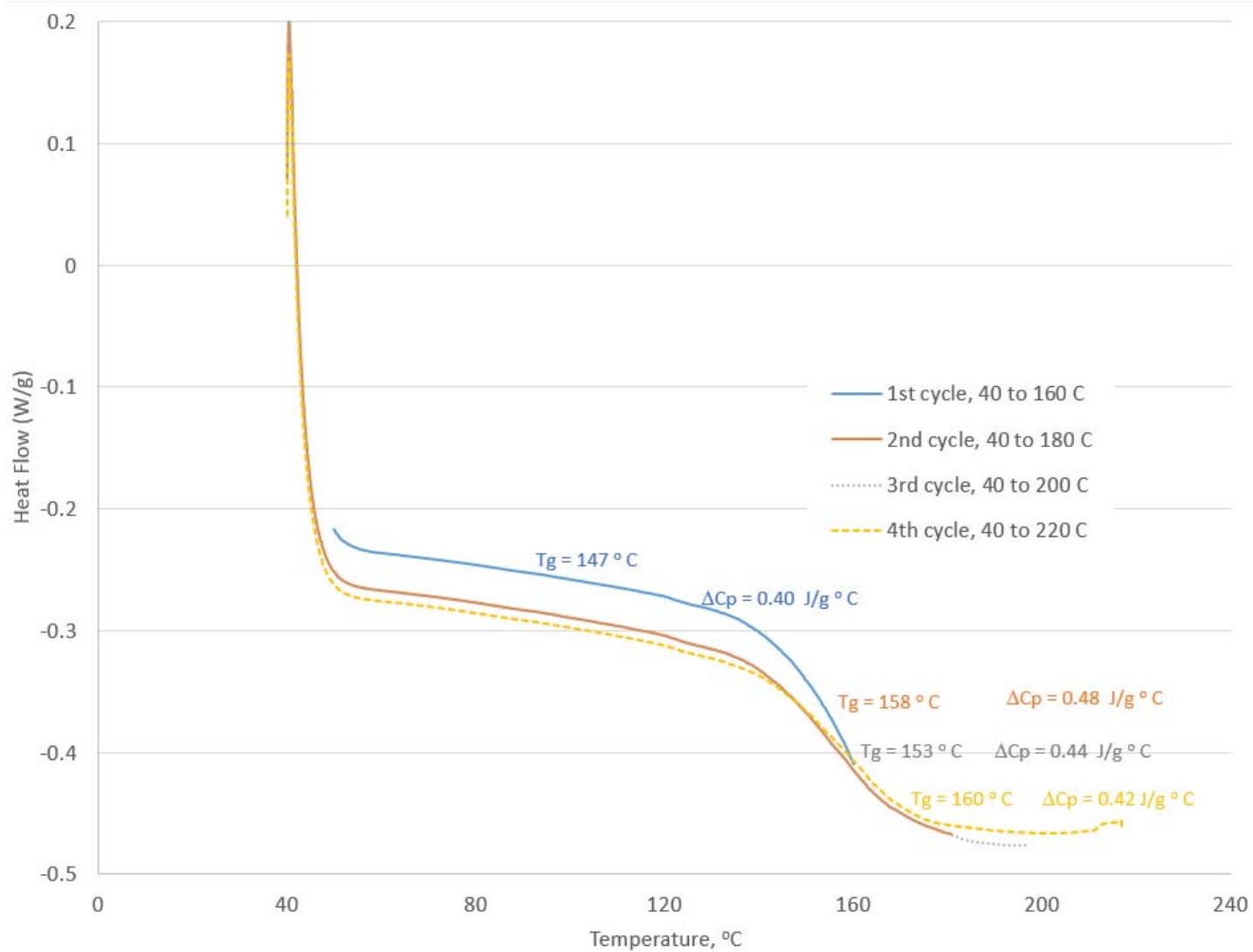


Figure 1.19 DSC scan of softwood kraft lignin showing the T<sub>g</sub> at each cycle

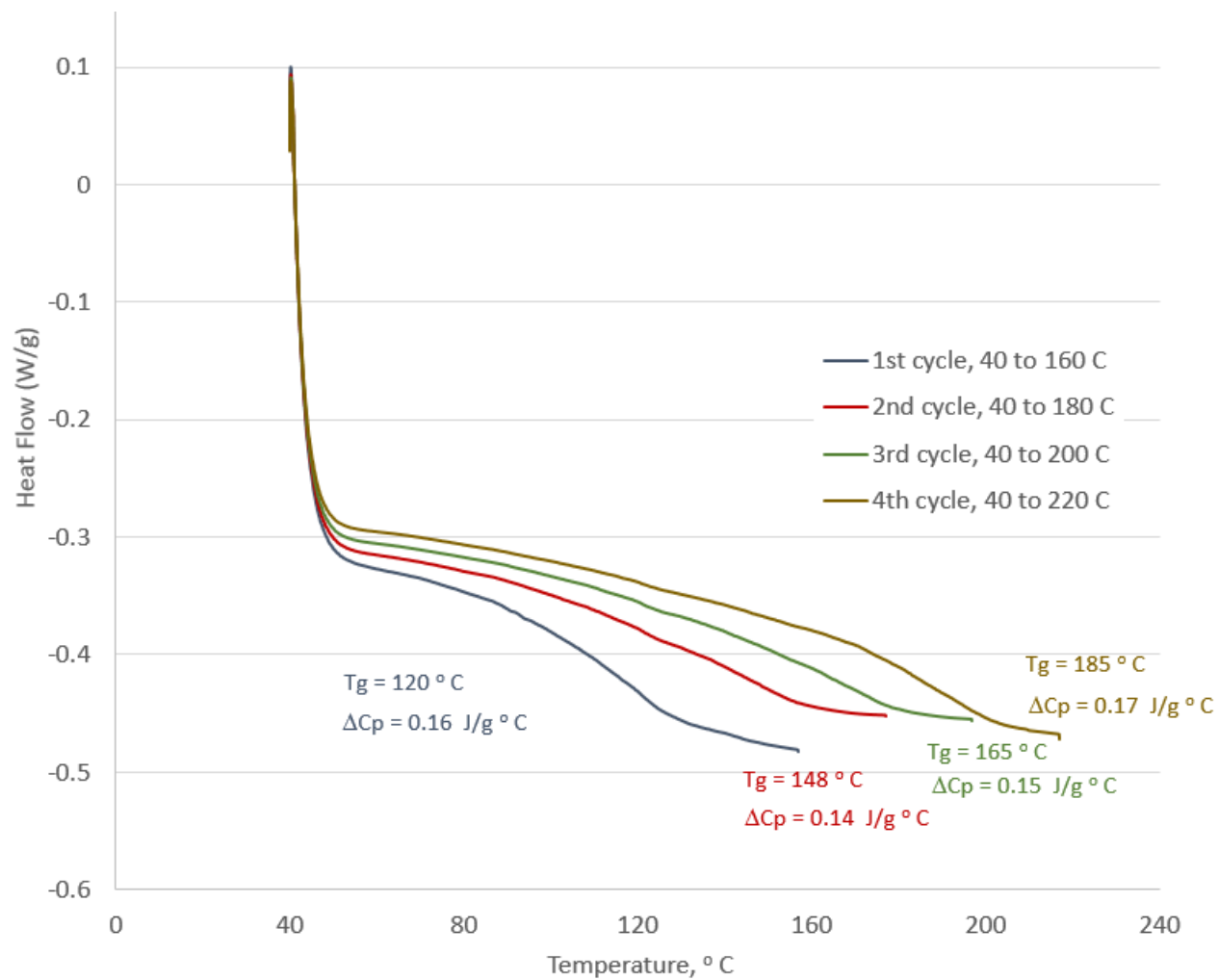


Figure 1.20 DSC scan of phenolated lignin made at 8 hours reaction showing the T<sub>g</sub> each cycle

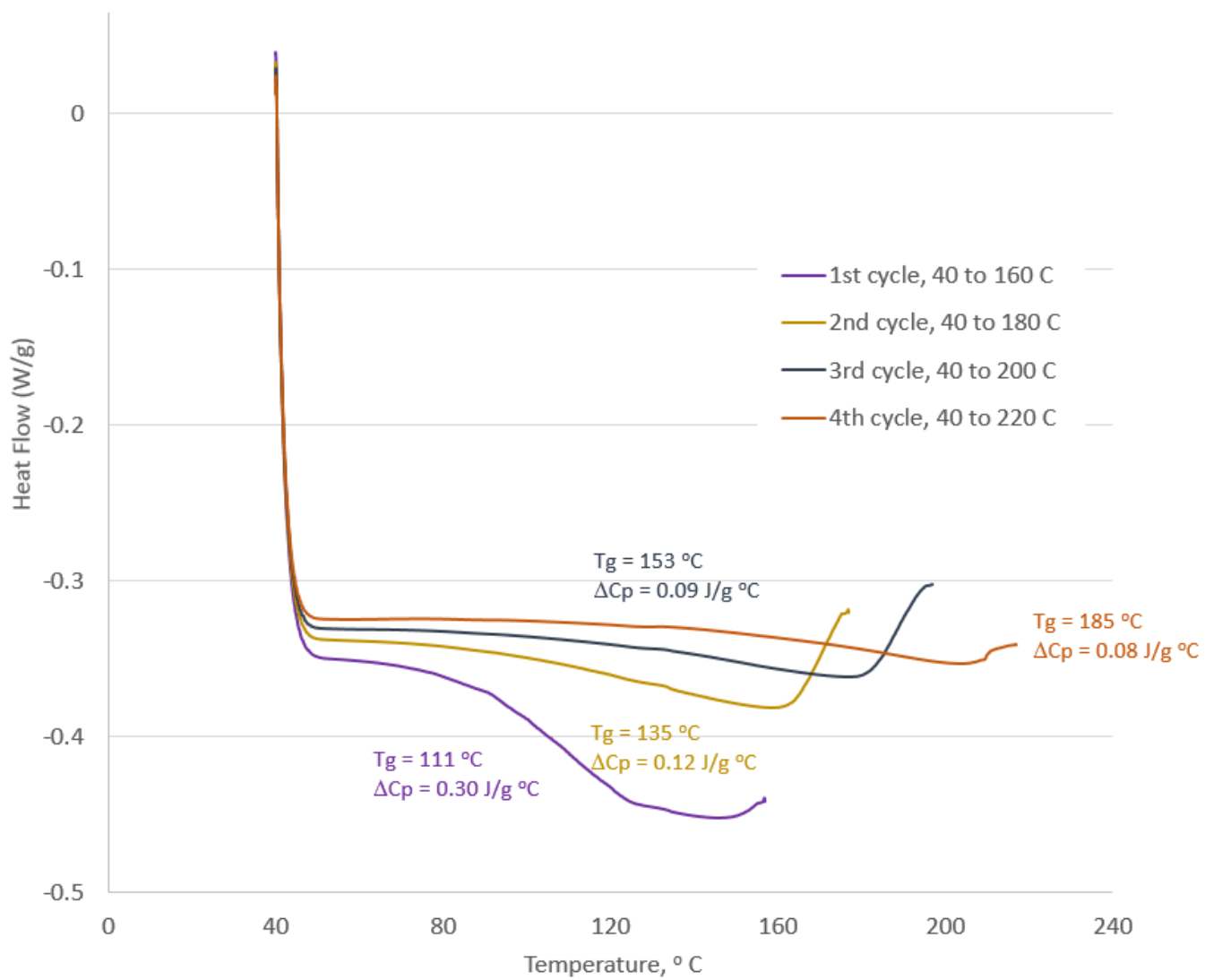


Figure 1.21 DSC of 1-naphthanolated lignin made at 8 hours reaction showing the T<sub>g</sub> at each cycle

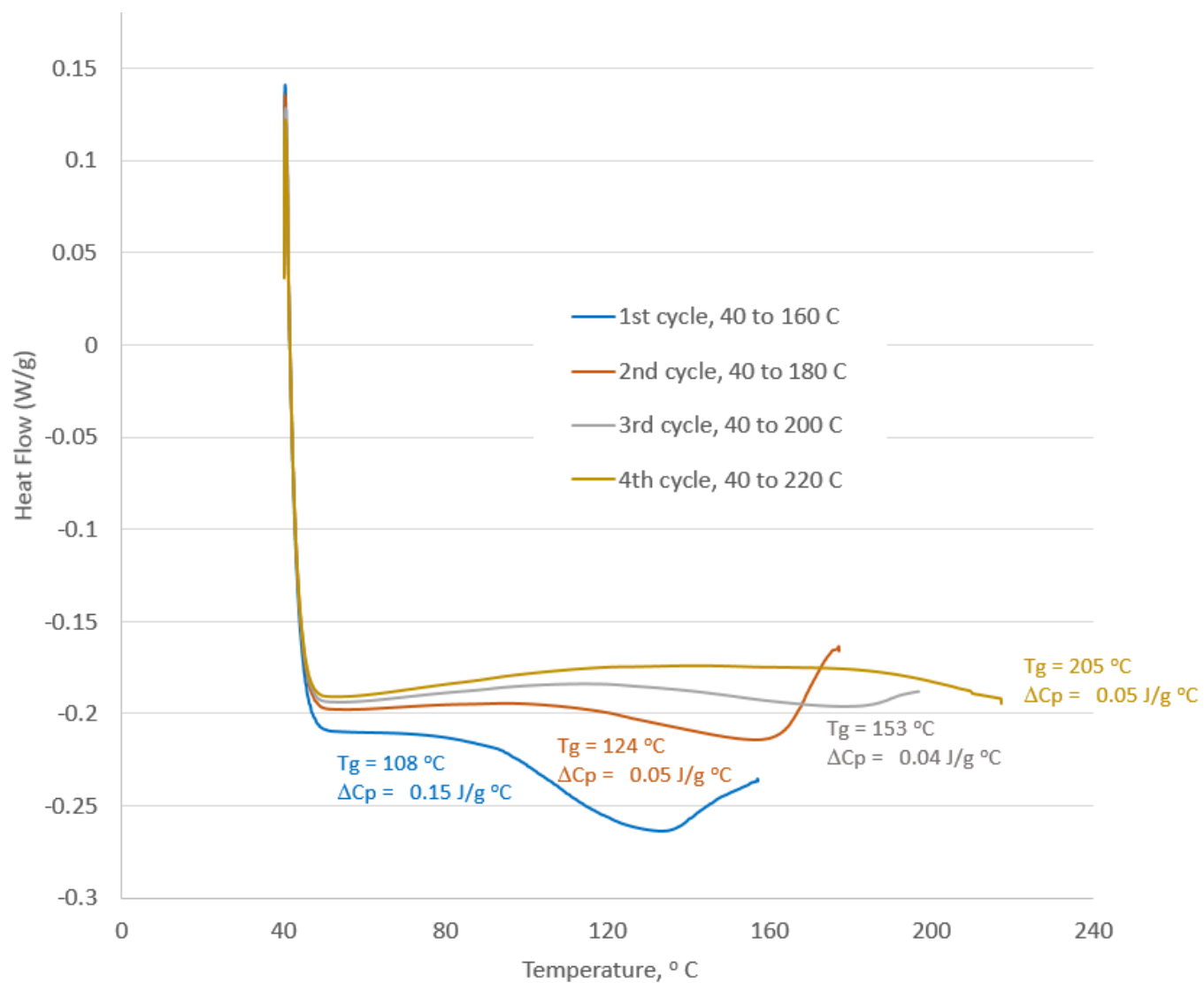


Figure 1.22 DSC of 2-naphthanolated lignin made at 8 hours reaction showing the T<sub>g</sub> at each cycle

Table 1.7 summarizes the  $T_g$  and changes in heat capacities at the  $T_g$  for the softwood kraft lignin and chemically modified lignin over several heating and cooling cycles. Heat capacities measured at W/g are converted to J/g °C using the heating rate at 20°C per minute. The degree of substitution is presented with  $T_g$ , the differences between the  $T_g$  of the consecutive DSC cycles, and the changes in heat capacity, J/g °C, for each cycle. The same method of obtaining  $T_g$  and heat capacities in the subsequent heating and cooling cycles are performed.

Table 1.7 Glass transition temperatures of lignin chemically modified with phenol and naphthanol over 4 cycles of heating and cooling at different temperature ranges at a rate of 20 °C per minute with an isothermal hold after heating

Chemically modified lignin at 2 hours reaction time at 90 ° C

Temperature range, °C	Degree of Substitution	moles of reactant per mole of C <sub>9</sub> unit	Glass transition temperature, T <sub>g</sub> , °C				Differences in the T <sub>g</sub> , °C (from previous cycle)			Changes in the heat capacity, J/g °C			
			40 to 160	40 to 180	40 to 200	40 to 220	40 to 180	40 to 200	40 to 220	40 to 160	40 to 180	40 to 200	40 to 220
heating and cooling cycle			(first)	(second)	(third)	(fourth)	(second)	(third)	(fourth)	(first)	(second)	(third)	(fourth)
Sample	Reaction time, hours												
softwood kraft													
Lignin	none	0.00	148	154	153	155	6	-1	2	0.36	0.48	0.43	0.40
phenolated lignin	2	0.60	122	155	174	195	33	19	21	0.39	0.17	0.11	0.14
1-naphthanolated lignin	2	0.17	124	119	156	not detected	-5	37	not detected	0.01	0.00	0.00	none

Chemically modified lignin at increasing reaction time at 100 ° C

Temperature range, °C	Degree of Substitution	moles of reactant per mole of C <sub>9</sub> unit	Differences in the T <sub>g</sub> , ° C										
			Glass transition temperature, T <sub>g</sub> , ° C				Differences in the T <sub>g</sub> , ° C (from previous cycle)			Changes in the heat capacity, J/g °C			
			40 to 160	40 to 180	40 to 200	40 to 220	40 to 180	40 to 200	40 to 220	40 to 160	40 to 180	40 to 200	40 to 220
heating and cooling cycle			(first)	(second)	(third)	(fourth)	(second)	(third)	(fourth)	(first)	(second)	(third)	(fourth)
Sample	Reaction time, hours												
softwood kraft													
Lignin	none	0.00	143	161	160	161	18	-1	1	0.47	0.73	0.61	0.56
			146	158	153	160	12	-5	7	0.40	0.48	0.44	0.42
phenolated													
lignin	1	0.12	120	142	164	185	22	22	21	0.36	0.28	0.27	0.27
	2	0.09	132	147	162	183	15	15	21	0.62	0.44	0.42	0.45
	4	0.10	122	153	173	190	31	20	17	0.15	0.11	0.11	0.12
	8	0.15	121	148	165	185	27	17	20	0.16	0.14	0.15	0.17
1-naphthanolated													
lignin	4	0.02	113	136	160	184	23	25	23	0.28	0.14	0.11	0.12
	8	0.07	111	135	153	185	24	18	32	0.30	0.12	0.09	0.08
2-naphthanolated													
lignin	4	0.24	96	135	153	195	39	18	42	0.28	0.09	0.05	0.08
	8	0.29	108	124	153	205	16	29	52	0.15	0.05	0.04	0.05
condensed													
lignin (control)	1	not applicable	120	122	151	176	1	29	25	0.49	0.39	0.40	0.47
	4	not applicable	131	138	164	190	7	26	26	0.50	0.13	0.19	0.19
	8	not applicable	122	121	163	185	-1	42	21	0.70	0.48	0.30	0.52

For the first set of samples made in 2 hours reaction time at 90 °C, the phenolated and naphthanolated lignin samples showed lower  $T_g$  values (122 and 124 °C, respectively) than the starting material, softwood Kraft lignin (148 °C) in the first heating and cooling cycle from 40 to 160 °C. Another interesting observation for the set of lignin samples prepared in 2 hours reaction time at 90 °C was that the 1-naphthanolated lignin did not show any consistent increases in the glass transition temperatures (124, 119, 156 °C and no  $T_g$ , detected from the first, second, third and fourth heating and cooling cycles respectively) compared to the increasing  $T_g$  values for the 1-naphthanolated lignin prepared at 4 hours reaction time (113, 136, 160 and 184 °C from the first, second, third and fourth heating and cooling cycles respectively). This observation might be explained by the low degree of substitution for the 1-naphthanolated lignin at 2 hours (DS = 0.17) compared to the same material prepared at 4 hours (DS = 0.24).

For the second set of samples made at increasing reaction time at 100 °C, SKL chemically modified with phenol and 1-naphthanol show lower  $T_g$  than SKL in the first heating and cooling cycle. For instance, as shown in Table 1.7, at 4 hours reaction time, the  $T_g$  values of phenolated lignin (122 °C), 1-naphthanolated lignin (113 °C) and 2-naphthanolated lignin (96 °C) are lower than the  $T_g$  of SKL (143 °C).

Table 1.7 showed that after repeated heating and cooling cycles, the  $T_g$  increased. However, there are no observed regular increments or differences between the  $T_g$  for the consecutive heating and cooling cycles. At the first heating and cooling cycle, incorporation of phenol or naphthanol increased the free volume of the polymeric segments of the lignin. By increasing the free volume of the polymeric segments in the lignin, incorporation of naphthanol or phenol is expected to allow these segments to reach the phase transitions from glassy to rubbery phases at a lower temperature. Heating from 40 °C to higher temperatures (180, 200, and 200 °C) in the

second, third and fourth heating cycles with an isothermal hold after heating, resulted in simultaneous thermal degradation and random cross-linking or condensation between the lignin molecules. As a result, macromolecular structures were formed with less mobility, lower free volume and a higher molecular weight. Thus, a higher temperature for a phase transition to happen.

SKL, as well, is known to undergo thermal degradation and self-polymerization 20 °C above the  $T_g$  under nitrogen atmosphere, resulting in slight increase in molecular weight (Hatakeyama & Hatakeyama, 2004). As shown in Table 1.7 thermal degradation and self-polymerization can occur for SKL during the third cycle when the temperature reached 200 °C, which is 20 °C above the detected  $T_g$  at 160 °C. This phenomenon was also expected for the chemically modified lignin samples and control SKL samples during the first cycle up to the fourth cycle, where the differences in the  $T_g$  and the highest temperature in each cycle is at least 20 °C.

Condensation or cross-linking of the chemical moieties in lignin happen at the aromatic side chains where there is free-radical polymerization induced by heat. NMR studies on stabilization of lignin under an air atmosphere for carbon fiber production (Foston et al., 2013) and on the effects of pulping (Balakshin, Capanema, Chen, & Gracz, 2003) on softwood lignin chemical moieties suggested that heating of lignin induces simultaneous degradation of the aliphatic side chains (carbonyl and carboxyl groups) and aromatic side chain condensation reactions among aryl carbons, forming aryl-O-aryl (4'-O-5), biphenyl (5-5'), diarylmethane (5-CH<sub>2</sub>-5') linkages between two monolignol units.

The experimental  $T_g$  of the lignin were consistent with the values reported in the literature. Experimental  $T_g$  results were consistent with reported  $T_g$  values for SKL in the literature, which were 148°C and 144 ° C in studies on thermal properties of Bio Choice Lignin™ in our research

group (Ayoub et al., 2014; Pawar et al., 2016); and 153°C for Indulin AT from MeadWestVaco (Li & McDonald, 2014) with a different DSC heating rate (0.5°C/min). Another compilation of SKL thermal properties (Gellerstedt, 2015) showed 140 - 155 °C for Indulin AT and other sources, although these samples might have different heating and cooling rates or isothermal hold steps in their DSC scans.

In order to confirm weight loss due to thermal degradation and demonstrate changes in the weight of the sample over the same range of DSC operating temperatures for these lignin samples prepared at increasing reaction time, TGA of these materials were performed from 40 to 200 °C at the same heating rate of 20 °C per minute with an isothermal hold at 8 minutes at 200 °C. These TGA plots in Figures 1.23 to 1.26 showed 89 to 94 weight % at 200 °C, which is an evidence of evaporation of residual solvents in the lignin materials in addition to thermal degradation over a DSC temperature range from 40 up to 200 °C.

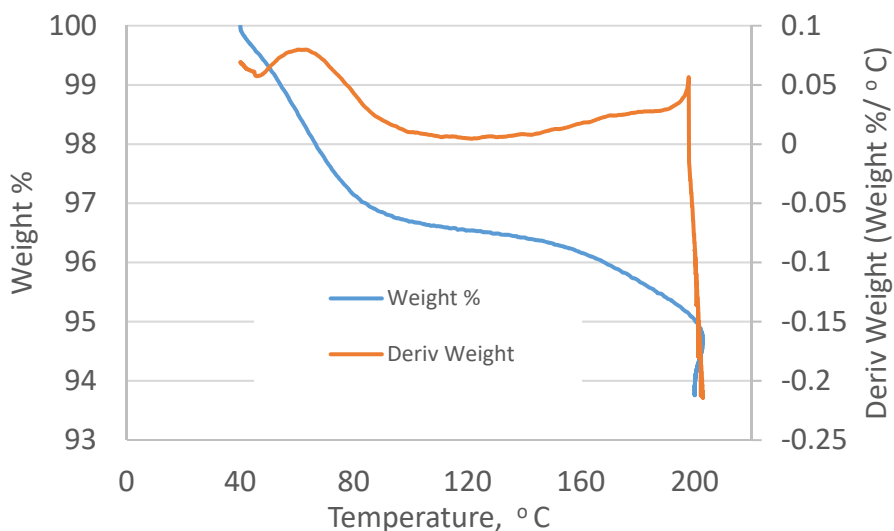


Figure 1.23 TGA curve of softwood Kraft lignin heated at 20 °C per minute from 40 to 200 °C with an isothermal hold at 8 minutes at 200 °C

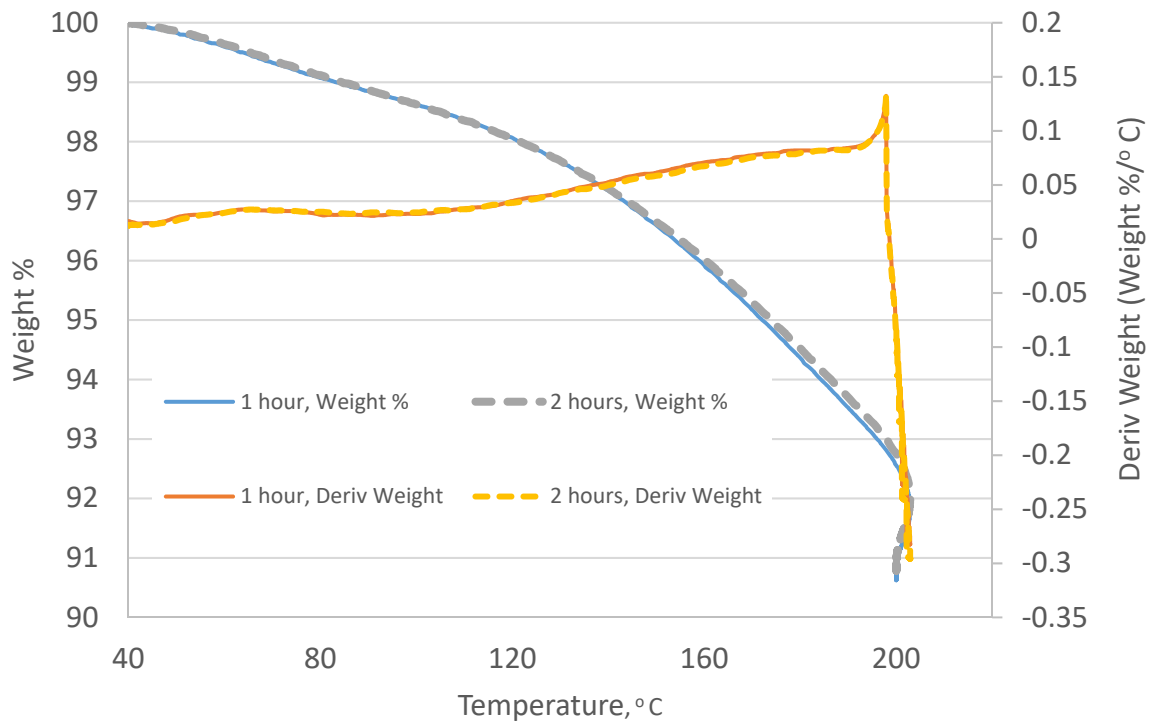


Figure 1.24 TGA curve of phenolated lignin made in 1 and 2 hours reaction time, heated at 20 °C per minute from 40 to 200 °C with an isothermal hold at 8 minutes at 200 °C

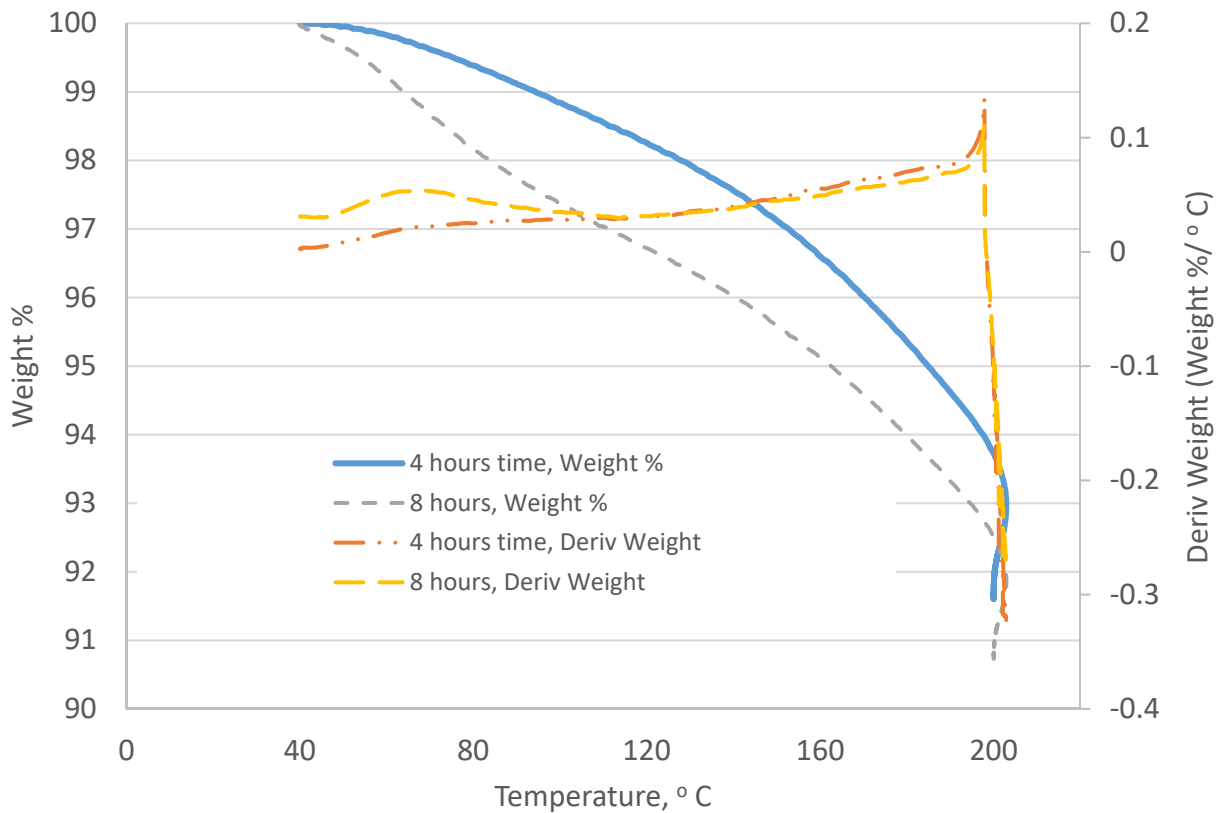


Figure 1.25 TGA curve of 1-naphthanolated lignin made in 4 and 8 hours reaction time, heated at 20 °C per minute from 40 to 200 °C with an isothermal hold at 8 minutes at 200 °C

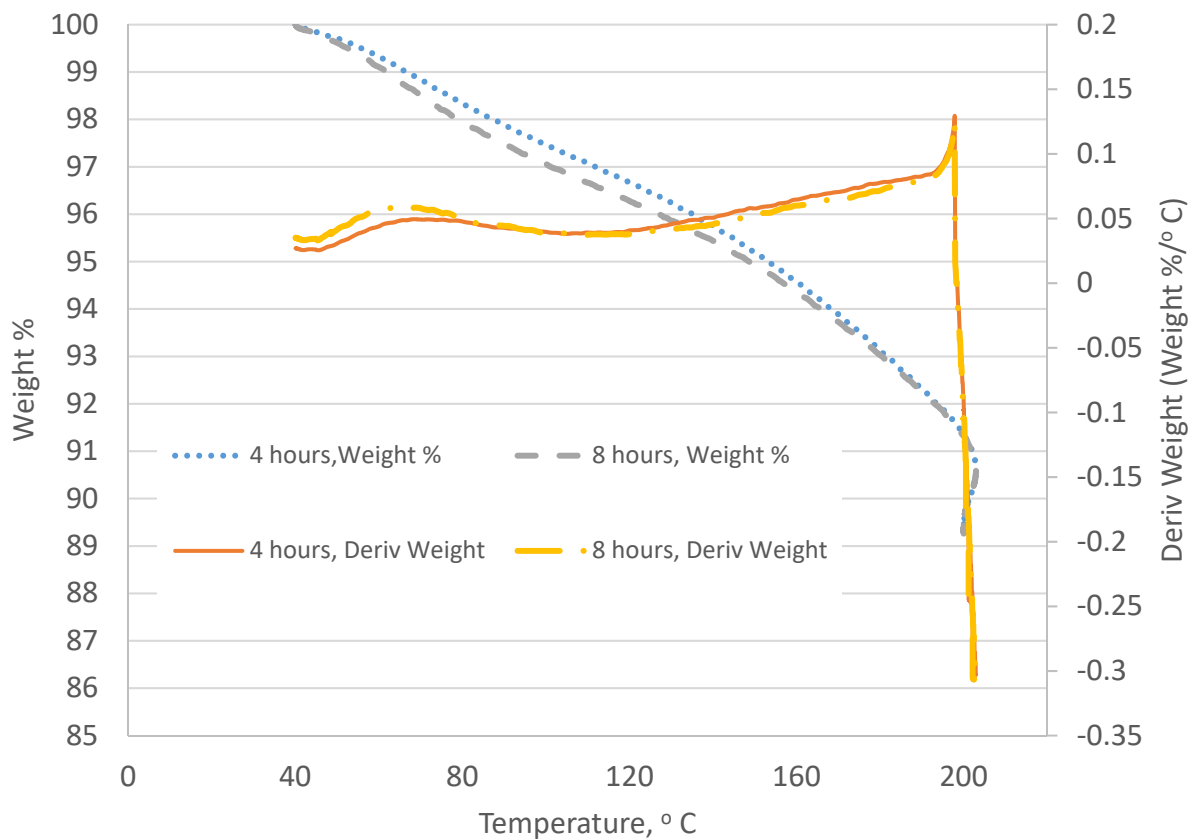


Figure 1.26 TGA curve of 2-naphthanolated lignin made in 4 and 8 hours reaction time, heated at 20 °C per minute from 40 to 200 °C with an isothermal hold at 8 minutes at 200 °C.

An evidence to show condensation of these lignin samples is when the heated material from TGA did not completely dissolve in tetrahydrofuran (THF) or N,N dimethylformamide (DMF) which are solvents that demonstrate high solubility for lignins and used for characterization of lignin by chromatography. The heated SKL and phenolated lignin were samples from TGA at 200 °C. The heated material is assumed to be cross-linked or condensed SKL and phenolated lignin. These samples were not completely soluble in THF at 0.1 mg/mL for  $M_w$  determination using GPC. Therefore, dispersed samples at 0.1 mg/mL were filtered through a 0.2 micron filter and loaded into the GPC. The number-average  $M_n$ , and weight-average molecular weight,  $M_w$ , are shown in Table 1.8. The lower  $M_w$  for the cross-linked lignins indicate the solubilized fraction is the only portion of the sample that was measured, not the  $M_w$  of a representative sample. These samples were also not completely soluble in DMF at 0.1 mg/mL. Likewise, the naphthanolated lignins were also assumed to have the same solubility behavior in these organic solvents.

Table 1.8 Molecular weight ( $M_w$  and  $M_n$ ) of softwood kraft lignin and phenolated lignin heated in TGA heated from 40 °C to 200°C at 20 °C/minute and then held at 200 °C for 8 minutes

	$M_w$ , g/mol	$M_n$ , g/mol
Softwood Kraft Lignin (Bio Choice Lignin)		
Starting material	1703	1038
Heated material	781	306
Phenolated Lignin		
Starting material	1855	558
Heated material	1642	306

### 1.3.2.3 Recommended Thermal Processing Conditions for Fiber Formation

From the thermal properties measured in this study, the temperature range suggested for processing these lignin samples would be above the  $T_g$  but below the temperature where the mass loss is at 5 % (without the solvent content). In addition, the  $T_g$  is the lower temperature limit where the lignin changes as a viscous rubbery material, as it is extruded with another polymer. The temperature where the mass loss at 5% can be set as an upper limit to prevent any further weight loss due to thermal degradation. These lower and upper temperature limits are shown in Figure 1.26. For each lignin sample, the  $T_g$  of the first, second, third and fourth DSC cycles are shown in increasing values and the temperature at 5% weight loss from TGA is shown last.

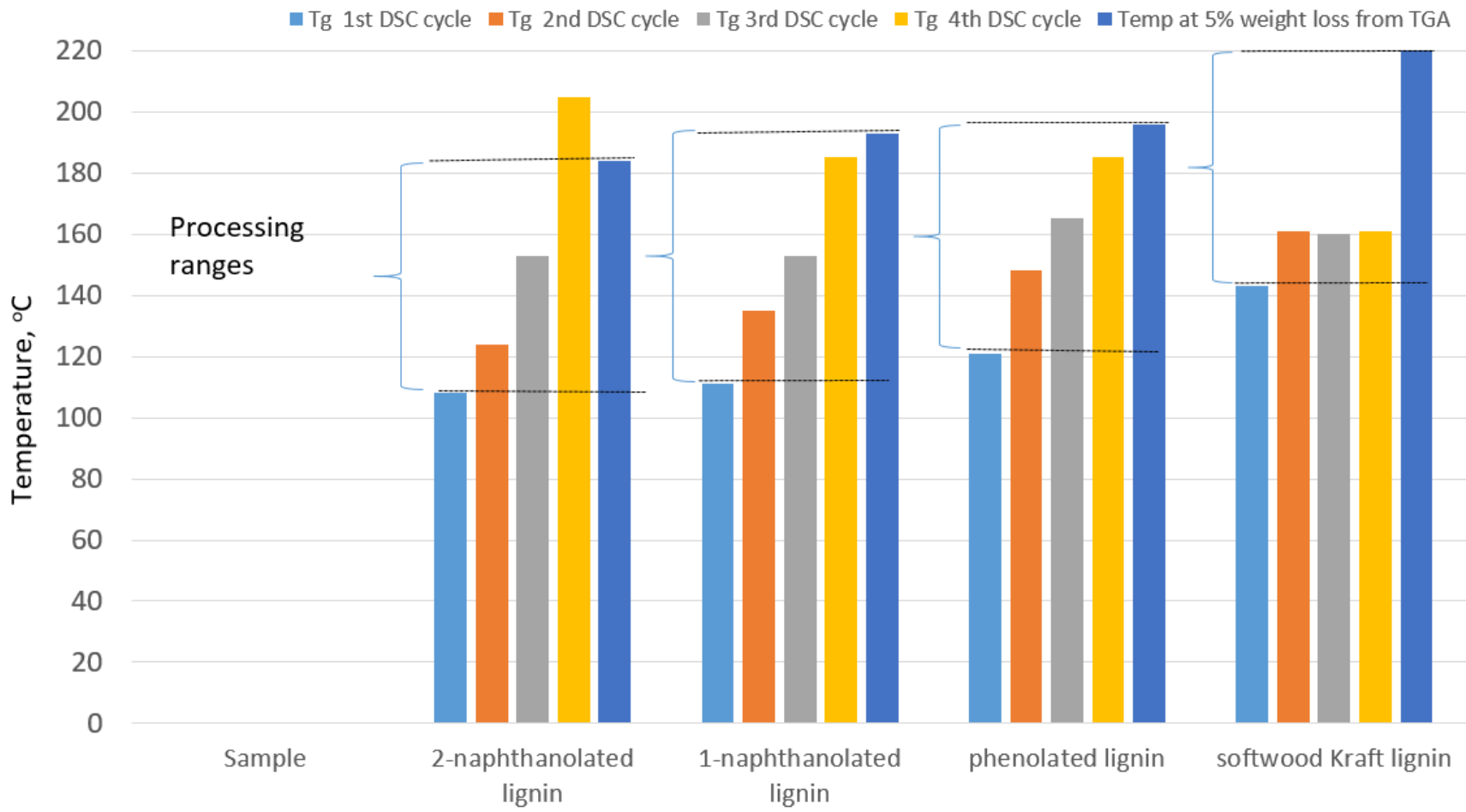


Figure 1.27 Suggested processing range of the modified lignins for thermal processing based on the  $T_g$  and temperature at 5% weight loss (without residual solvent content) for the lignin samples, prepared at 8 hours reaction time

As shown on Figure 1.27, the suggested thermal processing range for the chemically modified lignin materials would be approximately between 110 to 200 °C, while for softwood Kraft lignin, the temperature range would be 145 to 220 °C. At these temperature ranges, condensation or cross-linking reactions induced by heat occurred during the melt-spinning or extrusion for fiber formation. According to a review of fiber spinning studies on lignin-based carbon fibers (Dallmayer & Kadla, 2014), the thermal extrusion approach for spinning lignin into fibers is to heat lignin above its  $T_g$ , which is measured by DSC, to temperatures not exceeding its degradation temperature, measured by TGA, in order to generate a fiber that maintains suitable mechanical properties for handling during further processing such as thermostabilization and carbonization. In this study, the temperatures at 5% weight loss are in the range of 175 to 224 °C as shown in Table 1.6. However, melt extrusion on SKL at 180 °C resulted in a brittle material. Thus, lignin can be extruded with a melt-spinnable polymer, such as polyethylene. High density polyethylene melts at 180 °C and can thus be a carrier polymer for forming fiber composites at a recommended thermal processing temperature range of 110 to 200 °C.

### 1.3.3 Relationships between Chemical Properties and Thermal Properties

The relationship of  $T_g$  with DS and molecular weight can be correlated by polymer mixing equations relating these chemical and thermal properties shown in Tables 1.1, 1.2, 1.3, 1.6 and 1.7. The Fox equation can correlate  $T_g$  with DS while the Fox-Flory equation can relate the  $T_g$  with the molecular weight. These correlations have underlying assumptions, which have limitations on their applications on lignin as not a polymer with repeating units.

However, correlations are useful for interpolating chemical and physical properties within the range of the experimentally measured properties.

In order to correlate the  $T_g$  with the mass fraction, the DS values were converted from moles of reactant per mole of  $C_9$  unit to % mass of reactant added using the equations in Figure 1.1

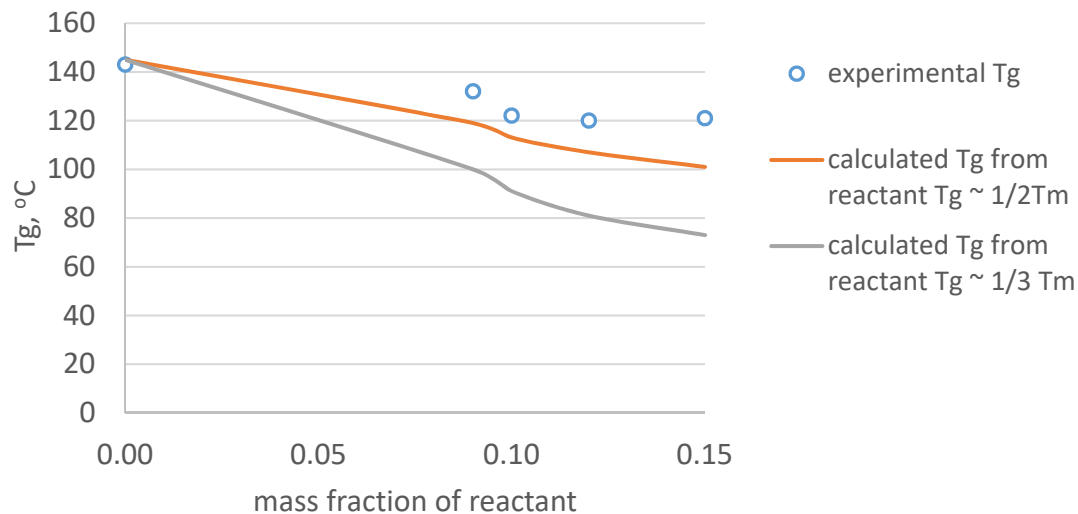
The Fox equation estimated the glass transition temperature (in Kelvin) from the mass fraction of the reactant, phenol or naphthanol (as component 1) and softwood Kraft lignin (as component 2).

$$\frac{1}{T_g} = \frac{w_1}{T_{g1}} + \frac{w_2}{T_{g2}}$$

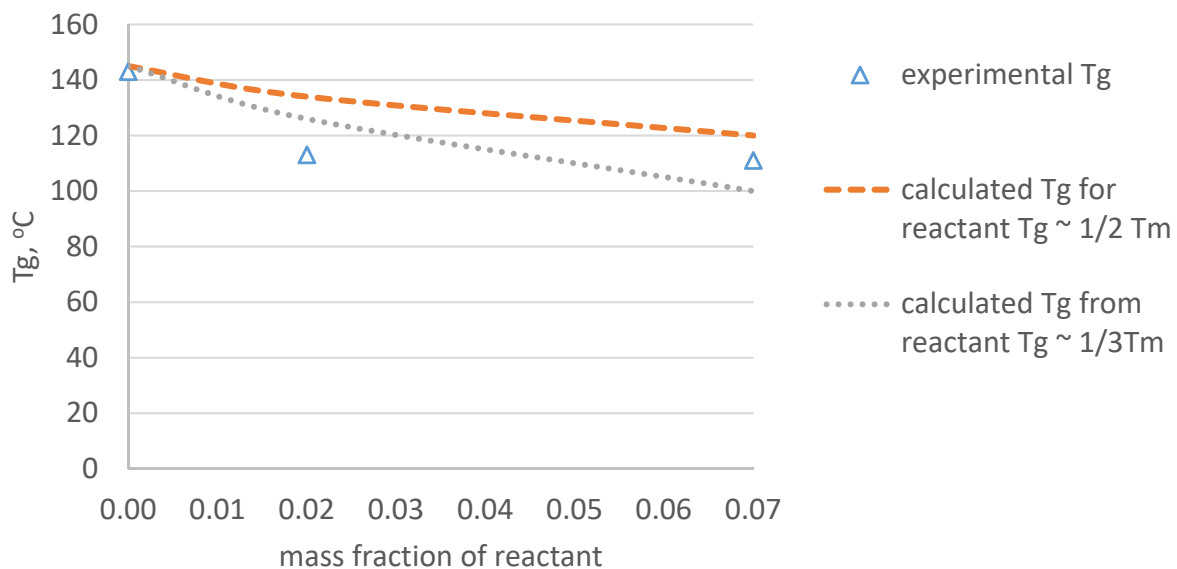
w1 - weight fraction of component 1  
w2 - weight fraction of component 2  
T<sub>g1</sub> - glass transition temperature of component 1  
T<sub>g2</sub> - glass transition temperature of component 2

Figure 1.28 Correlation of the Mw and  $T_g$  using the Fox Flory equation for the chemically modified lignins prepared in this study

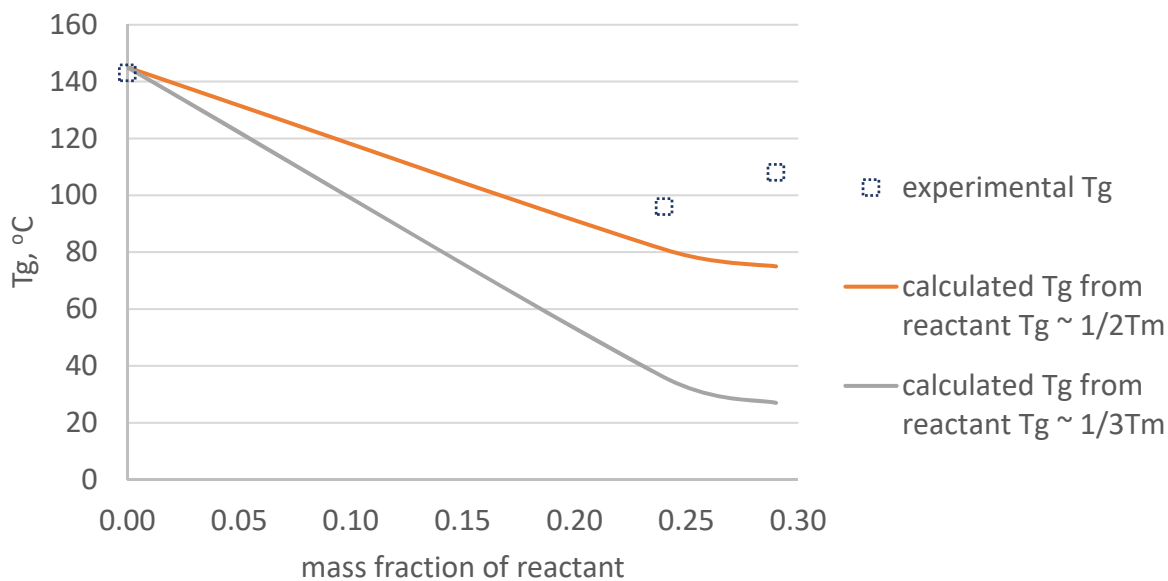
Figure 1.29 shows the experimental  $T_g$  of the chemically modified softwood Kraft lignin (SKL) with the predicted  $T_g$  using Fox equation with the  $T_g$  of reactant (phenol or naphthanol) estimated as 1/2 or 1/3 of the melting temperature ( $T_m$ ). The literature values of the melting temperatures of phenol, 1-naphthanol or 2-naphthanol are 314, 368 and 394 K, respectively. The  $T_g$  of SKL (418 K) is the experimental value obtained from DSC. The  $T_m$  is considered an adjustable parameter in the Fox equation. The correlated  $T_g$  from the reactant  $T_g$  at 1/2 of its melting temperature ( $T_m$ ) show closer values to the experimental  $T_g$ . A review paper on lignin-based thermoplastic materials (Wang, Chao; Venditti, 2016) showed that reported  $T_g$ s in the literature increase with the weight-average molecular weight,  $M_w$ , for softwood and hardwood Kraft lignins. In this study, the trends in increasing  $T_g$  as the reaction time increased (shown in Table 1.7) but was not correlated with slight increases in molecular weight (from 400 to 1000 g/mol) for the lignin samples (shown in Tables 1.2 and 1.3). Differences between data points and model predictions is possibly due to the approximation of the  $T_g$  values as well as due to slight changes in molecular weight.



(a)  $T_g$  of phenolated lignin



(b)  $T_g$  of 1-naphthanolated lignin



( c )  $T_g$  of 2-naphthanolated lignin

Figure 1.29 Glass transition temperatures,  $T_g$ , of (a) phenolated and (b) and (c) naphthanolated lignins correlated using Fox equation

The Fox Flory equation for correlating the  $M_w$  and  $T_g$  for polymers did not show any correlation with the experimental data (shown on Figure 1.30).

$$T_g = T_{g,\infty} - \frac{K}{M_n}$$

where the  $T_{g,\infty}$  and  $K$  are correlation parameters for fitting the  $T_g$  versus the  $1/M_n$  as a linear plot. This lack of correlation is due to the low degree of substitution of the phenol or naphthanol in the lignin, resulting in only slight increases in the molecular weight. The changes in the DS were also not taken as well into consideration with this equation and therefore did not provide a large enough range of molecular weights to be modeled.

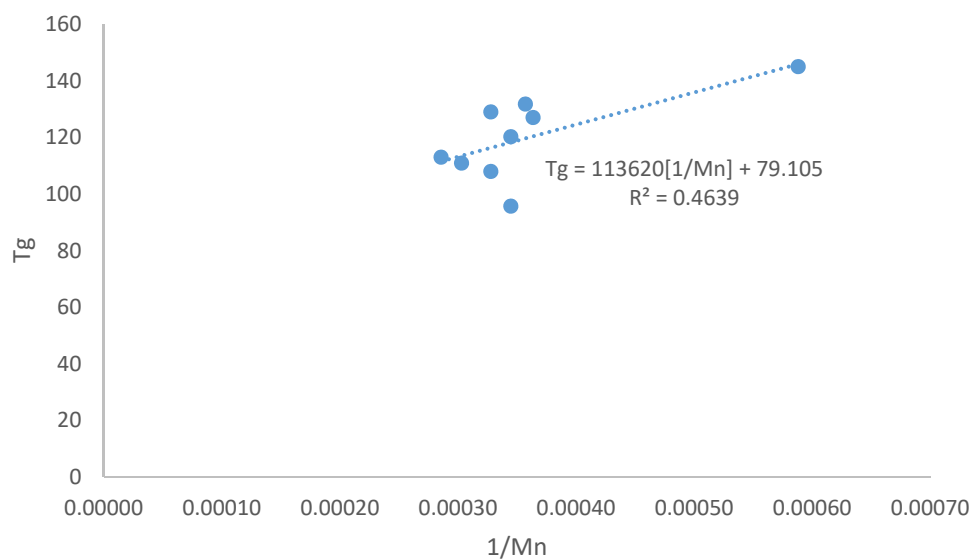
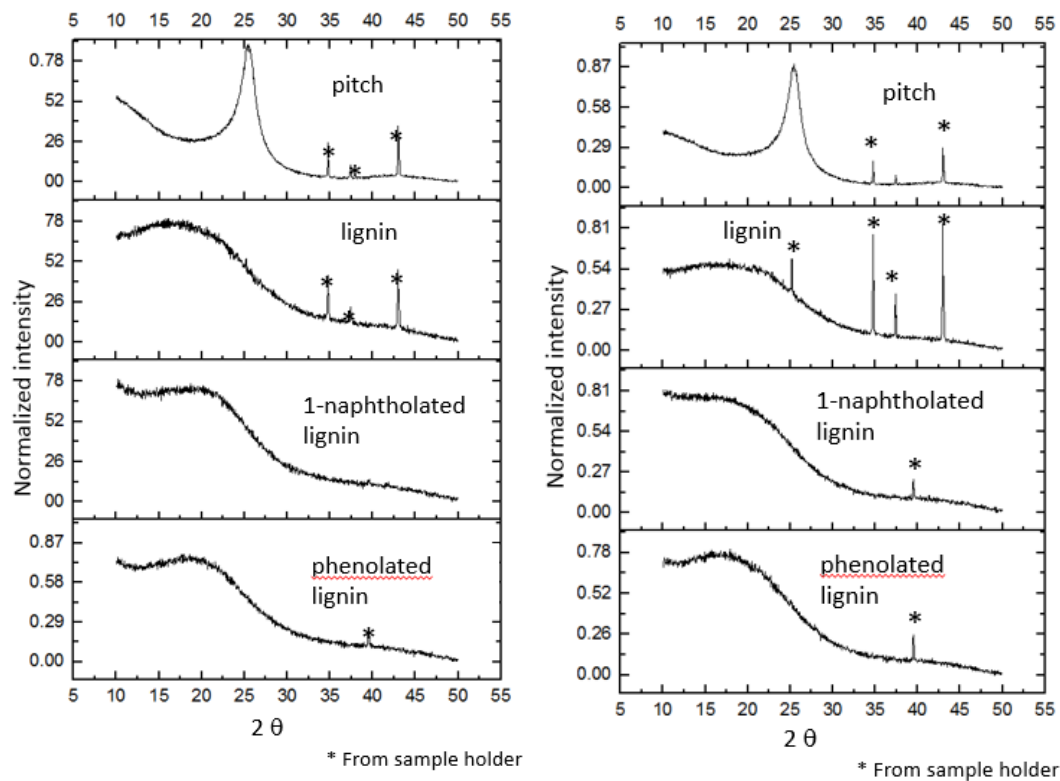


Figure 1.30 Correlation of the  $M_n$  and  $T_g$  using the Fox Flory equation for the chemically modified lignins prepared in this study

### 1.3.4 Molecular Ordering of Chemically Modified Lignin for Fiber Formation

To measure the degree of ordering of the lignin and its chemically modified forms during heating over the same range of temperatures when the thermal properties in this study were measured, the X-ray Diffraction (XRD) patterns were measured in situ during heating from room temperature to 300 °C, then cooled to room temperature. Petroleum pitch, a carbon fiber precursor, was also tested as a material for comparison. Figure 1.31 showed the XRD pattern of petroleum pitch and lignin



At room temperature before heating  
temperature

After heating then cooled to room  
temperature

Figure 1.31 X-ray diffraction patterns of 1-naphthanolated lignin and phenolated lignin samples, compared with petroleum pitch at room temperature

Petroleum pitch is a mesophase carbon which showed an ordered crystallite peak at 25.

During in-situ XRD the petroleum pitch softens during heating and solidified after cooling to room temperature. The cooled petroleum pitch has a crystallite peak with higher intensity due to rearrangement after cooling to room temperature. The XRD patterns of the lignin and its chemically modified derivatives did not show carbon peaks like petroleum pitch. Thus, a lack of ordering of chemically modified lignin compared to petroleum pitch showed that chemical modification cannot induce order as a material during fiber spinning. However, in a study on XRD of chemically modified Bio Choice Lignin (Pawar et al., 2016), the lignin showed carbon peaks from 5 to 10 degrees, which was not measured in this study.

Ordering is important during fiber spinning when the materials have to align to the fiber axis to form a mechanically strong fiber. Parallelization and extension of structural units as individual macromolecules, crystallites, aggregates, along the fiber axis in the course of spinning is one of the most important structural processes in fiber-spinning technology (Narayanan, 2014). Since X-ray diffraction revealed no ordering after heating and cooling these lignin samples, one of the possible ways to induce ordering during fiber formation is by blending lignin with petroleum pitch.

#### 1.4 SUMMARY AND CONCLUSIONS

Softwood Kraft lignin (SKL), an inexpensive renewable raw material, was modified with phenols and naphthanol as a potential carbon fiber precursor, a value-added product.

Characterization of these materials with Gel Permeation Chromatography (GPC), Thermogravimetric Analysis (TGA), Differential Scanning Calorimetry (DSC), Proton Nuclear Magnetic Resonance ( $^1\text{H}$  NMR) and In-situ X-ray Diffraction (XRD) were conducted.  $^1\text{H}$  NMR showed that the degree of substitution of 2-naphthanolated lignin is higher than phenolated lignin because of its reactivity as an ortho-director. After heating the samples at 700 °C in TGA, the carbon yields of the chemically modified lignin samples and SKL were comparable. As shown in DSC, chemical modification lowered the  $T_g$  of SKL with phenolation and naphthanolation. XRD did not show ordering of the modified lignin. DSC showed that  $T_g$  increased after repeated heating cycles for the modified and unmodified lignins consistent with chemical crosslinking. Increasing the reaction time, increased the degree of substitution, lowered the  $T_g$  but did not significantly change the carbon yield and the molecular weight. TGA and DSC data suggested the range of possible processing temperatures from 110 to 200 °C for utilizing chemically modified lignin in carbon fiber precursor production.

## 1.5 REFERENCES

- Alonso, M. V., Oliet, M., Rodríguez, F., García, J., Gilarranz, M. a., & Rodríguez, J. J. (2005). Modification of ammonium lignosulfonate by phenolation for use in phenolic resins. *Bioresource Technology*, *96*, 1013–1018.  
<https://doi.org/10.1016/j.biortech.2004.09.009>
- Alonso, M. V., Rodríguez, J. J., Oliet, M., Rodríguez, F., García, J., & Gilarranz, M. A. (2001). Characterization and structural modification of ammoniac lignosulfonate by methylation. *Journal of Applied Polymer Science*, *82*(11), 2661–2668.  
<https://doi.org/10.1002/app.2119>
- Argyropoulos, D. S., Sen, S., & Patil, S. (2015). Thermal Properties of Lignin in Copolymers, Blends, and Composites; A Review. *Green Chem.*  
<https://doi.org/10.1039/C5GC01066G>
- Ayoub, A., Venditti, R. a., Jameel, H., & Chang, H.-M. (2014). Effect of irradiation on the composition and thermal properties of softwood kraft lignin and styrene grafted lignin. *Journal of Applied Polymer Science*, *131*(1), n/a-n/a. <https://doi.org/10.1002/app.39743>
- Bajpai, P. (2013). *Update on Carbon Fibers*. Shrewbury: Smither Rapra.
- Balakshin, M. Y., Capanema, E. a., Chen, C. L., & Gracz, H. S. (2003). Elucidation of the structures of residual and dissolved pine kraft lignins using an HMQC NMR technique. *Journal of Agricultural and Food Chemistry*, *51*, 6116–6127.  
<https://doi.org/10.1021/jf034372d>
- Banu, D., El-Aghoury, A., & Feldman, D. (2006). Contributions to characterization of

poly(vinyl chloride)-lignin blends. *Journal of Applied Polymer Science*, 101(5), 2732–2748. <https://doi.org/10.1002/app.23026>

Dallmayer, I., & Kadla, J. (2014). Lignin-based Carbon Fibers. In K. Oksman, A. Matthew, A. Bismarck, O. Rojas, & M. Sain (Eds.), *Handbook of Green Materials Volume 4* (pp. 24–47). American Chemical Society.

Das, S., Warren, J., West, D., Schexnayder, S. M., Das, S., Warren, J., Schexnayder, S. M. (2016). *Global Carbon Fiber Composites Supply Chain Competitiveness Analysis*. Oak Ridge National Laboratory. Knoxville, Tennessee.

Fleming, I. (2010). *Molecular Orbitals and Organic Chemical Reactions*. Chichester West Sussex: Wiley.

Foston, M., Nunnery, G. A., Meng, X., Sun, Q., Baker, F. S., & Ragauskas, A. (2013). NMR: a critical tool to study the production of carbon fiber from lignin. *Carbon*, 52, 65–73. <https://doi.org/10.1016/j.carbon.2012.09.006>

Gellerstedt, G. (2015). Softwood kraft lignin: Raw material for the future. *Industrial Crops and Products*, 77, 845–854. <https://doi.org/10.1016/j.indcrop.2015.09.040>

Gottlieb, H. E., Kotlyar, V., & Nudelman, A. (1997). NMR Chemical Shifts of Common Laboratory Solvents as Trace Impurities. *The Journal of Organic Chemistry*, 62(3), 7512–7515. <https://doi.org/10.1021/jo971176v>

Hatakeyama, T., & Hatakeyama, H. (2004). *Thermal Properties of Green Polymer and Biocomposites*. Kluwer Academic Publishers.

Jacobs, A., & Dahlman, O. (2000). Absolute molar mass of lignins by size exclusion

chromatography and MALDI-TOF mass spectroscopy. *Nordic Pulp and Paper Research Journal*, 15(2), 120–127. <https://doi.org/10.3183/NPPRJ-2000-15-02-p120-127>

Kadla, J. F., Kubo, S., Venditti, R. A., Gilbert, R. D., & Compere, A. L. (2002). Lignin-based carbon fibers for composite fiber applications. *Carbon*, 40, 2913–2920.

Leskinen, T., Kelley, S. S., & Argyropoulos, D. S. (2015). Refining of Ethanol Biorefinery Residues to Isolate Value Added Lignins. *ACS Sustainable Chemistry & Engineering*, 150612140030007. <https://doi.org/10.1021/acssuschemeng.5b00337>

Li, H., & McDonald, A. G. (2014). Fractionation and characterization of industrial lignins. *Industrial Crops and Products*, 62, 67–76. <https://doi.org/10.1016/j.indcrop.2014.08.013>

Matsushita, Y., Sano, H., Imai, M., Imai, T., & Fukushima, K. (2007). Phenolization of hardwood sulfuric acid lignin and comparison of the behavior of the syringyl and guaiacyl units in lignin. *Journal of Wood Science*, 53(1), 67–70. <https://doi.org/10.1007/s10086-006-0814-3>

Narayanan, Ganesh.(2014). Electrospinning of Poly ( $\epsilon$ -caprolactone) Fibers Functionalized with Cyclodextrins and their Inclusion Complexes. PhD dissertation. Fiber and Polymer Science. North Carolina State University.

Paul, R., Burwell, D., Dai, X., Naskar, A., Gallego, N., & Akato, K. (2015). Recent Progress in Producing Lignin Based Carbon Fibers for Functional Applications. Retrieved from <http://www.osti.gov/scitech/biblio/1224680>

Pawar, S. N., Venditti, R. A., Jameel, H., Chang, H., & Ayoub, A. (2016). Engineering

physical and chemical properties of softwood kraft lignin by fatty acid substitution.

*Industrial Crops & Products*, 89, 128–134.

<https://doi.org/10.1016/j.indcrop.2016.04.070>

Podschun, J., Stücker, A., Saake, B., & Lehnen, R. (2015). Structure–Function Relationships

in the Phenolation of Lignins from Different Sources. *ACS Sustainable Chemistry & Engineering*, 150904101301000. <https://doi.org/10.1021/acssuschemeng.5b00705>

Saito, T., Perkins, J. H., Jackson, D. C., Trammel, N. E., Hunt, M. a., & Naskar, A. K.

(2013). Development of lignin-based polyurethane thermoplastics. *RSC Advances*, 3, 21832. <https://doi.org/10.1039/c3ra44794d>

Sudo, Kenichi; Shimizu, K. (1994). Method for manufacturing lignin for carbon fiber spinning. US Patent 5,344,921

Svensson, E. (2014). Flexibility to seasonal demand variations in pulp mill steam production:

The effect of steam savings leading to off-design heat loads. *Applied Thermal Engineering*, 70(2), 1180–1188. <https://doi.org/10.1016/j.applthermaleng.2014.04.059>

Upton, B. M., & Kasko, A. M. (2016). Strategies for the Conversion of Lignin to High-Value

Polymeric Materials : Review and Perspective. *Chemical Reviews*, 116(4), 2275–2306. <https://doi.org/10.1021/acs.chemrev.5b00345>

Wang, Chao, Venditti, R. and Kelley, S. (2016). Lignin Based Thermoplastic Materials.

*ChemSusChem*. 9 (8), 770-783. 1-15.doi: 10.1002/cssc.201501531

Wang, C., & Venditti, R. a. (2015). UV Cross-Linkable Lignin Thermoplastic Graft

Copolymers. *ACS Sustainable Chemistry & Engineering*, 3 (8), 1839-1845

<https://doi.org/10.1021/acssuschemeng.5b00416>

- Yang, H., Yan, R., Chen, H., Lee, D. H., & Zheng, C. (2007). Characteristics of hemicellulose, cellulose and lignin pyrolysis. *Fuel*, 86(12–13), 1781–1788. <https://doi.org/10.1016/j.fuel.2006.12.013>
- Yang, S., Wen, J., Yuan, T., & Sun, R. (2014). Characterization and phenolation of biorefinery technical lignins for lignin-phenol-formaldehyde resin adhesive synthesis. *RSC Advances*, 4, 57996–58004. <https://doi.org/10.1039/C4RA09595B>
- Zhang, M., Jin, J., & Ogale, A. (2015). Carbon Fibers from UV-Assisted Stabilization of Lignin-Based Precursors. *Fibers*, 3(2), 184–196. <https://doi.org/10.3390/fib3020184>
- Zhang, M., & Ogale, A. (2014). Carbon fibers from dry-spinning of acetylated softwood kraft lignin. *Carbon*, 69, 626–629. <https://doi.org/10.1016/j.carbon.2013.12.015>

## CHAPTER 2

### Production and Properties of Activated Biochar and its Utilization as Adsorbent Material

#### ABSTRACT

Biomass, from pine wood chips and switchgrass, was initially converted to biochar and then made into a higher value product, activated biochar, to investigate the effects of heat treatment on the adsorption behavior of the activated biochar. The specific surface area and concentration of acidic and basic groups on the surface of the biochar after steam activation were also measured. The intermediate biochar batches were made through pyrolysis at 500 °C followed by activation at 900 °C using moist nitrogen. The specific surface area of the biochar increased after steam activation (from 4 to 562 m<sup>2</sup>/g for pinewood and 3 to 128 m<sup>2</sup>/g for switchgrass), although these specific surface area values for the activated biochar are lower than the commercially available steam activated carbon from wood (975 m<sup>2</sup>/g). The basic surface groups on the biochar increased while the acidic surface groups decreased after steam activation. In this study, two organic compounds were selected for adsorption experiments, furfural and gallic acid. They represent examples of relevant bioprocessing or environmental contaminants, respectively. Furfural is a by-product created during the process of autohydrolysis of biomass, and interferes with a subsequent fermentation process of converting sugar to ethanol. Gallic acid is a phenolic compound that is representative of chemicals found in industrial food processing wastewater. Pine wood and switchgrass activated biochars were observed to adsorb 310 and 255 mg furfural per gram; and 102 and 28 mg gallic acid per gram, respectively. This study demonstrated the use of moist nitrogen

for increasing the adsorption of biochar for furfural and gallic acid, which is consistent with the increase in surface area and basic functional groups after activation.

#### ABBREVIATIONS

AC Activated Carbon

ABC Activated Biochar

BET Brunauer-Emmett-Teller

MC Moisture Content

## 2.1 INTRODUCTION

Activated biochar (ABC) is a value-added biomass-derived product made from biomass or biochar. Biochar can be the primary product from a manufacturing operation or a by-product, (e.g., from a bio-oil biorefinery). According to a 2013 report by the International Biochar Initiative, which surveyed the commercial activity of 23 biochar companies in the United States, non-activated biochar sold at an average price of \$2.74 per kilogram (\$2.96/kg with inflation of 2% to 2017). This non-activated biochar is blended with compost for home gardening, high-end horticulture or specialty crops (Tomlinson & Jirka, 2014). Another study of non-activated biochar production in Washington state showed that the value of crude biochar, based on their energy content as a fuel, without additional treatment is approximately \$0.07 per kg (Garcia-Perez, Garcia-Nunez, Lewis, Kruger, & Kantor, 2011). Biochar, when converted to AC, can be sold commercially for its use for industrial water treatment. For example, commercially available AC for water treatment, Jacobi Aquasorb™ G9 PAC-S (steam activated from wood) sells at \$3.30/kg [information obtained through personal communication with Jacobi customer service representative in February 2017]. Moreover, an analysis of the AC industry revealed a projected U.S. market revenue of \$2.5 billion by 2024 for powdered and granulated AC. The current market involves industrial manufacturers and municipal water treatment facilities that use AC for purification of drinking water or process water, removing odors from air, and clarification of waste streams.

This study aimed to use biochar as a source for producing activated biochar (ABC), and evaluate its use as an adsorbent material. The ABC can be used for removal of furfural, which is an inhibitor for sugar fermentation in a biorefinery. Another application is to utilize the ABC to remove phenolics found in food processing wastewater. To meet these potential applications of ABC, biochar is produced from pine wood chips and switchgrass through slow pyrolysis, and subsequently activated using moist nitrogen, and tested for its adsorption properties on a hydrophilic compound (furfural) and a phenolic compound (gallic acid). The surface area of the biochar and ABC were used as an initial evidence for their activation. This work is based on the hypothesis that the increased surface area should result in an increase in the sorption capacities of the biochar after activation using moist nitrogen.

Activated carbon can be produced from an array of starting materials, including coal, wood, coconut shell and agricultural residues. Activation of char can be done using either 'physical' or 'chemical' means. Physical activation involves steam, moist gas or carbon dioxide, while the chemical activation involves washing the acid or base. The advantages of physical activation involves lower water consumption and does not require costly purchase, handling, and recovery or disposal of acids or bases. However, the disadvantages of physical activation involves a higher energy requirement for generating steam, and the need for higher activation temperatures and handling materials at high temperature. Physical activation typically provides a lower yield than chemical activation as shown in studies on the conversion of coal tar pitch carbon fibers [6 % versus 27-47%] (Moore, Cazorla-Amor, & Maci, 2004); and steam and KOH activation of biochar [57% versus 75% from the intermediate biochar] (Azargohar & Dalai, 2008). Nevertheless, in this study, steam activation was chosen as a

simpler and more sustainable method of activating biochar. The following sections discuss the different methods of steam activation of biochar, and also sorption studies on the performance of ABC for aqueous systems.

## 2.2 RELATED STUDIES ON STEAM ACTIVATION OF BIOCHAR

This literature review is a compilation of laboratory-based processes designed for steam activation of biochar. Before activation, an intermediate biochar can be produced from biomass via pyrolysis. The composition of the intermediate biochar depends on the pyrolysis temperature and residence time, which in turn dictates the relative amounts of residual hemicellulose, cellulose and lignin. Thermogravimetric analysis (TGA) is a commonly used material characterization technique used to study the thermal degradation of biomass.

Biomass degradation includes a complex series of reactions including simultaneous bond cleavage, free radical formation, depolymerization, and evaporation of the degradation products. Below 225 °C, biomass hemicelluloses undergoes initial internal rearrangements (bond breakage), formation of free radicals, formation of carbonyl groups, reduction of the molecular weight and evolution of water, CO<sub>2</sub> and CO (Smith, 2016; H. Yang et al., 2007). Between 225-300 °C the hemicelluloses begin to rapidly decompose into a series of anhydro-sugars, acids, furans and aldehydes. At 300 °C and above, biomass continues to have a series of decomposition reactions including the condensation of volatile compounds with the residual char and degradation of lignin moieties, except for the aromatic rings in its chemical structure. As the temperature increases, the aromatization of the lignin continues via

oxidation and condensation (C-O, C-H) reductions that increase the carbon percentage of the remaining char.

In physical activation of biochar, water vapor is used either by itself or in combination with non-reactive gases such as carbon dioxide, argon or nitrogen at temperatures between 700 to 1000 °C. The high temperature degradation reactions and associated mass loss create pores in the biochar, producing carbon with high porosity and surface area. The mechanism of steam activation involves the removal of the biochar's internal mass to obtain a well-developed porous carbon structure (as shown on Figure 2.1). Steam at a higher temperature created a higher carbon content (with the loss of hydrogen and oxygen), a larger surface area and pore volume than biochar or coal (Henning & von Kienle, 2012; Nowicki, Carr, & Capp, 2016).

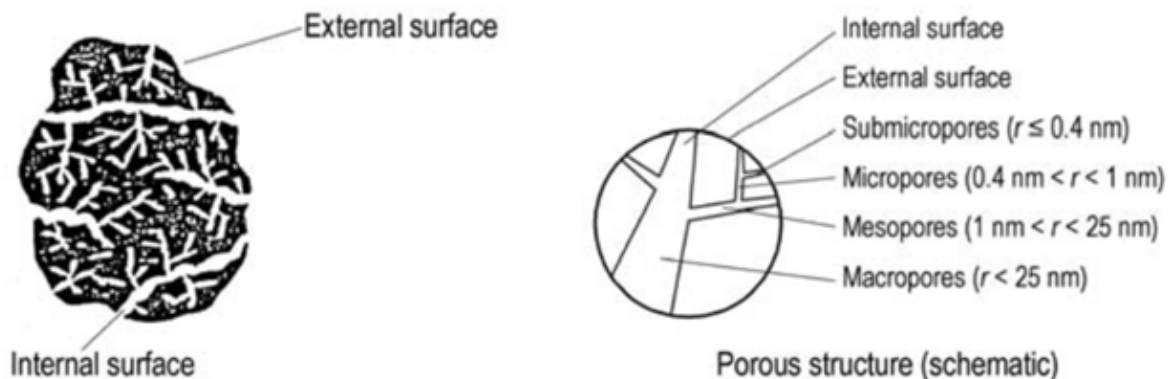


Figure 2.1 Schematic model of activated carbon affected by type of activation and biomass source (Henning & von Kienle, 2012)

During steam activation, chemical changes occurs in the biochar, involving vaporization of moisture, decomposition of organic compounds, gas-solid phase reactions and gas phase reactions. The major products of these decomposition reactions are condensable vapors (C<sub>6</sub>-

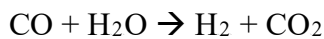
C<sub>10</sub> hydrocarbons, water, methanol, acetic acid, acetone) and non-condensable gases (CO, CO<sub>2</sub>, H<sub>2</sub>, CH<sub>4</sub> and other C<sub>2</sub>-C<sub>5</sub> hydrocarbons). During the steam activation, gas-solid reactions convert the solid carbon into gases, such as CO, CO<sub>2</sub>, H<sub>2</sub> and CH<sub>4</sub> (Franco, Pinto, Gulyurtlu, & Cabrita, 2003):

Water-gas (steam) reaction rate

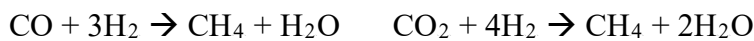


Gas-phase reactions involve the following:

Water-gas shift reaction



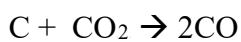
Methanation reactions



Steam-reforming reactions



Boudouard reaction



Porosity is developed by penetration of the hot inert gases in the internal structure of char and removal of carbon atoms by the above reactions, which results in the creation of pores, and opening of the inaccessible pores (Abbas, 2014). Activation using steam or a mixture of water vapor and inert gases, involves opening of the blocked pores in the char and developing micropores and widening of the developed micropores. The water –gas (steam) reaction between C and H<sub>2</sub>O is assumed to be the predominate reaction at activation

temperatures of 700 to 1000 °C. The resulting production of H<sub>2</sub>, CO and CO<sub>2</sub>, can initiate methanation and Boudouard reactions, producing CH<sub>4</sub> and CO (Franco et al., 2003). The resulting product has a higher surface area and more pores, which are usually measured using Brunauer-Emmett-Teller (BET) isotherm equipment.

The following experimental systems are reviewed to compare and contrast the different steam activation conditions such as temperature, activation time, type of gas and gas flow rates. The resulting product properties (BET specific surface area) and yields from different biomass feedstocks are summarized in Table 2.1.

Abbas and coworkers activated biochar from wheat straw using an activation reactor shown in Figure 2.2. This activation set up consists of a vertical furnace which can be heated up to 1200 °C. Inside the furnace is a tube with a small case at the bottom. The case contains char and has a porous bottom to ensure that incoming steam/nitrogen mixture flows through the char bed. The char was made into pellets to prevent any mass loss in the porous char bed and also to reduce the pressure drop for steam during the reaction through a porous plate. After activation, the pellets are easy to handle, store and transport. These biochar pellets were activated at 750 °C with a nitrogen flowrate at 500 mL/min passing through the pellets bed at the start and a steam flowrate of 75 mL/min passing through the bed during activation. A reaction time of 1 hour at temperature was used for all samples. After 1 hour, the steam flow was replaced with nitrogen gas and the reactor tube cooled. In this process, a major downside of this process is that the pellets are less porous compared to a packed bed.

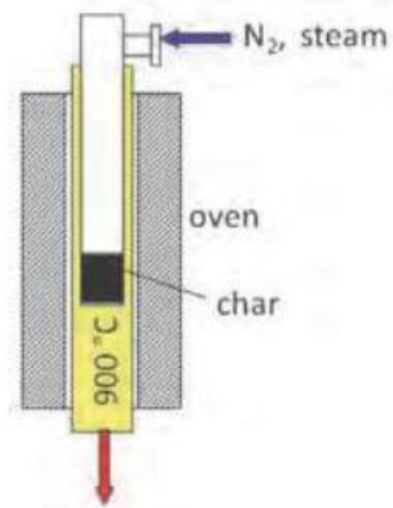


Figure 2.2 Steam activation of biochar using a porous case fixed in a reactor tube (Abbas, 2014)



**A)**



**B)**



**C)**

Figure 2.3 Biochar pellet press (a), pellets (b) and physical activation equipment (Abbas, 2014)

Azargohar and Dalai produced AC from biochar by combining nitrogen and water vapor into a fixed bed tubular reactor set-up shown in Figure 2.4. A furnace mounted vertically on a steel frame was installed to supply heat to the reactor. The bed temperature was recorded by

placing a thermocouple in the middle of the char bed. A mass flow controller at 138 mL/min controlled nitrogen flow (as the carrier gas) at STP into the reactor. This set up was operated to a maximum temperature of 1200 ° C. The steam was generated in a boiler consisting of a stainless steel tube embedded in a cylindrical insulated aluminum block. The water was injected to the boiler. To condense the steam-nitrogen mixture coming from the reactor for disposal of degradation products dissolved in the steam, an ice-bath was used to contain the volatile degradation products. This apparatus was used for steam activation of biochar and petroleum coke (Azargohar, R; Dalai, 2006; Azargohar & Dalai, 2008; Rambabu, Azargohar, Dalai, & Adjaye, 2013).

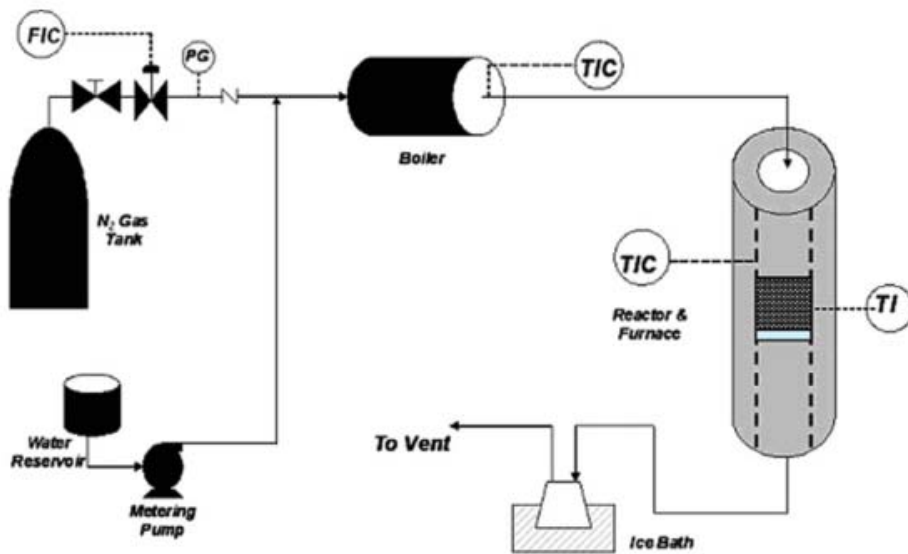


Figure 2.4 Steam activation set-up with nitrogen and water combined and fed to a reactor (Azargohar & Dalai, 2008)

Antal and coworkers made AC from Hawaiian macademia nut shells. In their process, the shells were ground, screened, and carbonized at 950 °C for 14 minutes to remove volatile matter, reacted with oxygen dissolved in flowing hot liquid water at 100 bar and temperatures between 100 and 200 °C for 20 minutes. The oxygenated biomass contained 87% carbon. Then the resulting material was carbonized a second time at 950 °C in air for 14 minutes (Antal, Sakurai, & Conesa, 2000). Figure 2.5 shows the experimental system for this study. This system involves a pre-heated reactor to completely decompose hydrogen peroxide into oxygen and water, followed by a packed bed reactor in which the charcoal feed is oxidized, and including downstream gas sampling and pressure maintenance equipment. The reactor was pressurized and externally heated with flowing deionized degassed water. When the temperature and pressure were stable at the desired experimental conditions, the feed solution switched from water to hydrogen peroxide.

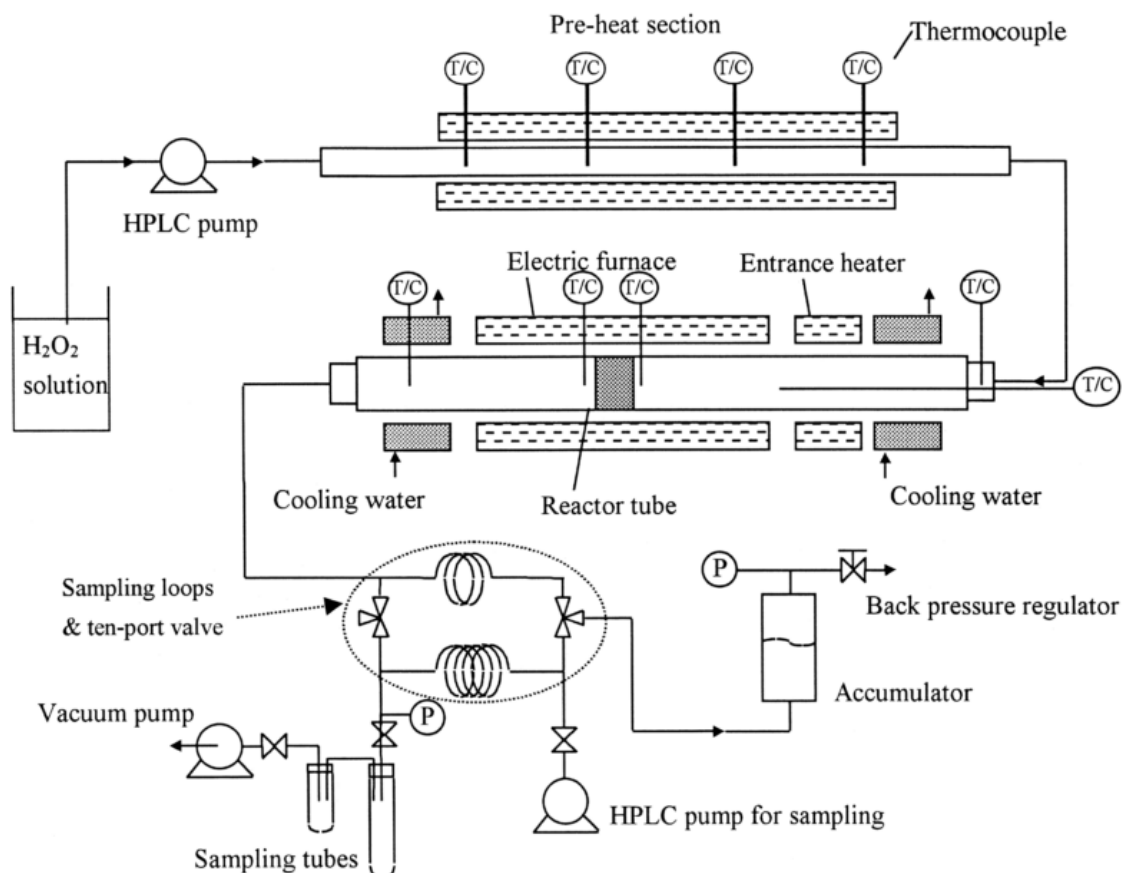


Figure 2.5 A packed bed reactor for carbonization, oxygenation and activation of biomass for production of activation carbon by a controlled, low temperature oxidation of biomass charcoal in liquid water (Antal & Grønli, 2003)

Baklanova and colleagues thermally activated biochar from cedar nutshells and lignin using a rotating reactor with a reaction volume of 0.5 L. A thermocouple placed in the center of the reactor zone was used for temperature measurement. Argon was used as a carrier gas and water vapor was produced in an electric steam generator. The activation procedure included the increase of temperature to 800 °C with argon at 10 °C/min and then char activation in a flow of steam at 800 °C for a duration of 5 - 120 minutes. After the activation, the reactor was cooled under argon to room temperature (Baklanova, Plaksin, Drozdov, Duplyakin, & Chesnokov, 2003).

Colomba activated biochar from various feedstocks (canola, miscanthus, switchgrass, willow, sunflower residue, sorghum, olive residue, Kraft lignin and birch bark) using a jigged bed reactor under a flow of steam/carbon dioxide at 100 mL/min. When the set temperature was reached, the biomass was injected into the reactor and the carbon dioxide flow was bubbled through water at 90 °C to obtain a mixture of 25 mole % steam and 75 mole % carbon dioxide (Colomba, 2015).

Chang and coworkers converted Korean pine sawdust biochars into AC by selecting activation temperatures suggested by their TGA studies. A sample of the washed air-dried ground pine sawdust in TGA showed a weight loss at 350 °C, indicating a compositional change of biochar and after 500-550 °C, the biochar's weight remained relatively stable. Steam activated biochar was produced in a furnace where the samples were treated with steam at 5 mL/min for 45 minutes at these chosen temperatures of 300 and 550 °C.

Fu and his research group performed activation of biochar prepared from Chinese pine nut shell. Prior to activation, oven dried pine nut shell was pyrolyzed initially at temperatures between 300 to 700 °C using a lab scale fixed bed pyrolysis reactor. Samples of about 50 g were used for each experiment at a nitrogen flowrate of 400 mL/min. This initial treatment consisted of rapidly heating the pine nut shell from room to the target temperature (300 to 700 °C), maintaining the sample at temperature for 10 minutes and cooling. The resulting biochar was collected for further activation and analysis. For the activation of the biochar, approximately 15 grams of biochar was placed in small furnace, that was then purged with nitrogen to remove air. The temperature was increased inside the unit to the pre-set temperature under nitrogen. After the steam activation was turned on for a period of 40-120 minutes, the inlet steam was cut off, and the furnace was cooled to room temperature to obtain the activated biochar. In this study, the optimal activation conditions were 850 °C and 80 minutes with a steam to biochar ratio of 1.5 (Chen, Chen, Sun, Zheng, & Fu, 2016).

Girgis, Soliman and Fathy used steam activation from char obtained from soybean, cottonseed, sunflower and beans. The washed dried biomass feedstocks were milled and screened. Three standard schemes of treatment were applied for these biomass feedstocks:

(1) static pyrolysis at 500 °C for 2 hours in the absence of the flowing air, (2) steam activation of the char from step 1, at 850 °C under a flow of steam-nitrogen for 2 hours, and (3) chemical activation of raw materials with phosphoric acid, which involved soaking with 50% phosphoric acid and leaving the material overnight followed by pyrolysis at 500 °C for 2 hours. Their previous studies demonstrated that temperatures around 500 °C were efficient to produce maximum development of porosity, although carbonization of the material may be incomplete (Girgis, Soliman, & Fathy, 2011).

Jia and Lua activated biochar from oil-palm shells. During the activation process, the chars were heated under nitrogen atmosphere from room temperature to 900° C at a heating rate of 10 °C/min. Having reached the final temperature of 900 °C, steam from an electric steam generator was introduced. The hold time during steam activation was 1 hour.

Daud and his research team activated biochar from Malaysian palm shell in a fluidized bed reactor connected to a steam generator at 820 °C. The fluidizing gas is either nitrogen for the carbonization process or a mixture of 80% steam in nitrogen for activation. Figure 2.6 shows the experimental set up of their process (Daud et al., 2000).

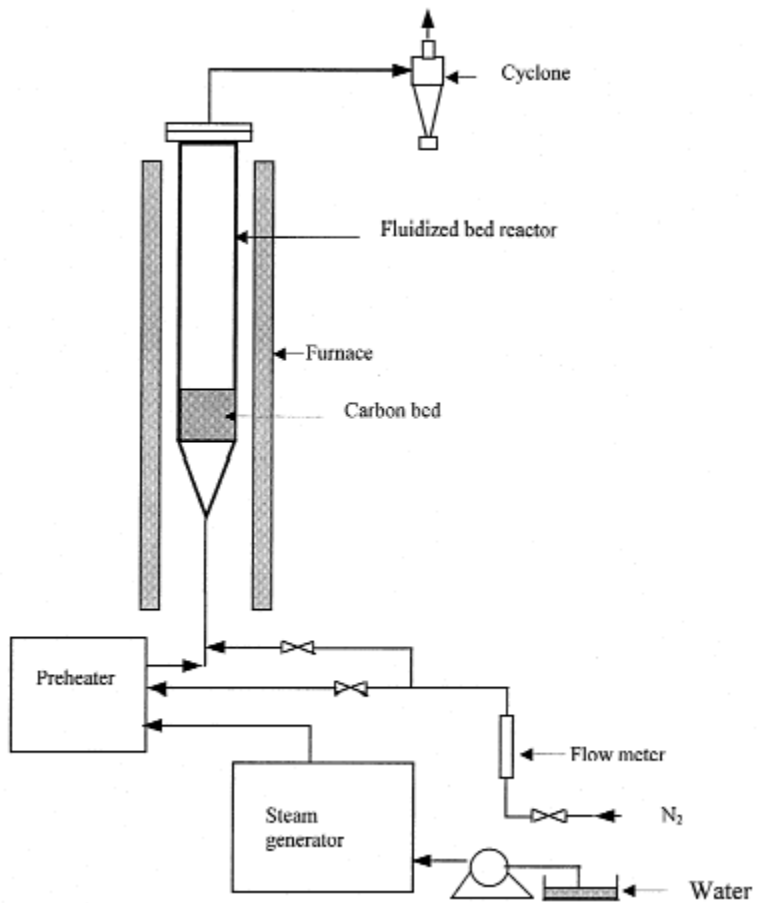


Figure 2.6 Experimental set up for steam activation of biochar using the same set-up for making biochar (Daud et al., 2000)

Sun and Jiang performed steam activation of biochar from rubber-seed shell. To prepare the biochar, pyrolysis of fresh rubber-seed shell was performed in a carbonization device under a flow of nitrogen gas. The sample was heated at 10 °C/min from room temperature to the range of 400–650 °C. Physical activation by steam following the carbonization, the pretreated samples were activated in the same pyrolysis equipment, but at temperatures between 800–900 °C, and under water vapor or stream. To obtain a high specific surface area and pore volume in the AC, the steam activation conditions were optimized and found to be at 880 °C, steam flow at 6 kg/hr, and a residence time of 60 min (Sun & Jiang, 2010).

The following table summarizes these aforementioned biochar activation processes, by showing the biomass feedstock, process conditions (temperature, duration, flowrate and type of gas mixtures), the yield of the product, and the specific surface area of the activated biochar with its intended applications as a carbonized adsorbent material. These studies suggests that the operating ranges for steam activation is 700-900 °C for a duration 1-2 hours. Preferably, nitrogen can be used as an inert gas before heating the system to the desired steam activation temperature, feeding the steam when the set temperature is reached and cooling the system with nitrogen only. The flow of steam or steam-inert gas mixture depends on the controls of the experimental set-up and had an effect on the yield and BET surface area. Some of these studies have optimized their process conditions to get maximum yield and BET surface area.

Table 2.1 Studies on activation of biochar using steam or steam-inert gas mixtures, the product properties and its intended application

Researchers Author (year) of Publication	Biomass	Activation Conditions			Product Properties		Intended Application
		Temperature ° C	Duration minutes	Gas Flowrate [Type of Gas]	Yield %	BET surface area m <sup>2</sup> /g	
Abbas (2014)	wheat straw	750	1 hour	500 mL/min [nitrogen], 75 mL/min [steam]	not reported	545	arsenic adsorption
Antal (2000)	macademia nuts	950	14 minutes	not specified [1st step: air, 2nd step: water and oxygen from H <sub>2</sub> O <sub>2</sub> decomposition, 3rd step: air]	25% (by weight of the dry raw feedstock)	620	value addition on macademia nut shells as an agricultural by-product
Azargohar and Dalai (2008)	whitewood (Spruce)	600 - 900	24 minutes – 2.5 hours	138 mL/min [nitrogen-steam]	57	568-893	water purification
Azargohar and Dalai (2013)	fluid petroleum coke	900	3 to 12 hours	15 grams/hr[steam]	30 to 91 %	359 - 482	catalysis and adsorption (desulfurization)
Baklanova (2003)	cedar nutshells, hydrolytic lignin	300 -1300	2 hours	not reported	not reported	407-865	gas purification
Colomba (2015)	canola, miscanthus, switchgrass, willow, sunflower residue, sorghum, olive residue, Kraft lignin, birch bark	800-900	20 minutes to 2 hours	20-400 mL/min [carbon dioxide-steam]	24 to 25	150-750	ammonia, naphthenic acids, mercury

Table 2.1 (continued). Studies on activation of biochar using steam or steam-inert gas mixtures, the product properties and its intended application

Researchers Author (year) of Publication	Biomass	Activation Conditions			Product Properties		Intended Application
		Temperature ° C	Duration minutes	Gas Flowrate [Type of Gas]	Yield %	BET surface area m <sup>2</sup> /g	
Chang et al (2016)	pine saw dust	300 and 550	45 minutes	not reported [steam]	not reported	189 to 397	phosphorus adsorption
Daud et.al. (2000)	Malaysian palm shell	500, 800, 900	20 to 250 minutes	15 L/min[steam- nitrogen]	20 to 60 (reported as % burn off)	0.08 to 0.16 cm <sup>3</sup> /g char (reported as absolute macropore volume, derived from BET surface area)	activated carbon production from palm shell as agricultural waste
Fu, et.al. (2016)	pine nut shell	750-900	40 to 120 minutes	not reported, steam/biochar ratio: 0.5 to 2.5	31.2 % (optimum)	850 to 1050	utilization of pine nut shell for activated carbon production
Girgis et.al. (2011)	seed hulls of peanut, soybean, cottonseed, lupine, broad beans, sunflower seeds	850	2 hours	not reported [steam-nitrogen]	10 to 15	437-1022	adsorption of pollutants in water or air
Jia, et.al. (2008)	oil-palm shells	900	1 hour	150 mL/min [steam]	not reported	700-950	phenol adsorption
Sun et.al. (2010)	rubber-seed shell	820 - 880	40 to 80 minutes	4 to 8 kg/hr [steam]	16 to 64	878 to 948	purification, separation of water or air; catalyst support, metals recovery

### 2.3 RELATED STUDIES ON ADSORPTION OF SELECTED MODEL COMPOUNDS ON ACTIVATED CARBON

Several studies have shown the removal of compounds from water using activated carbon over a wide variety of applications. For biorefinery applications, these compounds were furans and acids in woody hydrolysates (Lee, Venditti, Jameel, & Kenealy, 2011). For municipal drinking water and industrial process water treatment, perfluorinated compounds (Bender Dudley, 2012), biochemically active compounds (Deng, 2010), organic contaminants (Mezzari, 2006), phenanthrene (Park et al., 2013) and endocrine disruptors (Jung et al., 2013) have all been studied. These studies used commercially available activated carbons or chemically activated biochar.

In the forest biorefinery process, pretreated biomass is hydrolyzed into sugars using enzymes or strong acid, and then the sugars are fermented into alcohol. The presence of furfural and hydroxymethylfurfural (HMF) in the sugar-rich biomass hydrolysate, has been shown to inhibit the conversion of sugars to alcohol during fermentation. AC has been demonstrated to be effective for removal of almost 100% of the furfural and HMF in 1 hour with only a 5% carbon charge (Lee et al., 2011). This study utilized a commercial AC in preferentially adsorbing the HMF and furfural in the wood hydrolysates with 25% loss of the fermentable sugars in the hydrolysates. In a study by Martinez and colleagues, UV spectroscopy was used to monitor furans in dilute acid hydrolysates of biomass (Martinez, Rodriguez, York, Preston, & Ingram, 2000). Furfural and HMF were measured at a range of 0.05 to 10 mg/L in distilled

water at 284 nm. At 20 °C, furfural has solubility in water at 83 g/L (GESTIS Database), which suggests that furfural can be solubilized in a biomass hydrolysate up to 8.3 weight %. In food processing wastewater treatment, AC can remove water-soluble organic compounds such as phenolic compounds. One example of these compounds is gallic acid, which is found in food waste streams as a decomposition product of tannins, and can produce color in aqueous waste streams and react with chlorine in municipal water to produce harmful organic compounds (Utrera-Hidalgo, Moreno-Castilla, Rivera-Utrilla, Ferro-García, & Carrasco-Marín, 1992). In Mediterranean countries, 0.5 g/L of phenolic acids were found in agro-industrial wastewater related to manufacturing of olive oil and wine; and can be adsorbed on AC as shown by adsorption equilibrium studies on gallic acid with other phenolic compounds, syringic acid and p-hydroxybenzoic acid (García-Araya, Beltrán, Álvarez, & Masa, 2003; Utrera-Hidalgo et al., 1992). Gallic acid has a limited solubility in water, which is 1.5 weight % or 15 g/L at 298 K (Daneshfar, Ghaziaskar, & Homayoun, 2008), and therefore, the maximum amount that can be expected in wastewater streams from agro-industrial facilities. To measure the amount of gallic acid in water, another study (Mota, Queimada, & Pinho, 2008) measured the UV absorbance at 270 nm by interpolation in a calibration curve of absorbance versus gallic acid concentrations at 0.5 to 2.5 mg/L in water. For adsorption experiments, the amount of an organic compound adsorbed on the AC ( $q_e$ ) was determined from the liquid phase concentration and equilibrium concentration

$$q_e = \frac{C_o - C_e}{m} V$$

where  $C_o$  and  $C_e$  are the initial and equilibrium concentrations, respectively.  $V$  is the volume

of the solution and  $m$  is the mass of the activated carbon. The initial concentration is from the known added amounts of the organic compound in water. The equilibrium concentration is the amount of organic compound in the solution that has reached a constant value over a period of time; and experimentally measured by taking the concentration of filtered samples at increasing contact times (Ali & Gupta, 2007). In this study, the amount of furfural or gallic acid adsorbed on the biochar or activated biochar are quantified using this equation.

## 2.4 MATERIALS AND METHODS

Wood chips from loblolly pine chips (*Pinus taeda*) were provided by the Southeastern Partnership for Integrated Biomass Supply System (IBSS) consortium. Switchgrass (*Panicum virgatum*) was harvested in August 2011 from the Cherry Research farm of the State Department of Agriculture in Goldsboro, NC, USA (Ayoub, Venditti, Pawlak, Salam, & Hubbe, 2013). The pine wood chips and switchgrass were stored indoors and allowed to equilibrate to room temperature for at least 4 weeks prior to use. Nitrogen (Ultra-high purity) was provided by Airgas (Raleigh, NC, USA) and deionized water was produced in the Environmental Analysis laboratory, Weaver Labs, NCSU. Boehm titration reagents were purchased from Fisher Scientific (Atlanta, GA, USA) and VWR (Radnor, PA, USA) and used as received. Furfural and gallic acid (> 98 % purity) were purchased from Fisher Scientific (Atlanta, GA, USA) and used as received. Jacobi Carbons (Columbus, OH, USA) provided commercially available Aquasorb G9 PAC-S, which is steam activated carbon from wood.

## 2.4.1 Biochar production

Figure 2.7 shows a schematic diagram of the process used for the production of the initial pine wood and switchgrass biochar. This experimental set-up was in an open shed in Weaver Labs at the NCSU Biological and Agricultural Engineering department, to allow proper ventilation of the furnace where the exit gases were vented to the atmosphere.

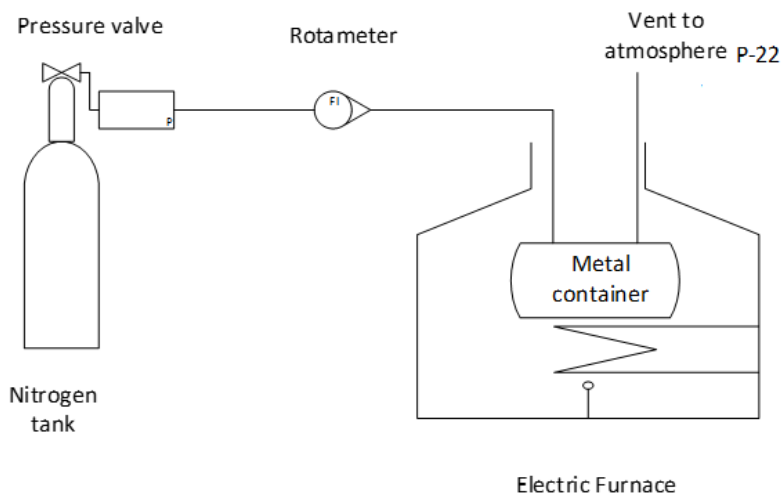


Figure 2.7 Process diagram for the pyrolysis of biomass



Figure 2.8 Muffle furnace containing the metal box container for heating the biomass

As shown in Figures 2.7 and 2.8, biomass was placed in a rectangular metal container and heated to 500 °C in a muffle furnace (Sentry Xpress 4.0, Paragon Industries, Mesquite, TX, USA). This rectangular metal container is connected to a nitrogen tank (Airgas USA LLC, Raleigh, NC, USA) which has a pressure set at 40 psi. The flowrate was set at 4-5 mL/min and monitored using a rotameter (Omega Engineering Inc., Norwalk, CT, USA). The rotameter and furnace were connected by metal fittings (Swagelok, Wake Forest, NC, USA). To produce biochar, the pine wood or switchgrass was heated to 500 °C at 14 °C per minute (average heating rate which is the maximum setting for the furnace), then held at 500 °C for 10 minutes. The furnace was cooled at a rate of 2 to 7 °C per minute. Twelve individual batches of pine and switchgrass samples were produced using this procedure. The resulting biochar was collected and kept in aluminum pans exposed to the air for 1 to 2 days to allow for oxidative reactions, and prevent any spontaneous combustion. The yield of the biochar or activated biochar is calculated as the percentage of the moisture-free biomass or biochar, respectively:

$$Yield = \frac{\text{moisture free biochar}}{\text{moisture free biomass}} \times 100 \%$$

$$\text{Moisture free activated biochar or biochar} = \text{weight} \left( 1 - \frac{\% \text{ moisture content}}{100} \right)$$

The percent burn-off is the percentage of the original moisture free biomass that was converted to the moisture free final activated carbon

$$\% \text{ Burn off} = \frac{\text{moisture free activated biochar}}{\text{moisture free biomass}} \times 100 \%$$

Since multiple batches of both the pine wood and switchgrass biochar materials were produced, there was a need to determine their individual properties before combining them to create a master batch. Elemental analysis and TGA were used to determine the key properties of the individual biochar batches. Prior to conducting TGA and elemental analysis, the coarse biochar was ground into a powder with a mortar and pestle. The elemental analysis and TGA procedures are described in the following sections on physical properties. Based on the results of elemental analysis and TGA, samples with similar carbon contents and TGA profiles were combined to create a master batch for pine wood and another one for switchgrass.

#### 2.4.2 Activation of biochar using moist nitrogen mixture

The biochar was activated using the same furnace system with a modification, shown on Figure 2.9. A 600-mL metal bubbler (MTI Corporation, Richmond, CA, USA) was connected between the nitrogen rotameter and the furnace using metal fittings (Swagelok, Wake Forest, NC, USA). A metal distribution plate (shown in Figure 2.10) was used to ensure good mixing

of the moist nitrogen throughout the cell when it was filled with the intermediate biochar.

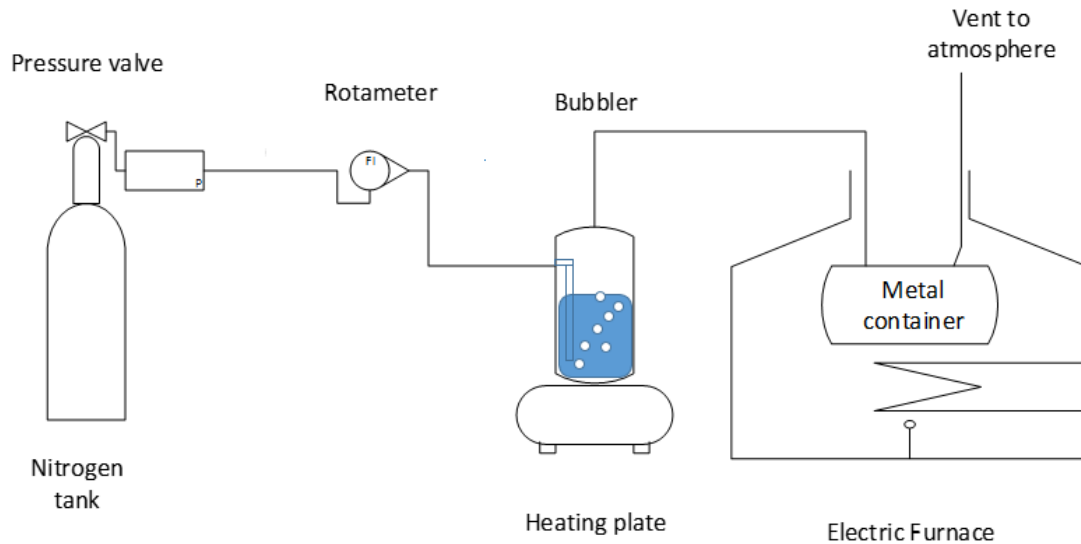


Figure 2.9 Steam activation set-up



Figure 2.10 Metal tube attachment at the inlet to the metal container for distribution of the moist nitrogen mixture

During steam activation, the bubbler was filled with 500 mL deionized water and fed with nitrogen at 4-5 mL/min. The metal tubing connecting the bubbler to the metal container were insulated with ceramic fiber wrapped with aluminum foil and packaging tape. Approximately 40 grams of unground biochar sample were placed in the metal container in the top holes to prevent clogging of the tube attachment for radial distribution of the moist nitrogen (Figure

2.10). Before heating the biochar, nitrogen was bubbled into the water inside the bubbler for 20 minutes to allow moist nitrogen to be uniformly distributed throughout the cell. For activation of the biochar, the water in the bubbler was heated at 70 to 90 °C to make hot moist nitrogen while increasing the temperature of the furnace to 900 °C at a heating rate of 7 °C/min, then holding the biochar at 900 °C for 2 hours, and cooling the furnace at 2 °C/min. During cooling, moist nitrogen was continuously flowed through the cell. The mass and the volume of the water that remained in the bubbler was measured to know the amount of water mixed with the nitrogen. The product (activated biochar) was weighed.

#### 2.4.3 Physical properties of biochar, activated biochar and commercially available activated carbon

Biomass, biochar, activated biochar and commercial steam-activated carbon from wood (Jacobi Aquasorb G9 PAC-S) were tested for moisture content and elemental composition (% carbon, % hydrogen, % nitrogen, % ash). All the samples were ground prior to elemental analysis and TGA.

##### 2.4.3.1 Elemental compositional analysis

Samples were analyzed for their carbon, hydrogen, and nitrogen content using Model 2400 Series II CHNS/O Elemental Analyzer (Perkin Elmer Corporation, Waltham, MA, USA) at the Environmental and Agricultural Testing Service Lab located in the Crop and Soil Sciences Department at NCSU. For determining the ash content, approximately 1 to 2 grams of samples were weighed into pre-weighed porcelain crucibles. The sample was placed in a Furnatrol II series 213 muffle furnace (Sybron/Thermlyne Corporation, Dubue, IA) and

burned at 500 °C overnight (approximately 12 hours). Upon cooling, the crucible containing the ash was weighed. The ash content was calculated as

$$\% \text{ ash content} = \frac{\text{weight of ash}}{\text{weight of sample}} \times 100$$

The percent oxygen (% O) is calculated by difference from the % C, H, N and ash. The elemental composition was also calculated on an ash free basis

$$\% C, H, N \text{ or } O = \frac{\% C, H, N \text{ or } O}{100\% - \% \text{ ash content}} \times 100$$

#### 2.4.3.2 Moisture content

Approximately 200 mg of each sample was weighed on an aluminum pan, conditioned in a room at 50 % relative humidity at 23 °C overnight, weighed the sample, dried for 30 minutes at 105 °C, cooled and weighed in the same humidity and temperature conditions. The moisture content is calculated from the differences in the weights before and after drying:

$$\% \text{ moisture content} = \frac{(\text{weight before drying} - \text{weight after drying})}{\text{weight before drying}} \times 100$$

#### 2.4.3.3 Thermogravimetric analysis of biochar

Thermogravimetric analysis was performed to compare the weight loss profiles of the biochar samples over a range of temperatures and estimate the yield of biochar when heated at 900 °C under nitrogen atmosphere. The biochar samples were tested in a TGA Q500 (TA Instruments, New Castle, DE). Approximately 10-20 mg of biochar were equilibrated at 50 °C, ramped at 20 °C per minute to 900 °C. The TGA curves were normalized at 100 weight % at 50 °C for comparison of their weight loss profiles.

#### 2.4.3.4 BET surface area

Brunauer-Emmett-Teller (BET) equipment was used to measure the specific surface areas of the biochar, activated biochar and commercially available AC (Jacobi Aquasorb G9 PAC-S). The BET equipment (Quantachrome Monosorb Model MS-17, Quantachrome Instruments, Boynton Beach, FL) was operated at the Department of Soil and Crop Science. Liquid nitrogen was obtained from the Center for Electron Microscopy in NCSU Gardner Hall. Approximately 60-70 milligrams of AC and ABC sample and 200 milligrams of biochar samples were oven-dried at 110-115 °C in a pre-weighed dried U-tube glass sample cell for at least 24 hours, outgassed at 110 °C with nitrogen for 15-30 minutes, immersed in liquid nitrogen bath and removed from the liquid nitrogen bath to desorb the nitrogen. After desorption, the sample in the glass U-tube was dried in an oven at 110 °C and weighed while hot to get the mass of the sample for calculating the specific surface area. The specific surface area is the ratio of the surface area to the oven dried mass of sample. Clay and alumina samples were used as standards with specific surface areas of 32 and 237 m<sup>2</sup>/g, respectively.

#### 2.4.3.5 Boehm titration for Surface chemistry

The surface chemistry of the ABC and AC were measured by classical wet methods, Boehm titration procedure, which measures the amount of surface-bound acidic and basic functional groups. In Boehm titration, 1 g of ABC or AC was contacted with 50 mL of HCl or NaOH, (0.05 M concentration for each solution) for 1 day in a water bath at 25 °C (Isotemp Shaking and General Purpose Water bath model B27, Fisher Scientific, GA, USA) followed by titration with NaOH and HCl (0.05 M concentration for each solution). The 0.05 M HCl is

prepared from a standardized 0.1 N HCl solution (Fisher Scientific, Atlanta, GA). The concentrations of the 0.05 M NaOH were determined using the standardized HCl solution. Phenolphthalein was used as an indicator for the neutralization endpoint (Boehm, Diehl, Heck, & Sappok, 1964; H. P. Boehm, 1994, 2002). The excess amount of acid or base added to a known mass of AC sample are titrated with the acid or base to quantify the moles of the acidic and basic groups.

*mmol of basic groups*

*= mmol of HCl added for the 24 hour reaction*

*– mmol of NaOH added to reach the endpoint using indicator*

*mmol of acidic groups*

*= mmol of NaOH added for the 24 hour reaction*

*– mmol of HCl added to reach the endpoint using indicator*

#### 2.4.4 Adsorption of model compounds

Furfural and gallic acid (> 98 % purity from Fisher Scientific; Atlanta, GA) were selected as model compounds and used as received. The concentrations of these compounds were quantified using UV spectrophotometer (Perkin Elmer Lambda XLS, CA, USA and Genesys 10S, Fisher Scientific, GA, USA). The concentration of the furfural solutions ranged between 5 and 500 mg/L. This concentration range represents the concentration of furfural in woody prehydrolysates (Lee et al., 2011). Approximately 50 grams of furfural solutions were mixed with 50 mg of biochar or activated carbon, placed in water bath (Isotemp Shaking and General Purpose Water bath model B27, Fisher Scientific, GA, USA) at 25 °C for 1-2 hours.

Approximately 5-10 mL of a uniformly dispersed mixture were sampled using a syringe (Becton Dickinson, Franklin Lakes, NJ); and filtered through a chemically inert nylon syringe filter with a pore size of 0.20 micron (DWK Life Sciences, Millville, NJ).

The amount of furfural was quantified by interpolation of the absorbance of the diluted sample in a calibration plot of absorbance versus concentration. For furfural, the wavelength of maximum absorbance for furfural was at 277 nm. Furfural solution with concentrations ranging from 1 to 5 mg/L show absorbance values between 0.2 to 0.8. The furfural solution samples from the sorption experiments were typically diluted to 1:1000 v/v as suggested by previous studies on using spectrophotometric measurements on furfural solutions (Martinez et al., 2000).

Similarly, gallic acid solutions were mixed and filtered using the same method performed for furfural. The starting concentration of the gallic solution is at 500 mg/L which is the amount of gallic acid reported in agro-industrial wastewater (García-Araya et al., 2003). The range of 5 to 500 mg/L of gallic acid was used as initial concentrations. The amount of gallic acid is also quantified in the same way as the furfural by interpolation of the measured absorbance at 270 nm on a calibration plot of absorbance vs concentration of gallic acid solutions.

To know the contact time when equilibrium is reached, a mixture with known amount of biochar, ABC or AC, and initial concentrations were sampled from 1, 2 and 3 hours. For furfural, the concentration of the samples did not change after 2 hours contact time while for gallic acid, the concentration did not have significant changes in the solution concentration (less than 10% difference) after 1 hour contact time.

## 2.5 RESULTS AND DISCUSSION

### 2.5.1 Yield, moisture content, elemental analysis and thermogravimetric analysis of biochar

For twelve batches of biochar produced from pine wood, the average yield of biochar (dry basis) from pine wood was  $33 \pm 2$  %. The starting material, pine wood had a moisture content of 3.6 % while the average moisture content of the pine wood biochar was 0.6%. For the twelve batches of biochar from switchgrass, the average yield of biochar (dry basis) from switchgrass is  $38 \pm 2$  %. The moisture content of the switchgrass was 4.1 % and the average moisture content of the switchgrass biochar was 1.0 %.

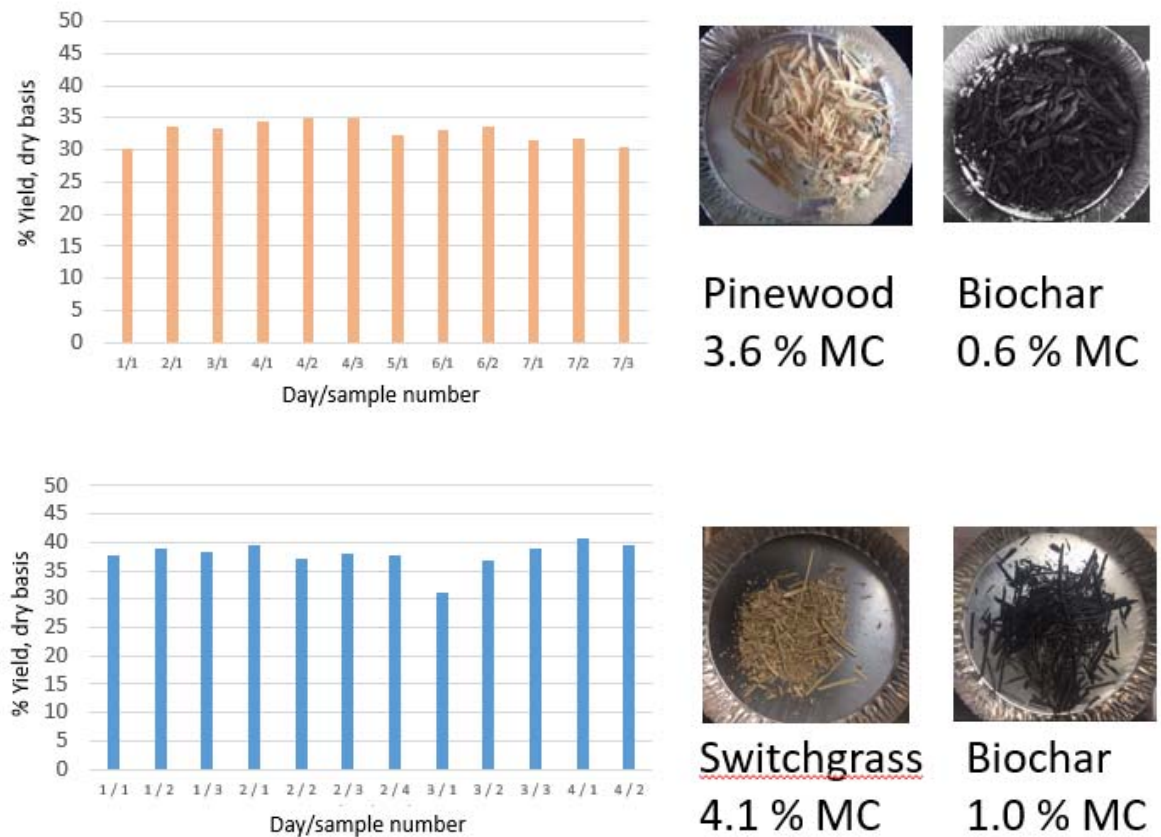


Figure 2.11 Yield and average moisture content (% MC) of the biochar batches from pine wood and switchgrass

From the elemental analysis and thermogravimetric analysis of the batches of biochars from pine wood and switchgrass (shown on Table 2.2 and Figure 2.12) and the biochar batches with higher % C and similar TGA profiles were combined for steam activation. The highlighted values in Table 2.2 show the batches of biochar that were combined, which provided at least 200 grams of starting material for activation. The combined pine wood and switchgrass biochar batches had 65 to 76 % and 55 to 62% carbon respectively.

Table 2.2 Percent Carbon and Weight % from TGA from elemental analysis of biochar batches from pine wood and switchgrass combined for activation

pine wood biochar properties			
Day/sample number	weight %		Reason for not including in activation
	% C from elemental analysis	at 900 °C from TGA	
1/1	70	61	anomalous TGA profile
2/1	65	67	
3/1	57	67	
4/1	66	68	
4/2	64	70	
4/3	62	62	anomalous TGA profile
5/1	71	70	
6/1	66	69	
6/2	67	70	
7/1	76	71	
7/2	60	72	low % C
7/3	62	71	low % C
switchgrass biochar properties			
Day/sample number	weight %		Reason for not including in activation
	% C from elemental analysis	at 900 C from TGA	
1 / 1	52	74	low % C
1 / 2	59	72	
1 / 3	57	70	
2 / 1	59	68	
2 / 2	58	73	
2 / 3	52	73	low % C
2 / 4	62	71	
3 / 1	55	75	
3 / 2	56	72	
3 / 3	59	70	
4 / 1	50	73	low % C
4 / 2	55	75	

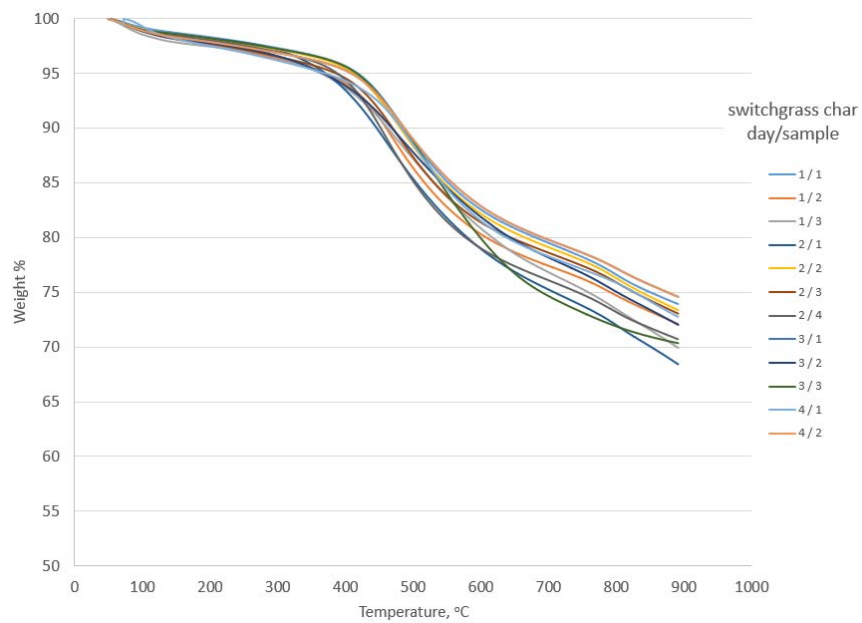
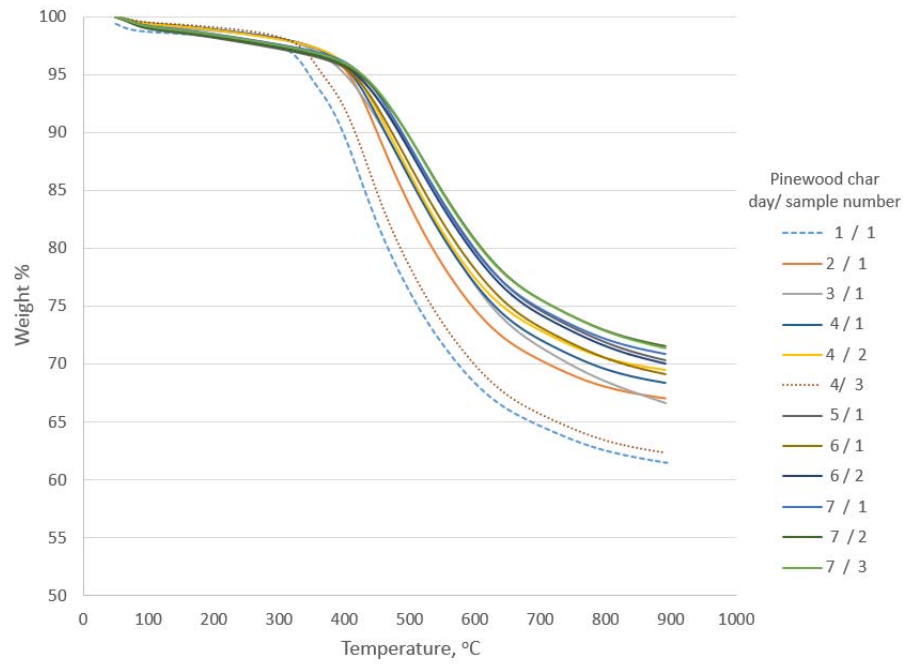


Figure 2.12 Thermogravimetric analysis of biochar batches from pinewood and switchgrass

### 2.5.2 Moisture content, elemental analysis and yield of the activated biochar

A comparison of the feedstock, initial biochar master batch and the activated biochar samples in terms of their moisture content and elemental analysis on an ash-free basis are shown in Table 2.3. The moisture content of the ABC were higher than the moisture content of the intermediate biochar, which is consistent with a higher surface area for the ABC materials. The measured moisture content of the commercial steam activated carbon, Jacobi G9, has a measured value of 5.7%, which is comparable with its reported value of 5% on its product specification sheet. The commercial activated carbon contained 9.4 % ash, which is comparable to its reported value of 8% on its product information sheet. The pine wood, pine wood biochar and pine wood ABC had 0.2, 0.9 and 1.9 % ash, respectively, while switchgrass, switchgrass char and switchgrass ABC had higher ash contents at 6.6, 17.3 and 21.1 %, respectively.

Table 2.3 Moisture content and elemental composition of the steam activated commercial activated carbon, biomass source, combined biochar batches and ABC

Sample	moisture content, weight %	elemental composition (ash-free), weight %				C / H ratio	% ash
		C	H	N	O		
Commercial activated carbon	5.7	87.7	0.8	0.3	11.1	114	9.4
Pine wood	3.6	47.0	4.0	0.1	49.0	12	0.2
Pine wood biochar	0.3	75.4	3.8	0.1	20.7	20	0.9
Pine wood ABC	3.1	92.8	0.2	0.1	6.9	455	1.9
Switchgrass	4.1	43.8	4.1	1.1	51.0	11	6.6
Switchgrass biochar	0.7	75.8	3.9	1.6	18.7	20	17.3
Switchgrass ABC	2.0	77.9	1.0	1.0	20.0	77	21.1

The yields were calculated on a moisture-free basis. The yield of ABC from the intermediate biochar for pine wood and switchgrass were 58 and 64 %, respectively. The % burn off is the percentage of the original biomass that was converted to the final activated carbon. The % burn-off for pine wood and switchgrass were 19 % and 24%, respectively. The yields are comparable with reported values for steam activated biomass in the literature for whitewood at 57% (Azargohar & Dalai, 2008) and Malaysian palm shell at 20-60% burn-off (Daud et al., 2000).

As expected, activation increases carbon content while simultaneously decreasing the oxygen content. The C/H ratio also increased consistently with the formation of a more condensed material. After activation, the hydrogen, oxygen and nitrogen contents all decreased. The intermediate biochars from pine wood and switchgrass have comparable ash-free carbon contents before activation. After activation, the pine wood has a higher carbon content than switchgrass.

### 2.5.3 Boehm titration for surface chemistry

Boehm titration was used to measure the surface basicity and surface acidity of the intermediate biochars, the activated biochars, and the commercial AC. The results of this analysis are shown in Table 2.4. After activation of the biochars, the surface basicity increased with a corresponding decrease in the surface acidity. This is consistent with the loss of oxygen functionality, e.g., the loss of carboxyl and phenolic hydroxyl groups. A study on biochars produced from poplar biomass (de Caprariis et al., 2017), reported a range of surface acidity and basicity on biochars and chemically activated biochars between 0.4 to

0.1 mmol/gram and 0.3 to 1.0 mmol/gram respectively, with comparable orders of magnitude seen on this study.

Table 2.4 Acidic and basic groups on the char and activated carbon

	Surface Basicity mmol/gram	Surface Acidity mmol/gram
Commercial activated carbon	1.7	0.5
Pine wood biochar	0.2	0.6
Pine wood ABC	0.8	0.2
Switchgrass char	1.0	1.1
Switchgrass ABC	1.9	0.4

#### 2.5.4 BET surface area

The BET surface area of the biochar and ABC, and the commercial AC are shown on Table 2.5. As expected, the steam activation increased the specific surface area of the ABC. These specific surface areas are comparable with reported values in the literature for wood and switchgrass. The surface area of the commercial AC measured in this work was 975 m<sup>2</sup>/g which is comparable to the reported value of 1050 m<sup>2</sup>/g on its product specification sheet. While steam activation significantly increased the surface area of the ABC samples, their surface areas are still well below that of the commercial AC. The specific surface area of pine ABC is 50% of the commercial sample, and thus is expected to perform reasonably well as an adsorbent. It is expected that the specific surface area of both the pine and switchgrass ABC could be increased through some combination of higher activation temperature or longer activation times, which needs further investigation.

Table 2.5 Comparisons of the BET surface area of the biochar and activated biochar samples with commercially available AC and reported values in the literature

	BET surface area m <sup>2</sup> /g		Literature value (type of biomass)	Source
		average		
Commercial activated carbon	1035 914	975	1050 (wood)	Jacobi AC G9 PAC-S product information sheet
Pine wood char	3 3	3	< 10 (whitewood Spruce)	Azargohar and Dalai (2008)
Pine wood ABC	590 533	562	568-893 (whitewood Spruce)	Azargohar and Dalai (2008)
Switchgrass char	4 4	4	< 10	
Switchgrass ABC	124 131	128	150-750 (switchgrass, miscanthus)	Colomba (2015)

### 2.5.5 Adsorption Behavior of Activated Biochar

The adsorption behavior of the ABC was measured along with the adsorption behavior of the initial biochars and commercially AC for comparison. In all cases, both furfural and gallic acid were used as model compounds.

The measurement protocols were reported in the Materials and Methods section. A representative UV spectrum, and the UV calibration curve are shown in Figure 2.14 and 2.16.

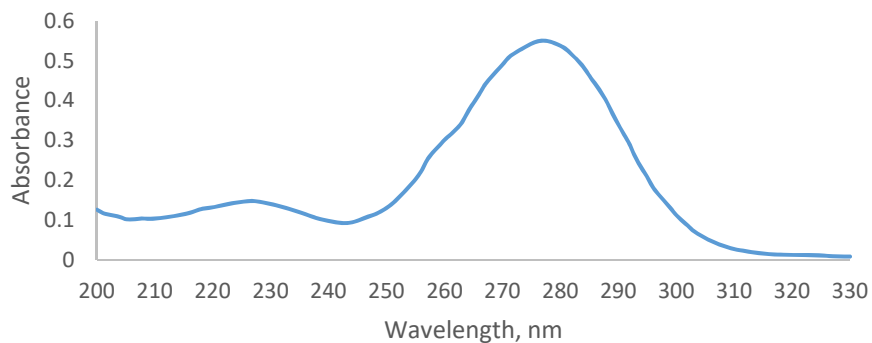


Figure 2.13 Absorbance of furfural solution (3.6 mg/L) from 200 to 330 nm, showing maximum absorbance at 277 nm

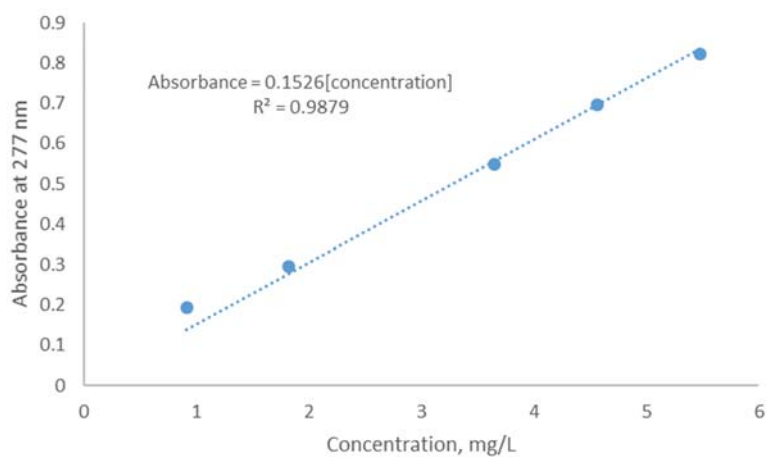


Figure 2.14 Absorbance of furfural solutions with known concentrations (0.9 to 5.5 mg/L) showing a linear relationship for interpolation on absorbance range of 0.2 to 0.8 for determining the concentration of unknown solutions from sorption experiments

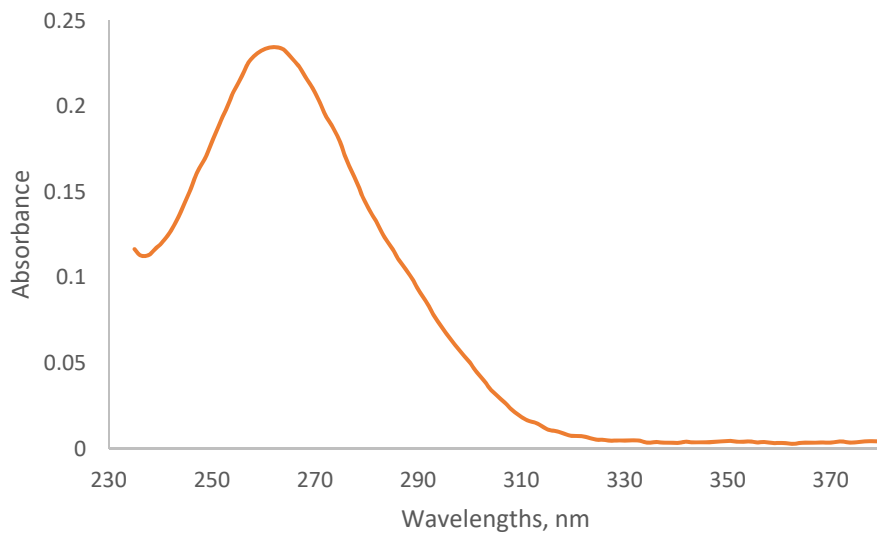


Figure 2.15 Absorbance of gallic acid solution (mg/L) from 235 to 380 nm, showing a maximum absorbance at 260 nm

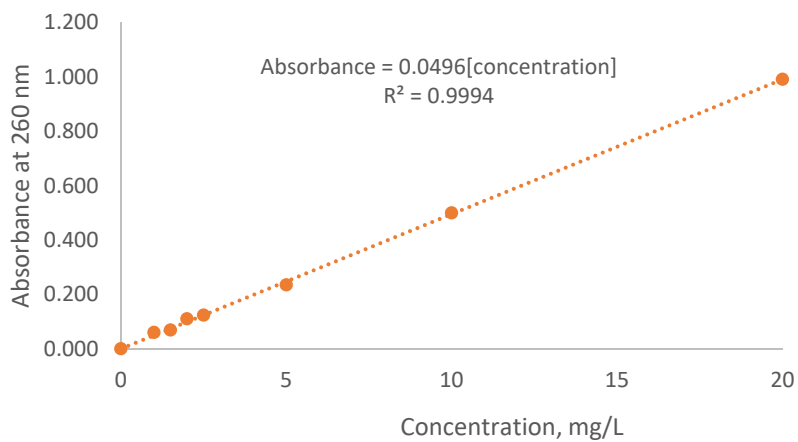


Figure 2.16 Absorbances of gallic acid solutions with concentrations from 1.0 to 20.0 mg/L, showing a linear relationship of absorbance and concentration for interpolation on absorbance range of 0 to 0.99 for determining the concentration of unknown solutions from sorption experiments

Figures 2.17 and 2.18 show the effectiveness of biochar, ABC and AC for adsorbing furfural and gallic acid. The milligrams of furfural and gallic acid adsorbed on the activated carbon and biochar were plotted against the equilibrium concentration.

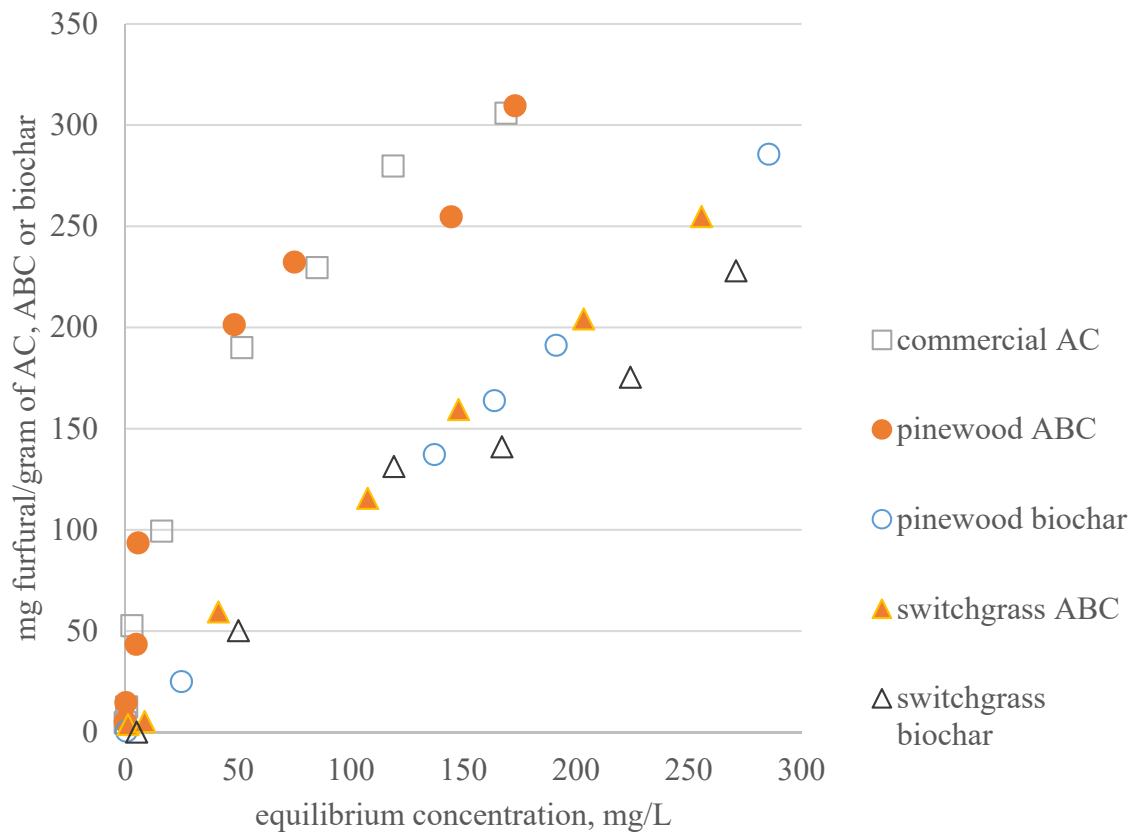


Figure 2.17 Batch adsorption isotherm indicating equilibrium concentrations at adsorption of furfural for 2 hours contact time at 25 °C

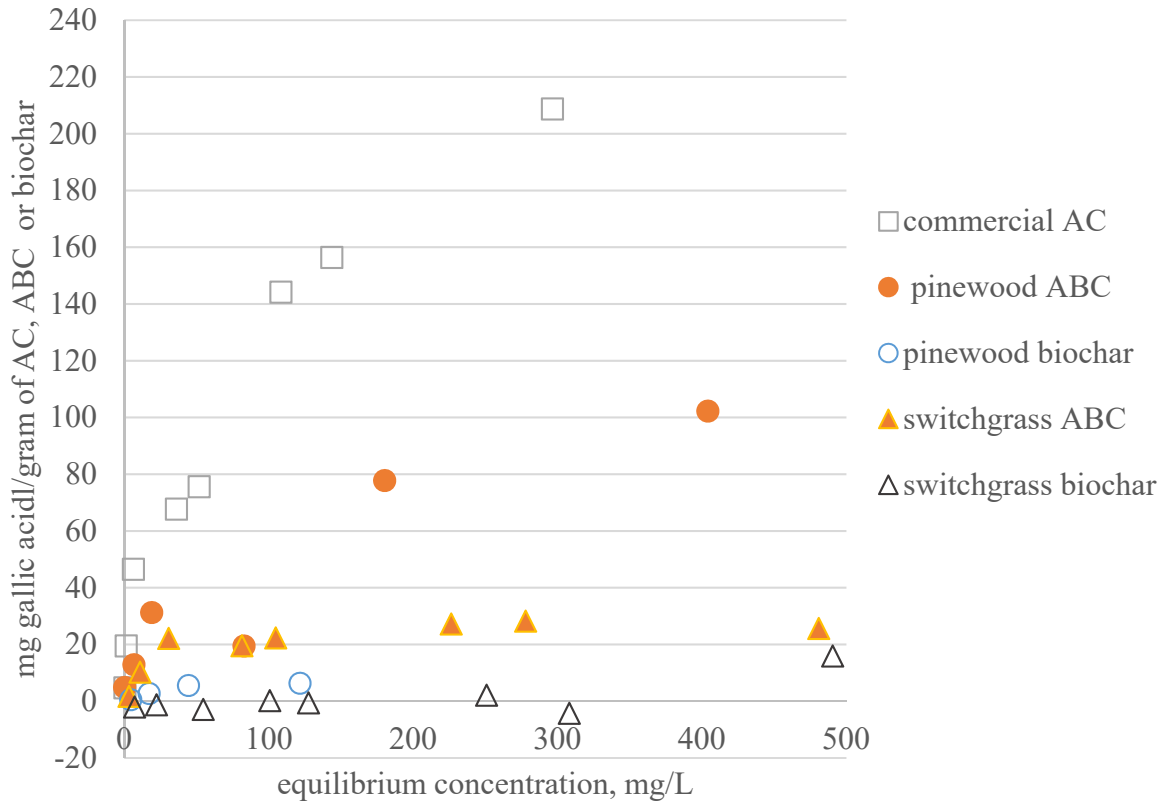


Figure 2.18 Batch adsorption isotherm indicating equilibrium concentrations of gallic acid at 1 hour contact time at 25 °C

Figure 2.17 shows that the pine wood ABC and the commercial AC had similar adsorption characteristics for furfural. The switchgrass and both intermediate biochar samples all had similar adsorption properties. These differences are to be expected as the commercial AC and pinewood ABC had significantly higher BET specific surface areas than the switchgrass ABC. However, while the commercial AC and pine wood ABC had essentially the same furfural adsorption capacity, the commercial AC had twice the specific surface area relative to the pinewood ABC.

The second set of samples, switchgrass ABC and the pine wood and switchgrass intermediate biochars, all had essentially the same furfural adsorption capacity, although the switchgrass ABC had a higher specific surface area by a factor of thirty compared to switchgrass biochar. Chemical analysis (shown on Table 2.3) of the commercial AC and pine wood ABC shows that they are similar, with very low oxygen content, high carbon, and C/H ratios. It is noteworthy that the pinewood ABC has even less oxygen than the commercial AC, which suggests that the pine wood ABC might have even greater potential for hydrophobic interactions, compensating for its lower specific surface area. For the second set of samples, it is worthwhile to note to they all had similar, relatively high oxygen content. Thus, it is possible that the furfural adsorption was dominated by a combination of phenomena including surface interactions, hydrogen bonding and swelling of the matrix material. These results also suggest that the surface acidity and basicity do not play a significant role in the adsorption of furfural, as the commercial AC, and the pine wood and switchgrass ABC were similar in these properties , but radically different in their adsorption responses.

It is also important to note that this sorption behavior is comparable with other studies on furfural (Klasson, Uchimiya, Lima, & Boihem, 2011) which demonstrated furfural adsorption of 350 mg furfural per gram of AC.

The adsorption results for the gallic acid are more complex. Clearly, the adsorption behavior of gallic acid by these five carbon samples is not dominated by the specific surface area.

While there is scatter in the data the commercial AC and both the pinewood and switchgrass ABC show similar behavior, and the two intermediate biochar samples show lower adsorption. In this case, there is potential for both the specific surface area and the surface

basicity to play a significant role in the adsorption, with the higher surface basicity of the switchgrass ABC compensating for its relatively low specific surface area, while the higher specific surface area of the pine wood ABC is moderated by its lower surface basicity. Both activated and unactivated switchgrass char showed low sorption than the pinewood biochar samples due to low specific surface area and even negative values of adsorbed amounts due to the solubilization of the blue-green complexes formed by gallic acid with the metals found in the ash. Prior work on adsorption of gallic acid by Utera-Hidalgo and coworkers (Utrera-Hidalgo et al., 1992) showed adsorption of 200 mg of gallic acid per gram of the carbonized material, which is higher than the highest adsorption values of 102 and 28 mg of gallic acid per gram for the pine wood and switchgrass ABC samples. Their work also suggested that the pH and presence of electrolytes also affected the sorption capacity for gallic acid as a weak acid and as a complexing agent with metal ions, on activated carbon.

## 2.6 SUMMARY AND CONCLUSION

This work has demonstrated that biomass can be converted to activated carbon making it useful for adsorbent applications including removal of organic compounds dissolved in water. In this work, biochar produced from an intermediate process was activated using moist nitrogen. Conversion of the biochar to activated carbon increases the value of the biochar, and thus may enhance the overall commercial viability of the bio-oil biorefinery. Another purpose of this study is to measure how steam activation can be used to increase the BET specific surface area, and also increase the concentration of acidic and basic groups on the surface of the activated biochar. After steam activation, BET specific surface areas of the biochars increased, but these values were still lower than the commercial steam activated carbon from wood. The basic surface groups on the biochar increased while the acidic surface groups decreased after steam activation. The adsorption behavior was measured with two model compounds, furfural and gallic acid, that represent relevant bioprocessing contaminants. For sorption experiments, a range of concentrations of the selected organic compounds were prepared based on reported concentrations of furfural and gallic acid in actual biomass hydrolysate and food processing wastewater studies, respectively. The adsorption on the biochars increased after steam activation due to increased specific surface area and changes in the surface chemistry. The adsorption of furfural seems to be dominated by the specific surface area of the adsorbent, while the adsorption of gallic acid seems to be governed by a combination of specific surface area, surface basicity and the presence of ash.

## 2.7 REFERENCES

- Abbas, M. M. (2014). *Alternative material use of fast pyrolysis char and its impact on the bioliq® process chain*. MS Thesis. Karlsruhe Institute of Technology, Tecnico Lisboa.
- Ali, I., & Gupta, V. K. (2007). Advances in water treatment by adsorption technology. *Nature Protocols*, *1*(6), 2661–2667. <https://doi.org/10.1038/nprot.2006.370>
- Antal, M. J., & Grønli, M. (2003). The Art, Science, and Technology of Charcoal Production. *Industrial & Engineering Chemistry Research*, *42*(8), 1619–1640. <https://doi.org/10.1021/ie0207919>
- Antal, M. J., Sakurai, M., & Conesa, J. A. (2000). Synthesis of a high-yield activated carbon by oxygen gasification of macadamia nut shell charcoal in hot, liquid water. *Carbon*, *38*(6), 839–848. [https://doi.org/10.1016/S0008-6223\(99\)00182-7](https://doi.org/10.1016/S0008-6223(99)00182-7)
- Ayoub, A., Venditti, R. A., Pawlak, J. J., Salam, A., & Hubbe, M. A. (2013). Novel hemicellulose-chitosan biosorbent for water desalination and heavy metal removal. *ACS Sustainable Chemistry and Engineering*, *1*(9), 1102–1109. <https://doi.org/10.1021/sc300166m>
- Azargohar, R; Dalai, A. K. (2006). Biochar As a Precursor of Activated Carbon. *Applied Biochemistry and Biotechnology*, *129*(6), 762–773.
- Azargohar, R., & Dalai, A. K. (2008). Steam and KOH activation of biochar: Experimental and modeling studies. *Microporous and Mesoporous Materials*, *110*(2–3), 413–421. <https://doi.org/10.1016/j.micromeso.2007.06.047>
- Baklanova, O. N., Plaksin, G. V, Drozdov, V. A., Duplyakin, V. K., & Chesnokov, N. V. (2003). Preparation of microporous sorbents from cedar nutshells and hydrolytic lignin.

- Carbon*, 41, 1793–1800. [https://doi.org/10.1016/S0008-6223\(03\)00149-0](https://doi.org/10.1016/S0008-6223(03)00149-0)
- Banu, D., El-Aghoury, A., & Feldman, D. (2006). Contributions to characterization of poly(vinyl chloride)-lignin blends. *Journal of Applied Polymer Science*, 101(5), 2732–2748. <https://doi.org/10.1002/app.23026>
- Bender Dudley, L.-A. M. (2012). *Removal of perfluorinated compounds by powdered activated carbon, superfine powdered activated carbon, and anion exchange resins*. MS Thesis. North Carolina State University.
- Boehm, H. P., Diehl, E., Heck, W., & Sappok, R. (1964). Surface Oxides of Carbon. *Angewandte Chemie International Edition in English*, 3(10), 669–677. <https://doi.org/10.1002/anie.196406691>
- Boehm, H. P. (1994). Some aspects of the surface chemistry of carbon blacks and other carbons. *Carbon*, 32(5), 759–769. [https://doi.org/10.1016/0008-6223\(94\)90031-0](https://doi.org/10.1016/0008-6223(94)90031-0)
- Boehm, H. P. (2002). Surface oxides on carbon and their analysis: A critical assessment. *Carbon*, 40(2), 145–149. [https://doi.org/10.1016/S0008-6223\(01\)00165-8](https://doi.org/10.1016/S0008-6223(01)00165-8)
- Brodin, I., Sjöholm, E., & Gellerstedt, G. (2009). Kraft lignin as feedstock for chemical products: The effects of membrane filtration. *Holzforschung*, 63(3), 290–297. <https://doi.org/10.1515/HF.2009.049>
- Chen, D., Chen, X., Sun, J., Zheng, Z., & Fu, K. (2016). Pyrolysis polygeneration of pine nut shell: Quality of pyrolysis products and study on the preparation of activated carbon from biochar. *Bioresource Technology*, 216, 629–636. <https://doi.org/10.1016/j.biortech.2016.05.107>
- Colomba, A. (2015). *Production of Activated Carbons from Pyrolytic Char for*

- Environmental Applications*. PhD Dissertation. The University of Western Ontario.
- Daneshfar, A., Ghaziaskar, H. S., & Homayoun, N. (2008). Solubility of Gallic Acid in Methanol, Ethanol, Water, and Ethyl Acetate. *Journal of Chemical & Engineering Data*, 53(3), 776–778. <https://doi.org/10.1021/je700633w>
- Daud, W. M. A. W., Ali, W. S. W., & Sulaiman, M. Z. (2000). Effects of carbonization temperature on pore development in palm-shell-based activated carbon. *Carbon*, 38(14), 1925–1932. [https://doi.org/10.1016/S0008-6223\(00\)00028-2](https://doi.org/10.1016/S0008-6223(00)00028-2)
- de Caprariis, B., De Filippis, P., Hernandez, A. D., Petrucci, E., Petruzzo, A., Scarsella, M., & Turchi, M. (2017). Pyrolysis wastewater treatment by adsorption on biochars produced by poplar biomass. *Journal of Environmental Management*, 197, 231–238. <https://doi.org/10.1016/j.jenvman.2017.04.007>
- Deng, Q. (2010). *Removal of Biochemically Active Compounds by Powdered Activated Carbon*. MS Thesis. North Carolina State University.
- Franco, C., Pinto, F., Gulyurtlu, I., & Cabrita, I. (2003). The study of reactions influencing the biomass steam gasification process. *Fuel*, 82(7), 835–842. [https://doi.org/10.1016/S0016-2361\(02\)00313-7](https://doi.org/10.1016/S0016-2361(02)00313-7)
- García-Araya, J. F., Beltrán, F. J., Álvarez, P., & Masa, F. J. (2003). Activated carbon adsorption of some phenolic compounds present in agroindustrial wastewater. *Adsorption*, 9(2), 107–115. <https://doi.org/10.1023/A:1024228708675>
- Garcia-Perez, M., Garcia-Nunez, J., Lewis, T., Kruger, C., & Kantor, S. (2011). *Methods for Producing Biochar and Advanced Biofuels in Washington State. Part 3: Literature Review of Technologies for Product Collection and Refining*. <https://doi.org/Ecology>

Publication Number 11-07-017

GESTIS Substance Database of the Institute of Occupational Health and Safety,

[www.dguv.de/ifa/gestis-database](http://www.dguv.de/ifa/gestis-database) Retrieved on April 25, 2017

Girgis, B. S., Soliman, A. M., & Fathy, N. A. (2011). Development of micro-mesoporous carbons from several seed hulls under varying conditions of activation. *Microporous and Mesoporous Materials*, *142*(2–3), 518–525.

<https://doi.org/10.1016/j.micromeso.2010.12.044>

Henning, K., & von Kienle, H. (2012). Carbon, 5. Activated Carbon. In *Ullmann's Encyclopedia of Industrial Chemistry* (pp. 23–44). Retrieved from

[http://onlinelibrary.wiley.com/doi/10.1002/14356007.n05\\_n06/full](http://onlinelibrary.wiley.com/doi/10.1002/14356007.n05_n06/full)

Jung, C., Park, J., Lim, K. H., Park, S., Heo, J., Her, N., Yoon, Y. (2013). Adsorption of selected endocrine disrupting compounds and pharmaceuticals on activated biochars. *Journal of Hazardous Materials*, *263*, 702–710.

<https://doi.org/10.1016/j.jhazmat.2013.10.033>

Klasson, K. T., Uchimiya, M., Lima, I. M., & Boihem, L. L. (2011). Feasibility of removing furfurals from sugar solutions using activated biochars made from agricultural residues. *BioResources*, *6*(3), 3242–3251.

Lee, J. M., Venditti, R. A., Jameel, H., & Kenealy, W. R. (2011). Detoxification of woody hydrolyzates with activated carbon for bioconversion to ethanol by the thermophilic anaerobic bacterium *Thermoanaerobacterium saccharolyticum*. *Biomass and Bioenergy*, *35*(1), 626–636. <https://doi.org/10.1016/j.biombioe.2010.10.021>

Martinez, A., Rodriguez, M. E., York, S. W., Preston, J. F., & Ingram, L. O. (2000). Use of

UV absorbance to monitor furans in dilute acid hydrolysates of biomass. *Biotechnology Progress*, 16(4), 637–641. <https://doi.org/10.1021/bp0000508>

Mezzari, I. (2006). *Predicting the Adsorption Capacity of Activated Carbon for Organic Contaminants from Fundamental Adsorbent and Adsorbate Properties*. MS Thesis. North Carolina State University. <https://doi.org/10.1017/CBO9781107415324.004>

Moore, B. C., Cazorla-amor, D., & Maci, J. A. (2004). Activation of coal tar pitch carbon fibres : Physical activation vs . chemical activation, *Carbon*, 42, 1367–1370. <https://doi.org/10.1016/j.carbon.2004.01.013>

Mota, L., Queimada, J., & Pinho, P. (2008). Aqueous Solubility of Some Natural Phenolic Compounds Fa. *Ind. Eng. Chem. Res.* 2008, 47(5182–5189), 5182–5189.

Nowicki, H., Carr, C., & Capp, R. (2016). Lignin Waste Transformed into Coconut-like Activated Carbon, 1–11. Retrieved from <http://www.wcponline.com/2016/06/15/lignin-waste-transformed-coconut-like-activated-carbon/>

Park, J., Hung, I., Gan, Z., Rojas, O. J., Lim, K. H., & Park, S. (2013). Activated carbon from biochar: Influence of its physicochemical properties on the sorption characteristics of phenanthrene. *Bioresource Technology*, 149, 383–389. <http://dx.doi.org/10.1016/j.biortech.2013.09.085>

Rambabu, N., Azargohar, R., Dalai, A. K., & Adjaye, J. (2013). Evaluation and comparison of enrichment efficiency of physical/chemical activations and functionalized activated carbons derived from fluid petroleum coke for environmental applications. *Fuel Processing Technology*, 106(2013), 501–510. <https://doi.org/10.1016/j.fuproc.2012.09.019>

- Smith, C. R. (2016). *Possible Sources and Impacts of Biochar Water Extractable Organic Compounds on Aquatic Microorganisms*. PhD Dissertation. Old Dominion University.
- Sun, K., & Jiang, J. (2010). Preparation and characterization of activated carbon from rubberseed shell by physical activation with steam. *Biomass and Bioenergy*, *34*(4), 539–544.  
<https://doi.org/10.1016/j.biombioe.2009.12.020>
- Svensson, E. (2014). Flexibility to seasonal demand variations in pulp mill steam production: The effect of steam savings leading to off-design heat loads. *Applied Thermal Engineering*, *70*(2), 1180–1188. <https://doi.org/10.1016/j.applthermaleng.2014.04.059>
- Tomlinson, T., & Jirka, S. (2014). *2013 State of the Biochar Industry A Survey of Commercial Activity in the Biochar Field*. International Biochar Initiative.
- Utrera-Hidalgo, E., Moreno-Castilla, C., Rivera-Utrilla, J., Ferro-García, M. A., & Carrasco-Marín, F. (1992). Activated carbon columns as adsorbents of gallic acid from aqueous solutions: Effect of the presence of different electrolytes. *Carbon*, *30*(1), 107–111.  
[https://doi.org/10.1016/0008-6223\(92\)90113-B](https://doi.org/10.1016/0008-6223(92)90113-B)
- Yang, H., Yan, R., Chen, H., Lee, D. H., & Zheng, C. (2007). Characteristics of hemicellulose, cellulose and lignin pyrolysis. *Fuel*, *86*(12–13), 1781–1788.  
<https://doi.org/10.1016/j.fuel.2006.12.013>